II-B.   Thermal Analysis

B.1.   General

(1) Thermal Designing

The transport packaging, type GP-01, consists of an outer receptacle and an inner receptacle which can be retrieved from the outer receptacle without dismantling. All the structural elements of the packaging are made of stainless steel. These structural elements do not include materials of different coefficients of thermal expansion. Thus, the model of packaging will not be deformed when the ambient temperature changes.

The outer receptacle has a multi-caisson-shaped double structure composed of frames, inner plates, and outer plates welded. The voids between the inner plates and the outer plates are filled with a heat insulating material (synthetic mineral fiber/ceramic fiber) to retard heat conduction to the inner receptacle which embraces the material for which the packaging GP-01 has been designed. This insulating material is made of an alumina-silica based synthetic mineral fiber which has a maximum service temperature of at least 1000°C. This material has several advantages. It is manufactured as a blanket-shaped lightweight material and can easily be formed into desired shapes. Even when deformed under compressive load, its insulating capability is not affected. A fusible plug is installed at an appropriate location on each of the outer faces of the outer receptacle. If exposed to a high-temperature environment, the solder will melt to offset the pressure difference between the inner and outer plates.

Fire-resisting rubber pieces are applied to the back of the lid of the outer receptacle. These rubber pieces will start to expand at approximately 200°C in accidental fire conditions to block up the gaps between the top of the body of the outer receptacle and the lid to prevent flames from entering.

Neither a specific cooling device nor an expansion tank is installed in the packaging.

(2) Thermal analysis

The package (packaging and contents) to be transported will be subjected to a thermal analysis to prove that it meets the technical requirements for "Type 'A' fissile package" defined in the "Regulations for transport of nuclear fuel materials outside the industrial facility and premises" (Ordinance No. 57 of the General Administrative Agency of the Cabinet of December 28, 1978; last revised in the decree No. 3 of the Ministry of Economy, Trade and Industry of April 15, 2008) (hereinafter referred to as "the Regulations") and in the Public Notice on particulars relative to the technical requirements for transport of nuclear fuel materials outside the industrial facility and premises" (Public Notice No. 5 of the Science and Technology Agency of November 28, 1990; last revised in the Public Notice No. 1 of the Ministry of Economy, Trade and Industry of December 26, 2006) (hereinafter referred to as "the Public Notice").

(a) Normal conditions of transport

The package considered is a Type "A" fissile package and therefore need not be subjected to the thermal tests under normal conditions of transport which Type "B" packages must be subjected to: it shall "be exposed to a solar radiation environment of 38°C for twelve hours a day for one week (seven cycles of 12-hour solar radiation and 12-hour no solar radiation)." In fact, the Regulations require Type "A" packages to "be exposed to a solar radiation environment of 38°C for twelve hours a day for one week (seven cycles of 12-hour solar

radiation and 12-hour no solar radiation) until it presents a constant surface temperature change pattern," before being evaluated in the thermal tests under accident conditions of transport which fissile packages must be subjected to. Considering the category of the package ("fissile package"), our analysis will be carried out for "Normal Conditions of Transport" using a no-damage model (Chapter II-B, section "B.4. Normal Conditions of Transport").

(b) Accident conditions of transport

Yi. The specimen is exposed to a solar radiation environment of 38°C for 12 hours a day for one week (seven cycles of 12-hour solar radiation and 12-hour no solar radiation) until it presents a constant surface temperature change pattern, and is then exposed to a heat radiation environment (ambient emittance: 0.9) of 800°C for 30 minutes. During the last period of 30 minutes, the package remains exposed to heat of solar radiation. The maximum design exothermic reaction is taken into account.

Ro. Following this exposure to heat radiation, the specimen is exposed to additional cycles of 12-hour solar radiation and 12-hour no solar radiation in an atmosphere of 38°C. The maximum design exothermic reaction is taken into account. During this period, no active cooling is performed.

The Regulations require that Drop I and Drop II tests should be carried out in such ways that the specimen suffers maximum damage during thermal tests. A thermally demanding condition for the specimen will be prepared when its corner strikes the test target during drop tests. The packaging flange (joint of lid and body of the inner/outer receptacles) is regarded most vulnerable to entry of heat. In fact, the specimen was dropped in the same orientation which would cause maximum damage and have en effect of superposition in Drop I and Drop II tests as part of the prototype tests: orientation with the corner facing downward so that it strikes the test target first. To enhance the conservatism, these Drop I and Drop II tests were preceded by free drops in this package orientation under normal conditions of transport. The specimen which was thus subjected to drop tests repeatedly in the same orientation before the thermal test. Our thermal analysis adopted a model which conservatively took into account the data on the deformations in the prototype packaging and the measured temperatures to evaluate the package. Appendix 1 to Chapter II-B shows results of the thermal tests of the prototype packaging.

An unsteady heat transfer analysis was carried out. More precisely, non-linear analysis methods which handle non-linear material constants and heat radiation were applied. The analytical code, Ansys version 11, was used for analytical calculations. This is a universal finite element analysis code. A preliminary analysis was carried out to check the definitive analytical model is justifiable in relation to the results of the thermal tests before proceeding to carry out the main part of the heat transfer analysis. Appendix 2 to Chapter II-B shows results of the preliminary check.

(3) Maximum quantity of decay heat

The quantity of decay heat of uranium oxides, the material to be contained in the package is very small and is neglected in the thermal analysis.

B.2.   Thermophysical Properties of Contents

Tables II-B-1 to II-B-4 show the thermophysical properties of the materials to be contained in the package (inner receptacle) which were used for the thermal analysis of the package.

Table II-B-1: Thermophysical Properties of Contents

Temperature (K)	Density (g/cm³)	Specific heat (J/kg·K)	Heat conductivity (W/m·K)	Temperature (K)	Density (g/cm³)	Specific heat (J/kg·K)	Heat conductivity (W/m·K)
293	3.646	462	4.83	693	3.598	535	5.28
313	3.644	466	4.82	713	3.595	539	5.33
333	3.643	470	4.82	733	3.592	542	5.38
353	3.641	473	4.81	753	3.589	546	5.43
373	3.638	477	4.81	773	3.586	549	5.49
393	3.636	480	4.82	793	3.583	552	5.55
413	3.634	484	4.83	813	3.581	555	5.61
433	3.631	487	4.84	833	3.578	557	5.67
453	3.629	491	4.86	853	3.575	560	5.73
473	3.626	494	4.88	873	3.572	562	5.80
493	3.624	498	4.90	893	3.569	564	5.87
513	3.621	502	4.93	913	3.566	566	5.94
533	3.619	505	4.96	933	3.563	567	6.01
553	3.616	509	4.99	953	3.560	568	6.08
573	3.614	513	5.02	973	3.556	569	6.15
593	3.611	517	5.06	993	3.553	569	6.23
613	3.608	521	5.10	1013	3.550	570	6.31
633	3.606	524	5.14	1033	3.547	569	6.39
653	3.603	528	5.18	1053	3.544	569	6.47
673	3.600	532	5.23	1073	3.541	567	6.55

Note: The contents were homogenized with the volumetric ratios of the different materials contained in the inner receptacle: 46.2 % for air, 16.6 % for uranium oxides, 21.8 % for stainless steel, and 15.4 % for neoprene rubber. The data on uranium oxides were cited from MATPRO-Version 11 and NFI's archives. The other data were cited from *Heat Transfer Engineering Data*, 4th revised edition, The Japan Society of Mechanical Engineers, 1986.

Table II-B-2: Thermophysical Properties of Aluminum Honeycomb Element

Temperature (K)	Density (g/cm³)	Specific heat (J/kg·K)	Heat conductivity (W/m·K)		
			X	Y	Z
300	0.0776	907	2.554	3.818	6.767
320	0.0775	921	2.552	3.814	6.759
340	0.0774	934	2.550	3.810	6.751
360	0.0772	946	2.548	3.806	6.743
380	0.0771	957	2.546	3.802	6.735
400	0.0770	966	2.543	3.798	6.727
420	0.0768	975	2.541	3.794	6.719
440	0.0767	983	2.539	3.790	6.711
460	0.0766	991	2.537	3.786	6.702
480	0.0765	998	2.534	3.782	6.694
500	0.0764	1005	2.532	3.778	6.686
550	0.0760	1022	2.526	3.768	6.665
600	0.0757	1040	2.520	3.758	6.645
650	0.0754	1060	2.491	3.712	6.562
700	0.0750	1083	2.462	3.667	6.480
800	0.0743	1140	2.404	3.577	6.315
900	0.0734	1213	2.345	3.487	6.150
1000	0.0725	1300	2.286	3.395	5.984
1100	0.0715	1391	2.226	3.304	5.817

Note: The thermophysical properties of the aluminum honeycomb element have been calculated. Refer to Appendix 2 to Chapter II-B.

Table II-B-3: Thermophysical Properties of Insulating Material

Temperature (K)	Density (g/cm³)	Specific heat (J/kg·K)	Heat conductivity (W/m·K)
291	0.16	1050	0.031
373	0.16	1050	0.036
473	0.16	1050	0.044
573	0.16	1050	0.053
673	0.16	1050	0.064
773	0.16	1050	0.081
873	0.16	1050	0.098
973	0.16	1050	0.120
1073	0.16	1050	0.145
1173	0.16	1050	0.173

Note: These data are cited from the technical data published by the manufacturer with some modifications. Refer to Appendix 2 to Chapter II-B.

Table II-B-4: Thermophysical Properties of Materials Adopted for Thermal Analysis

Component	Material	Temperature (K)	Density (g/cm³)	Specific heat (J/kg·K)	Heat conductivity (W/m·K)
Inner/Outer Receptacle	Stainless steel [1]	300	7.92	449	16.0
		400	7.89	511	16.5
		600	7.81	556	19.0
		800	7.73	620	22.5
		1000	7.64	644	25.7
Rubbers	Fire-resistant rubber [1][2]	300	0.86	2200	0.36
	Silicone rubber [1]	293	0.97	1600	0.20
		400	0.97	1500	0.19
	Neoprene rubber [1]	293	1.23	2200	0.25
		400	1.23	2200	0.23

Notes: (1) *Heat Transfer Engineering Data*, 4th revised edition, JSME, 1986

(2) The properties of ethylene propylene rubber (main component) are substituted.

B.3.   Characteristics of Packaging Components

The contents of the package consist of assemblies of storage boxes containing solid pellets of uranium oxides. The assemblies and the pellet storage boxes are made of stainless steel. There is no emission of gases from the pellets which are stable solids within the range of temperatures conceivable in safety analysis. Therefore, no valves such as safety valves are provided in the packaging. Since it is needless to increase or decrease the pressure in the packaging for storing the pellets, the applicable requirements for maximum service pressure are not relevant for this package.

The O-ring installed on the flange of the inner receptacle has been designed with the following specifications:

- Material: Silicone rubber
- Service temperature range: –50 to +180°C
- Thermal aging performance: No serious deterioration at 225°C for 72 hours
- Tensile strength: ≥ 3.4 MPa
- Hardness: 48 to 60 (measured with a Type "A" durometer)
- Elongation: ≥ 200 %
- Wire diameter: 10 mm.

B.4.   Normal Conditions of Transport

The package is a Type "A" fissile package and is therefore not subjected to the thermal tests under normal conditions of transport which Type "B" packages must subjected to. In fact, the Regulations require Type "A" packages to be exposed to a solar radiation environment of 38°C until it presents a constant surface temperature change pattern, before being evaluated in the thermal tests under accident conditions of transport to which fissile packages must be subjected. Our analysis was based on this prerequisite. The package was exposed to a solar radiation environment of 38°C for one week.

B.4.1.   Analytical Thermal Model

B.4.1.1.   Analytical model

(1) Geometrical model

In the preceding 1.2-meter free drop test under normal conditions of transport, Prototype No. 2 was made to drop with its corner facing downward to strike the test target first (refer to Appendix 1 to Chapter II-A). During that test, deformations occurred mainly in the zone of lifting attachment and scarcely in the main body of the package. The analytical model used in the analysis for integrating thermal test results conservatively involved a limited insulator zone and takes into account deformations under accident conditions of transport. This analytical model includes well the deformations observed in the 1.2-meter drop test. We removed from it those deformations under accident conditions to prepare an analytical model for use in our thermal analysis (refer to Appendix 2 to Chapter II-B). Our analysis for integrating thermal test results adopted the metal lead as dummy contents to ensure coherence with the conditions for the prototype tests. Our thermal analysis took into account uranium oxides as contents to simulate more precisely the real model of packaging.

Since the package to be analyzed has a symmetric shape, our thermal analysis was based on a modeled quarter symmetric zone (hatched zone in Fig. II-B-1) of the package. Our modeling excluded small parts of the packaging because they were regarded negligible in terms of thermal consequences.
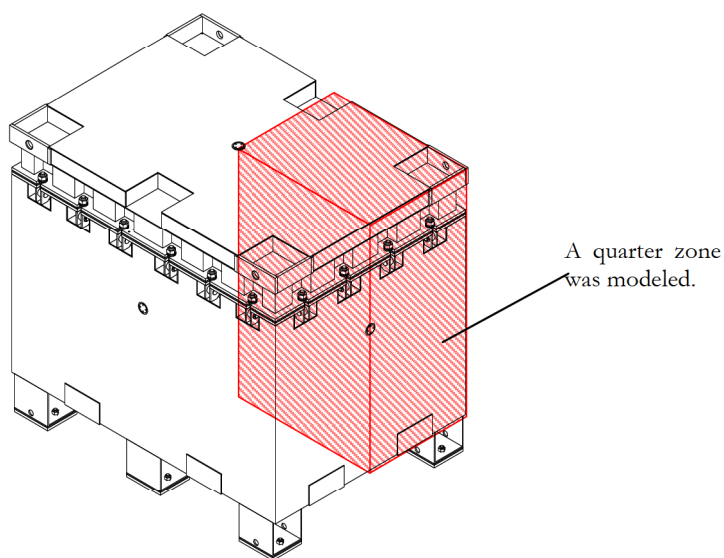

A quarter zone was modeled.

Fig. II-B-1: Modeled Zone for Analysis

We excluded from our analysis those portions of the lid of the outer receptacle which are located outside the frames. The model is all the more conservative because it has contiguous stacking recesses for the legs of another outer receptacle on the lid of the outer receptacle and contiguous bolt seats on the body of the outer receptacle. Moreover, to avoid reducing our conservatism, the honeycomb elements were assumed to be free from deformation and form heat conduction paths to the inner receptacle. Fig. II-B-2 illustrates the analytical model used for our thermal analysis.

(a) View from −Y direction   (b) View from +Y direction
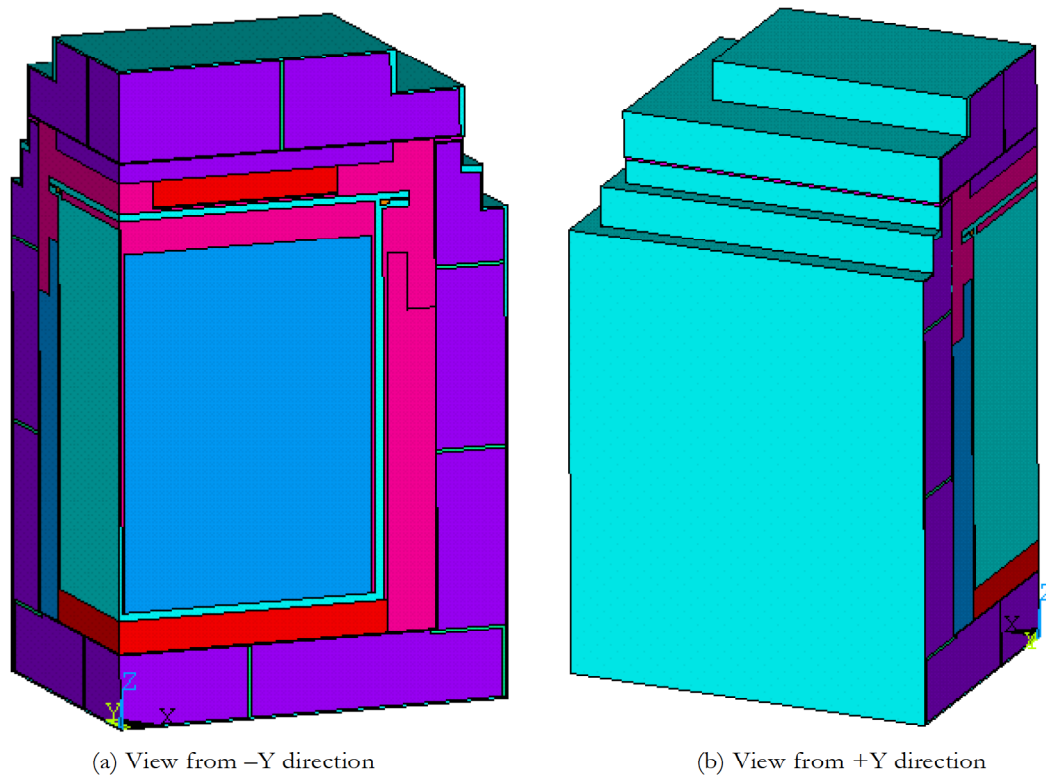
Fig. II-B-2: General View of Analytical Model

The analytical model is embraced by three elements created for analyzing heat transfer through air, heat transfer by radiation during natural cooling and heat transfer by radiation of flames, respectively. Heat transfer by radiation is taken into account for the border between the internal air and the surrounding structural components of the package.

The model has 101,917 nodes and 123,375 finite elements. Figs. II-B-3 to II-B-5 show the entire finite element model and its segments.
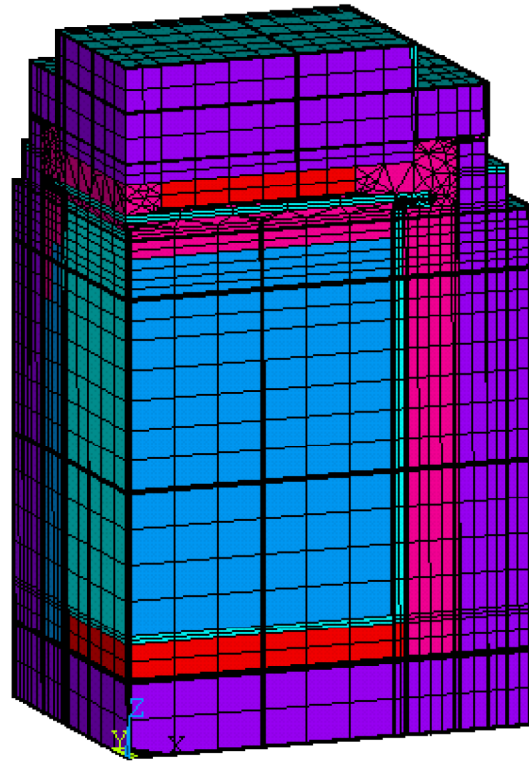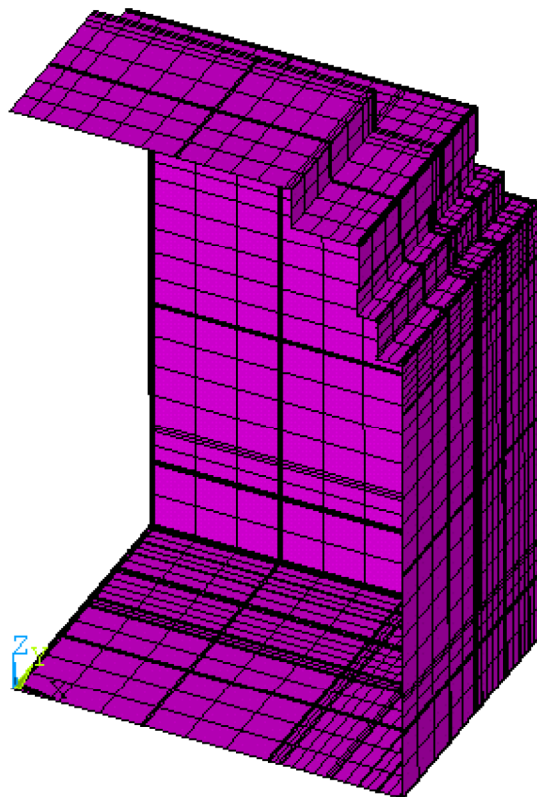
Fig. II-B-3: Finite Element Model (entire)

Fig. II-B-4: Finite Element Model (segment for calculating surface effect)
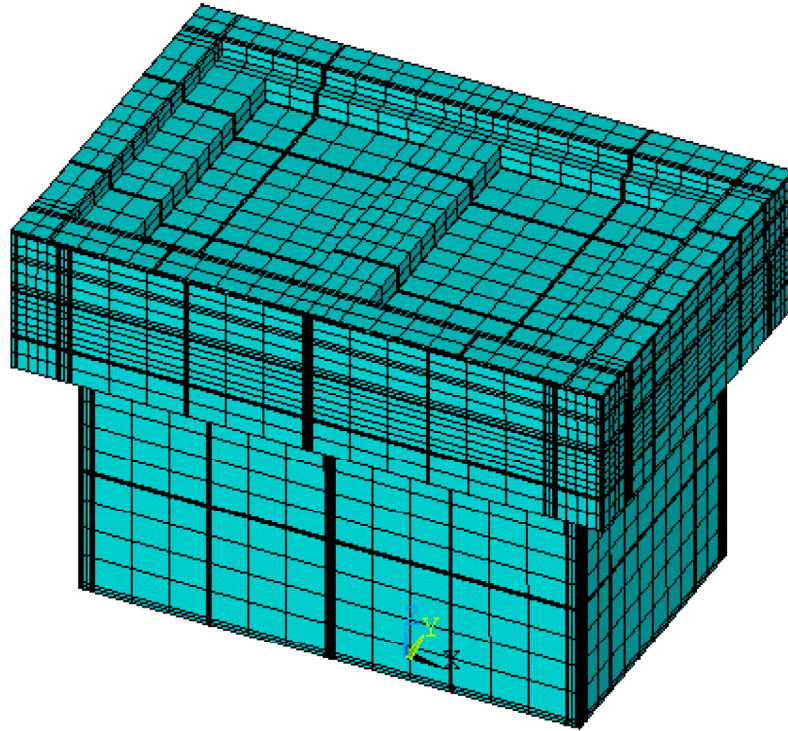
Fig. II-B-5: Finite Element Model (segment for calculating surface effect and internal radiation)

(2) Analysis conditions
The conditions specified in the Regulations should be adopted for our analysis. The following paragraphs summarize the analysis conditions adopted.

(a) Heat transfer between packaging components
All the components and parts of the packaging are assumed to be in tight contact with each other as long as they are in contact geometrically. No loss of heat transfer occurs in the analysis since the model was created with the nodes shared by the relevant elements.

(b) Heat transfer under Appendix 4-1 to Public Notice
The set of two conditions shown below is applied for 12 hours followed by an interval of 12 hours, this cycle being further repeated six times within one week (total: 7 cycles).
Yi: Applying a heat input with the specified heat flux and a heat release by radiation to simulate a thermal condition in the daytime
- According to the tables in Appendix 4-1 to the Public Notice, the following energies are applied:
800 W/m² to the external horizontal and upward-facing surfaces of the packaging
200 W/m² to the external vertical surfaces of the packaging.
These energies are directly applied with heat flux to the relevant external surfaces of the packaging.
- Applying radiation of heat from the external surfaces of the outer receptacle to the surrounding space (atmospheric temperature: 38°C). The outer receptacle is made of stainless steel. The *Heat Transfer Engineering Data* (4th revised edition, The Japan Society of Mechanical Engineers, 1986) includes data on the radiation

factor for stainless steel in Figure 1(a), page 184. It indicates a range of 0.1 to 0.2 for 0°C to 800°C. We adopted 0.1 to stay conservative. Ansys surface effect elements were used to apply the radiation.

Ro. Applying heat release by radiation to simulate a thermal condition in the nighttime
- Applying radiation of heat from the external surfaces of the outer receptacle to the surrounding space (atmospheric temperature: 38°C). A radiation factor of 0.8 was adopted in accordance with the IAEA transport regulations TS-G1.1 728.29. Ansys surface effect elements were used to apply the radiation.

(c) Heat transfer to packaging surfaces by convection of surrounding fluid

If the surrounding fluid is in the state of convection at 38°C, a heat balance occurs on the external surfaces of the packaging. This heat balance was applied. The coefficient of heat transfer α was regarded as function of Nusselt number. The Nusselt number was retrieved from the IAEA transport regulations TS-G1.1 728.31. Ansys surface effect elements were used to apply the heat transfer.

The coefficient of heat transfer α is as function of Nusselt number:

$$\alpha = Nu \cdot \lambda / l \quad (\lambda : \text{heat conductivity}, l : \text{representative length (outer receptacle height exc. legs} : 0.915 \text{ m})$$

The Nusselt number was calculated with the formula shown in the IAEA transport regulations TS-G1.1 728.31

$$Nu = 0.13(Pr\,Gr)^{1/3}$$

where

Prandtl number $Pr = \nu/\varkappa$ (ν: kinetic viscosity; $\varkappa$: coefficient of thermal diffusivity ($=\lambda/\varrho c$); ϱ: density; c: specific heat)

Grashof number $Gr = g \cdot \beta \, (T_w - T\infty) \, l^3 / \, \nu^2$ (g: gravitational acceleration; β: coefficient of volumetric expansion; T_w: wall temperature; $T\infty$: air temperature)

Table II-B-5 shows results of calculation for coefficients of heat transfer.

Table II-B-5: Coefficients of Heat Transfer

Temperature (K)	Coefficient of heat transfer (W/m²·K)	Temperature (K)	Coefficient of heat transfer (W/m²·K)
311	0	550	7.942
320	3.858	600	7.988
340	5.460	650	7.975
360	6.250	700	7.965
380	6.742	800	7.878
400	7.082	900	7.783
420	7.326	1000	7.619
440	7.509	1100	7.448
460	7.643	1200	7.273
480	7.748	1500	6.758
500	7.826	—	—

(d) Heat transfer by radiation through air in the packaging

A real package contains air between the external surfaces of the inner receptacle and the internal surfaces of the outer receptacle and between the internal surfaces of the inner receptacle and the external surfaces of the pellet storage box assemblies. Assuming that no convection is present in the internal air, this air was regarded as a heat transferring material (or solid for which physical properties corresponding to the air are applied) in our analysis. Heat transfer by radiation was applied to the internal surfaces of the packaging which are in contact with air. Aluminum honeycomb elements occupy most of the internal surfaces of the outer receptacle. The *Heat Transfer Engineering Data* (4th revised edition, The Japan Society of Mechanical Engineers, 1986) includes data on the radiation factor for aluminum in Figure 1(a), page 184. It indicates a range of 0.01 to 0.05. We adopted 0.1 to stay conservative. To carry out the analysis with a symmetric model, radiosity was used.

(e) Symmetry boundary condition

All the symmetric surfaces were handled as heat insulating conditions. Surfaces for which no condition is specified were regarded as heat insulating conditions in the heat transfer analysis.

(f) Initial temperature condition

The analysis was started with the object to be analyzed which had a uniform temperature of 38°C under normal conditions of transport.

Table II-B-6 shows the heat transfer conditions used.

Table II-B-6: Heat Transfer Conditions (normal conditions of transport)

Conditions		Heat transfer through surrounding air (heat transfer condition applied)	Inflow of solar radiation (heat flux applied)	Radiation by flames (heat transfer by radiation applied)	Radiation through surrounding air (heat transfer by radiation applied)	Radiation through the air in packaging voids (outer recept. internal surface⇔inner recept. external surface inner recept. internal surface⇔contents external surface)
Normal Conditions	Temperature rise solar radiation (daytime)	ON Surrounding air at 38°C Temperature-dependent coefficient of heat transfer	ON Horizontal/upward-facing surfaces: 800 Vertical surfaces: 200 Horizontal/downward-facing surfaces: 0	OFF	ON (ε packaging external surface=0.1)	ON (ε=0.1)
	Natural cooling (nighttime)		OFF			

(3) Flow of analysis
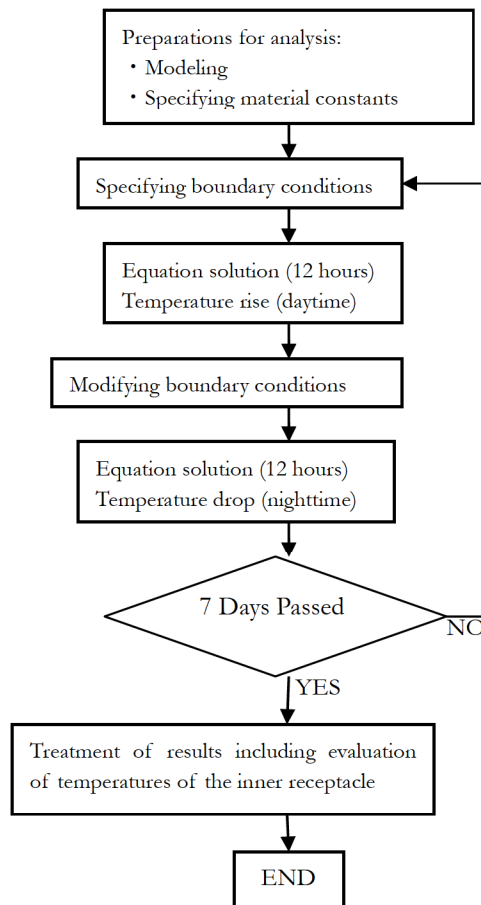
Fig. II-B-6 shows the flow of the thermal analysis.

```
┌─────────────────────────────────────┐
│ Preparations for analysis:          │
│   • Modeling                        │
│   • Specifying material constants   │
└─────────────────────────────────────┘
                  │
                  ▼
┌─────────────────────────────────────┐ ◄───┐
│ Specifying boundary conditions      │     │
└─────────────────────────────────────┘     │
                  │                          │
                  ▼                          │
┌─────────────────────────────────────┐     │
│ Equation solution (12 hours)        │     │
│ Temperature rise (daytime)          │     │
└─────────────────────────────────────┘     │
                  │                          │
                  ▼                          │
┌─────────────────────────────────────┐     │
│ Modifying boundary conditions       │     │
└─────────────────────────────────────┘     │
                  │                          │
                  ▼                          │
┌─────────────────────────────────────┐     │
│ Equation solution (12 hours)        │     │
│ Temperature drop (nighttime)        │     │
└─────────────────────────────────────┘     │
                  │                          │
                  ▼                          │
            ◇ 7 Days Passed ◇ ──── NO ───────┘
                  │
                 YES
                  │
                  ▼
┌─────────────────────────────────────┐
│ Treatment of results including      │
│ evaluation of temperatures of the   │
│ inner receptacle                    │
└─────────────────────────────────────┘
                  │
                  ▼
             ┌─────────┐
             │   END   │
             └─────────┘
```

Fig. II-B-6: Flow of Analysis under Normal Conditions of Transport

B.4.1.2.   Test model

This section is not applicable since no thermal tests were carried out with a prototype packaging under normal conditions of transport.

B.4.2.　Highest Temperatures

The analytical model of package as described in section "B.4.1.1. Analytical model" was analyzed with the analytical code ANSYS to evaluate temperatures of the package under normal conditions of transport. This evaluation was focused on the O-ring on the flange which was regarded as thermally most vulnerable of the components of the inner receptacle, containment boundary of the package. Fig. II-B-7 shows the time-varying temperatures. Fig. II-B-8 shows the items evaluated. The temperature raised by solar heat radiation practically attained equilibrium on the fifth day. The highest temperature of the O-ring was recorded on the seventh day: 68°C, lower than the maximum service temperature for normal service (180°C). The highest temperature (114°C) in the package was recorded in the insulator close to the outer receptacle lid center. Fig. II-B-9 and II-B-10 show the temperature distributions in the entire analytical model and in the O-ring and spacers, respectively when the highest temperature was attained.　Stainless steel is the main structural element of the transport packaging. Therefore, the temperature rise generated in the analysis will not adversely affect the packaging. The highest temperature (74.5°C) in the inner receptacle was generated near the lid center. Fig. II-B-11 shows the temperature distribution in the inner receptacle.
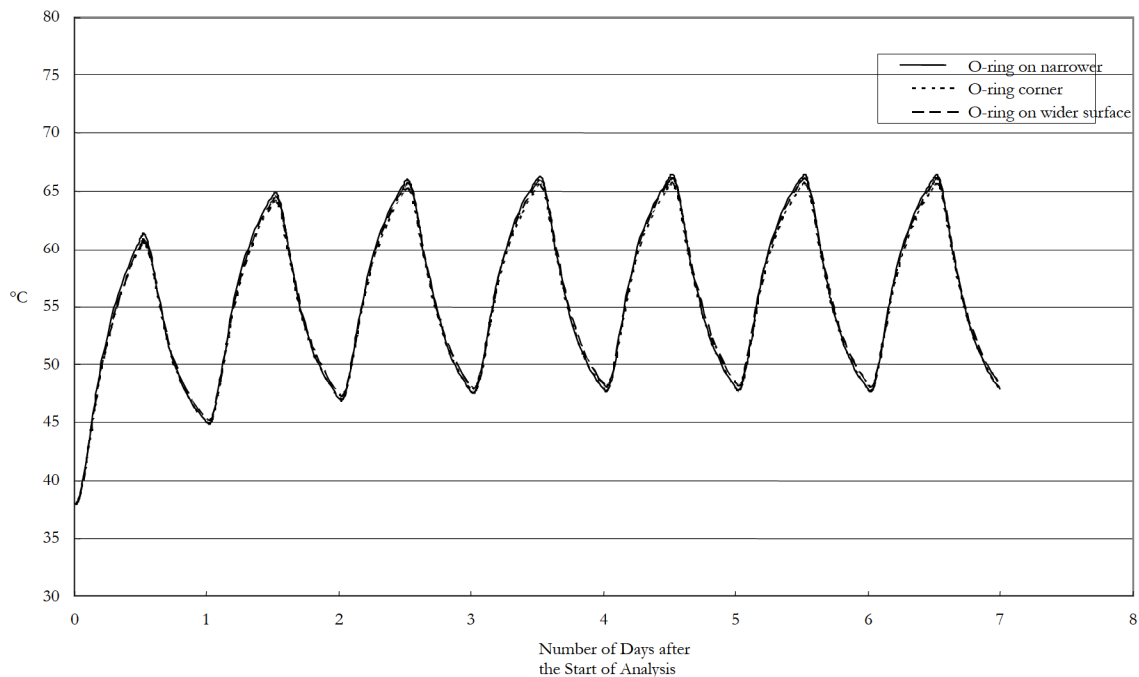
Fig. II-B-7: Temperatures Recorded under Normal Conditions of Transport
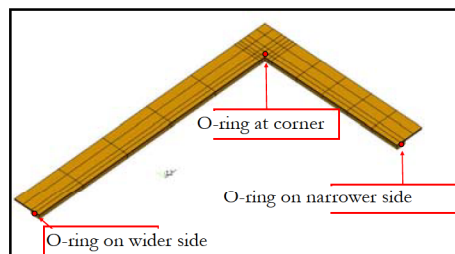
Fig. II-B-8: Points Evaluated for Temperature

II – B - 12
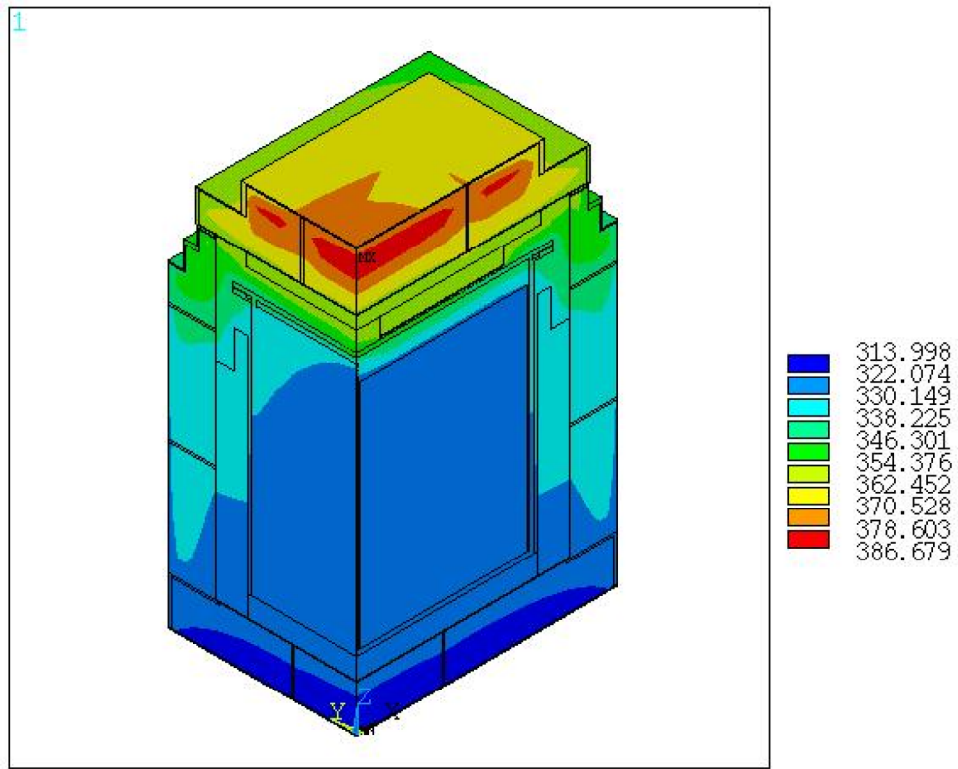
Fig. II-B-9: Temperature Distribution in the Entire Package at End of 7th Day (unit: K)
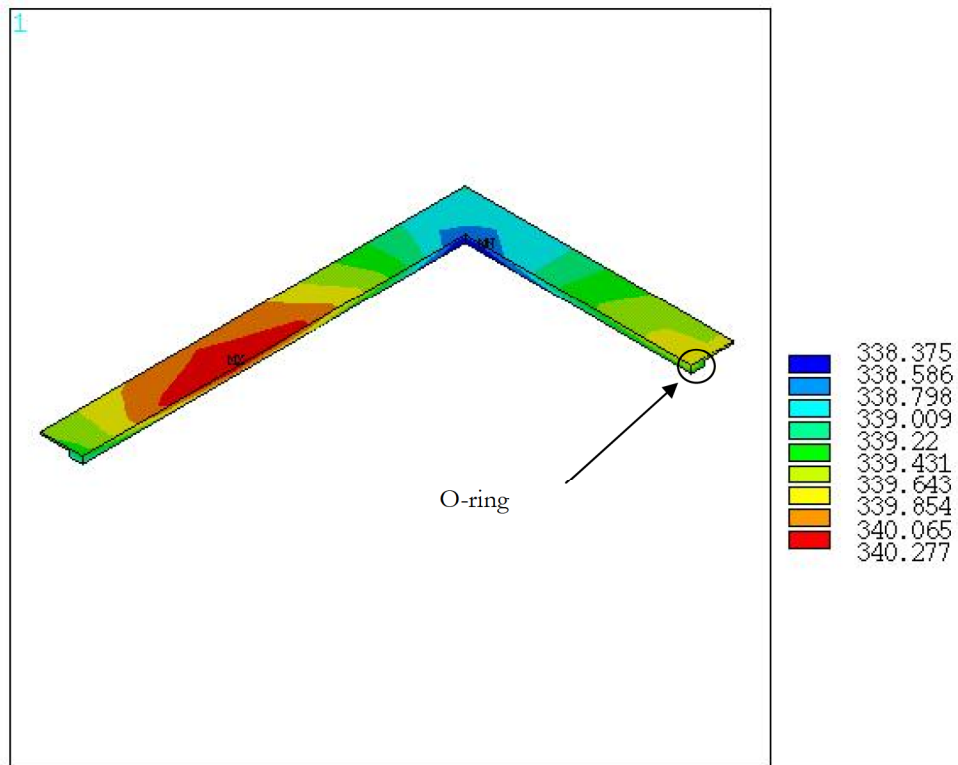
Fig. II-B-10: Temperature Distribution in Rubber near O-ring at End of 7th Day (unit: K)
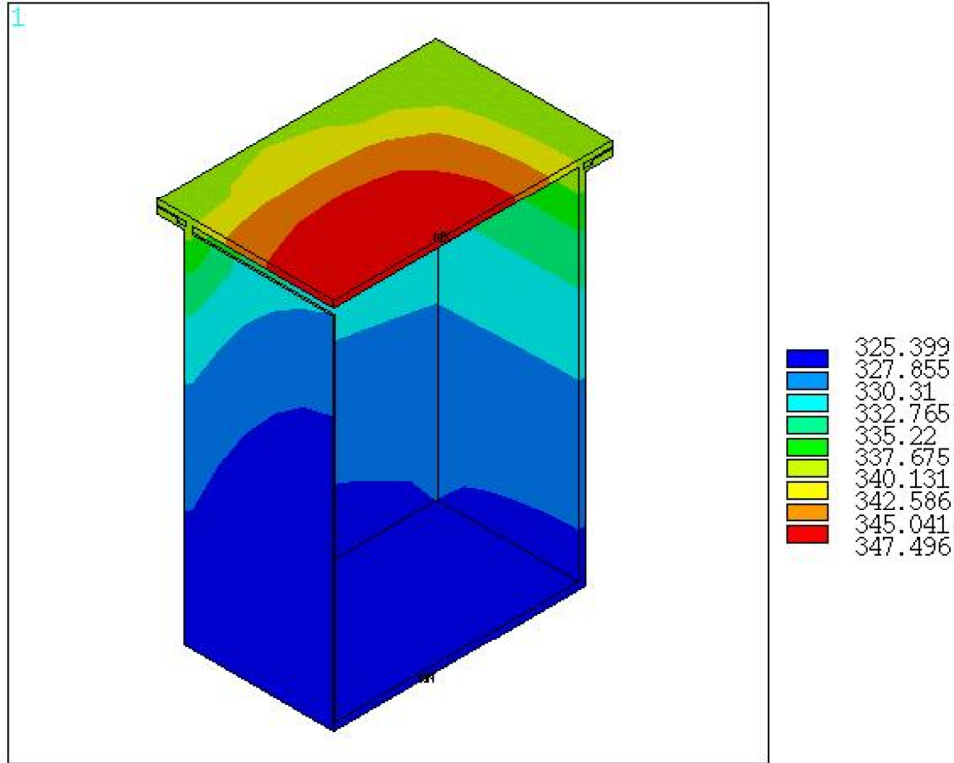
Fig. II-B-11: Temperature Distribution in Inner Receptacle in Middle of 7th Day (unit: K)

B.4.3.   Lowest Temperature

The lowest ambient temperature was assumed to be –40°C. The contents of the package are pellets of unirradiated uranium oxides. Therefore, we assumed that no decay heat is generated in the package. When solar radiation is neglected additionally, the lowest temperature which the package can attain was assumed to be the same as the assumed ambient temperature (–40°C).

Even if the temperature of the package is cooled down to –40°C, the materials of the packaging preserve their normal capabilities. The normal lowest service temperature for the O-ring is –50°C. Thus, no trouble will occur even at –40°C.

B.4.4.   Highest Inner Pressure

Results of the analysis under normal conditions of transport showed that the highest temperature (74.5°C) was attained near the inner receptacle lid center. The highest inner pressure was determined on the conservative assumption that the entire inner receptacle uniformly attains 75°C.

When the initial pressure in the inner receptacle is 101 kPa (absolute) at 0°C, the inner pressure P in the inner receptacle which has attained 75°C in solar radiation heat is

$$P = \frac{273 + 75}{273 + 0} \times 101 = 128 \quad \text{[kPa]}.$$

Hence, a gauge pressure of 27 kPa (=128 –101 [kPa]) which corresponds to the pressure difference between

the interior and the exterior of the inner receptacle acts on the internal surfaces of the inner receptacle.

B.4.5.   Highest Thermal Stress

A stainless steel of good heat conductivity is the main structural material of the transport packaging. Therefore, there will no steep temperature gradient in these structural stainless steel elements under normal conditions of transport (Figs. II-B-9 and II-B-11). The inner receptacle is not fixed anywhere in the outer receptacle. Even if thermally expanded, the inner receptacle will not suffer thermal stresses resulting from restraint and will not present deformation that might cause the contents to leak from the receptacle. Since different metals are not welded with each other in the packaging, no stresses will occur due to difference of thermal expansion.

B.4.6.   Summary of Results and Evaluation

The highest temperatures in different parts of the package under normal conditions of transport were shown in section "B.4.2 Highest Temperatures." A specific zone of the package may attain 114°C. Nevertheless, there will be no deterioration in the main structural elements made of stainless steel of the packaging. The O-ring made of silicone rubber may attain 68°C, far under the maximum service temperature.

A temperature of −40°C is taken into account as the lowest for the package. At this temperature, all the materials used for the packaging maintain their required capabilities. Temperatures foreseen will never be lower than the minimum service temperature for the O-ring.

When the inner pressure in the inner receptacle is assumed to have become uniform at the highest temperature for the inner receptacle, an inner pressure of up to 27 kPa may act on the internal surfaces of the inner receptacle. Any stresses due to a rise of the inner pressure in the inner receptacle will not affect the capabilities of the package as have been evaluated in section "A.5.1.3 Calculation of stresses."

Table II-B-7 shows summarized results of the thermal analysis and evaluations for normal conditions of transport.

Table II-B-7: Evaluations of Package under Normal Conditions of Transport

Item	Criterion	Results	Evaluation
Highest temperatures:			
O-ring	180 °C	68 °C	Meets the requirements
Entire package	–	114 °C	–
Inner receptacle	–	75 °C	–
Lowest temperature:			
O-ring	–50 °C	–40 °C	Meets the requirements
Highest inner pressure	–	27 kPa (g)	–
Highest thermal stress	–	–	Causes no problem

B.5.   Accident Conditions of Transport

For the accident conditions of transport, preliminary analyses were carried out to integrate the temperature data obtained during the preceding thermal test of a prototype packaging at 800°C for 30 minutes (refer to Appendix 2 to Chapter II-B). The analytical model for calculation was considered to be relevant for further analyses and was therefore adapted to the requirements of the real tests.

Analytical calculations were carried out consecutively for the three conditions to evaluate the temperature changes in the package:

(1) Initial conditions of thermal test

The specimen package is exposed to a solar radiation environment of 38°C for 12 hours a day (cycles of "12-hour solar radiation and 12-hour no solar radiation") until it presents a constant surface temperature change pattern.

(2) Conditions of thermal test

The specimen package is then exposed to a heat radiation environment of 800°C for 30 minutes. During this period, the specimen remains exposed to heat of solar radiation (the same radiation as that applied in the initial exposure).

(3) Conditions after thermal test

The specimen package is exposed to additional cycles of 12-hour solar radiation and 12-hour no solar radiation in an environment of 38°C for a period long enough to verify that the zone considered for evaluation has reached its highest temperature.

B.5.1.   Analytical Thermal Model

B.5.1.1. Analytical model

(1) Geometrical model

The analytical model which had been used for tests under normal conditions of transport was used for thermal test with some modifications related to the deformations produced during. the preceding drop tests. The model has the same geometry as that used for the analyses for integrating the results of the preceding test. Uranium was considered instead of lead, the material which had been considered in the analyses for integrating the results of the preceding test.

To be conservative, the geometrical model has a simplified zone which corresponds to the insulator in the outer receptacle lid and includes most of the deformations produced during the drop tests in that simplified zone. A compressed insulator would increase the volumetric insulating capability of the insulator. To remain conservative in this respect, the geometrical model was based on the assumption that the portions of insulator that were deformed during the actual tests should not change their thermal properties throughout the analysis. Accordingly, these portions were simply omitted.

In addition, we assumed that the aluminum honeycomb elements do not change their shape, and that in this way the paths for heat transmission are maintained.

Fig. II-B-12 shows the analytical model used. Figs. II-B-13 to II-B-16 show cutaway views of the damage model from different angles.

The model includes 102,279 nodes and 125,973 finite elements. Figs. II-B-17 to II-B-19 show the finite element models used.
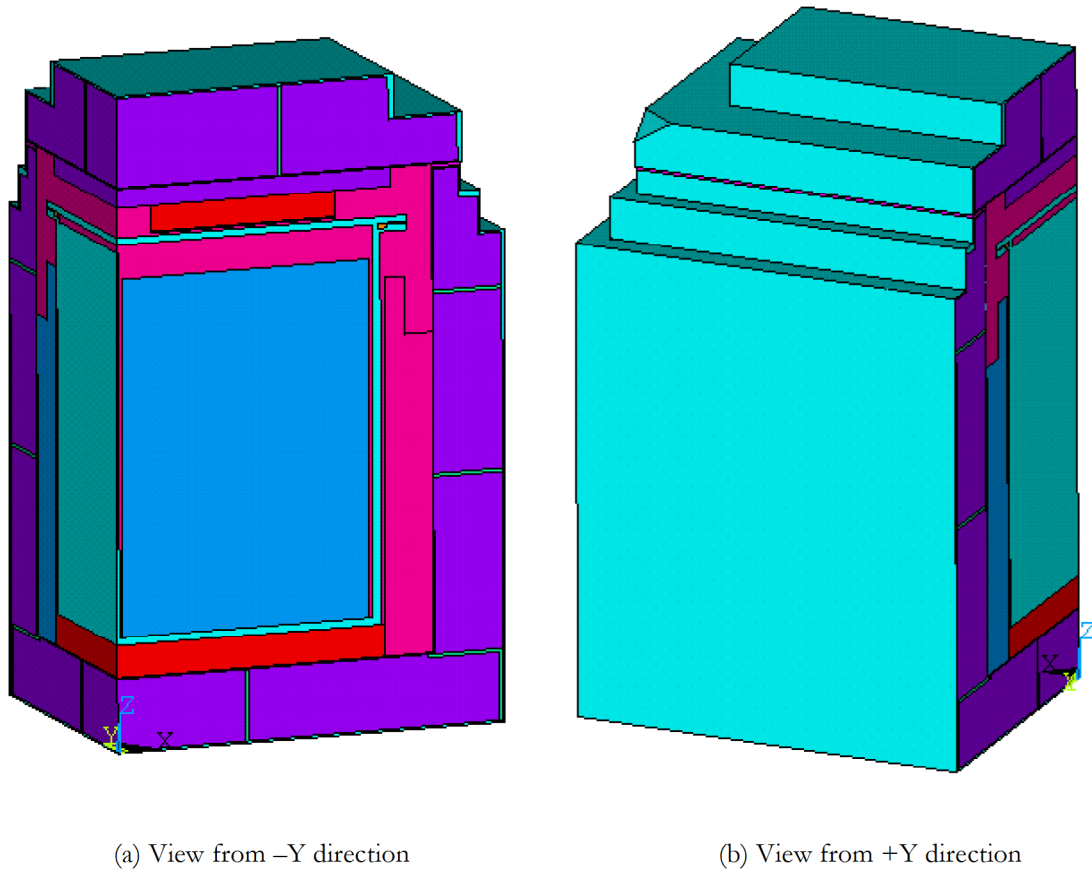

(a) View from –Y direction   (b) View from +Y direction

Fig. II-B-12: Analytical Model (Damage Model) (entire)
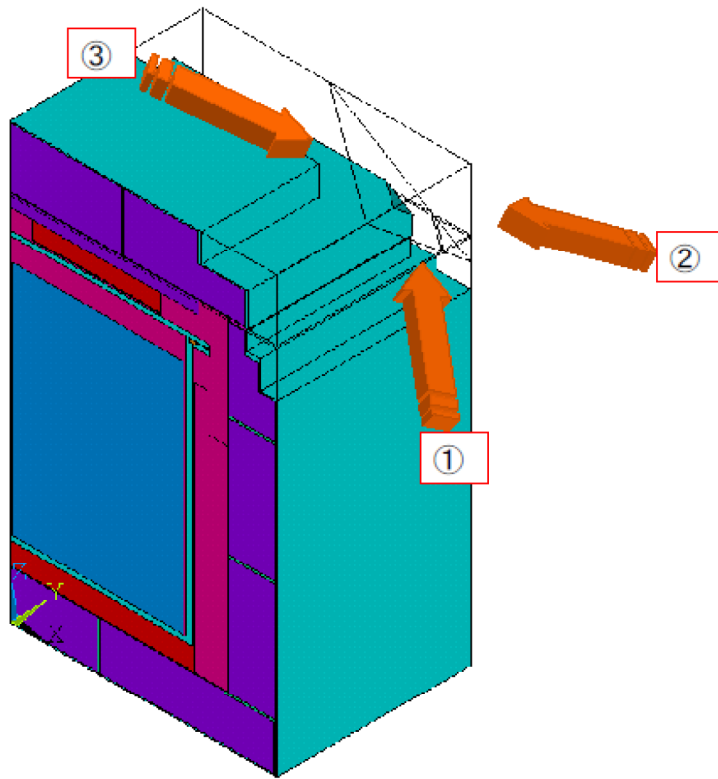
Fig. II-B-13: Cutaway View of Damage Model (1/4)
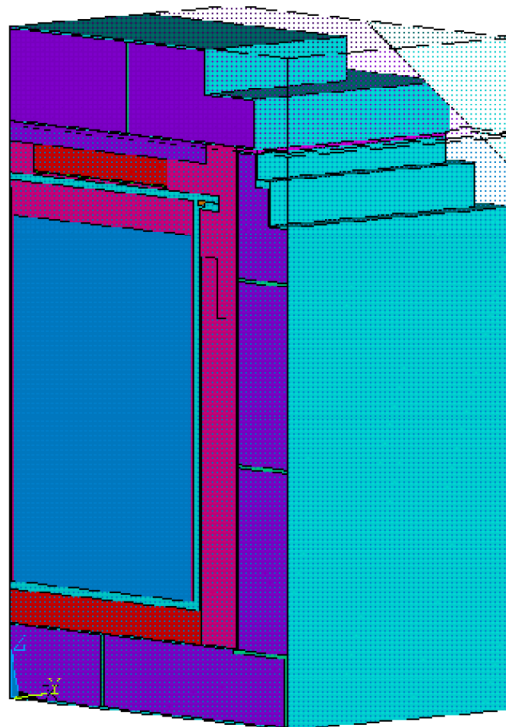
Fig. II-B-14: Cutaway View of Damage Model (2/4) (from ① direction)
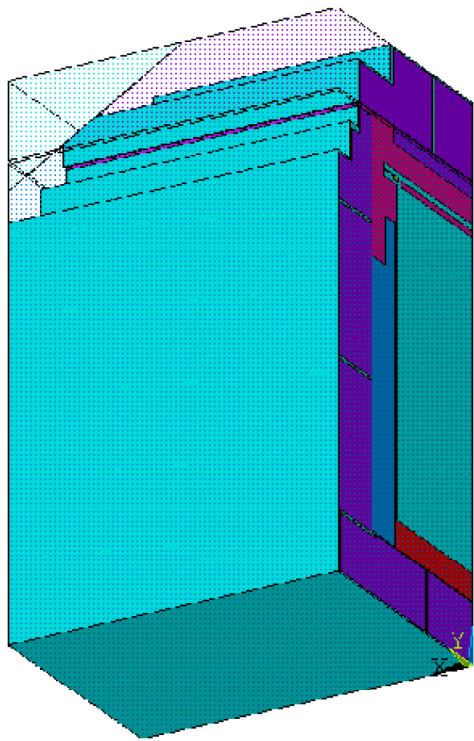
Fig. II-B-15: Cutaway View of Damage Model (3/4) (from ② direction)
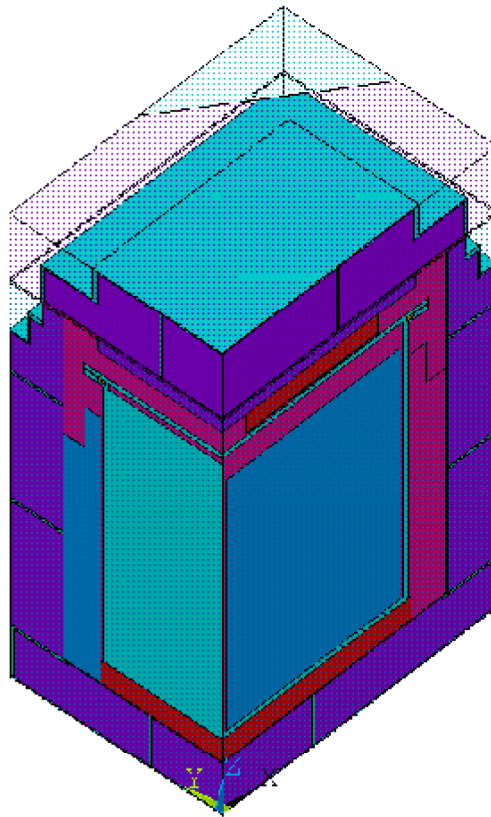
Fig. II-B-16: Cutaway View of Damage Model (4/4) (from ③ direction)
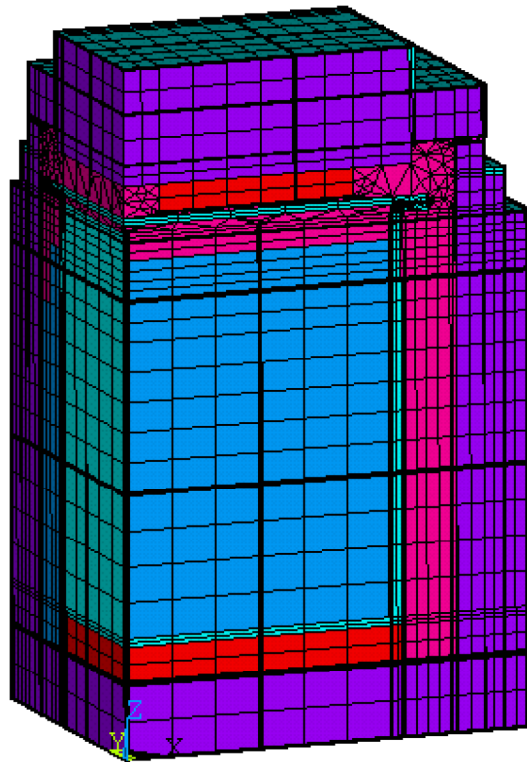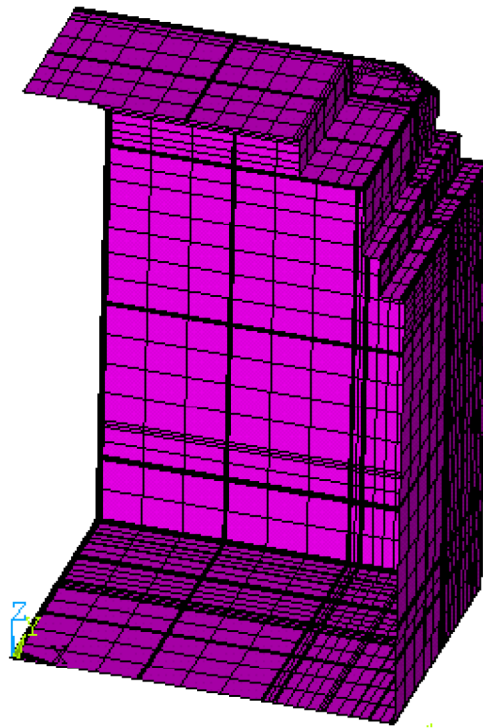
Fig. II-B-17: Finite Element Model (entire)

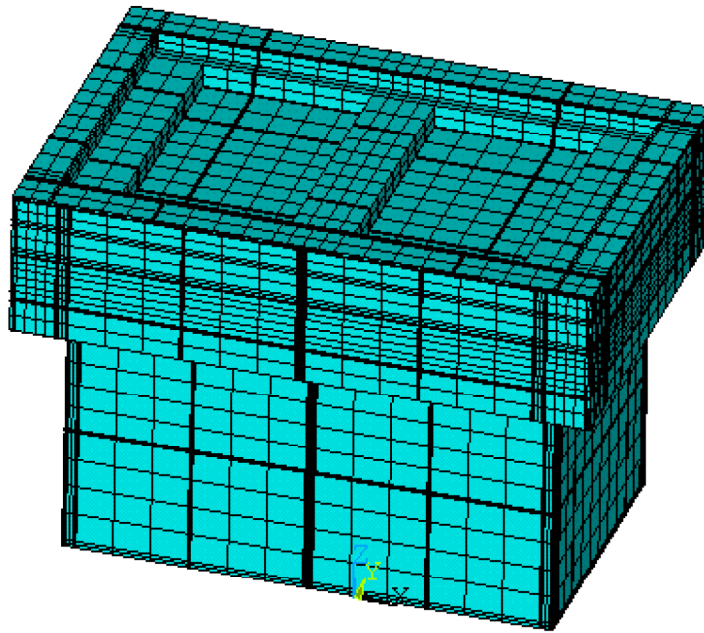Fig. II-B-18: Finite Element Model (surface effect elements)

Fig. II-B-19: Finite Element Model (for calculation of surface effect and internal radiation)

(2) Analysis conditions

Essentially, the analysis conditions adopted were the same as those used for tests under normal conditions of transport, except for the following particulars:

(a) Heat transfer according to Appendix 5-2 to Public Notice

The set of the three conditions shown below is made to occur consecutively:

Yi. Exposing the package to an environment of 38°C until it presents a constant surface temperature change pattern

- Performing the operation shown below in "(b) Heat transfer according to Appendix 4-1 to Public Notice" for 12 hours followed by an interval of 12 hours of no active heat transfer, and repeating this cycle until stable equilibrium is attained. These cycles of heat transfer should occur for a total period of 10.5 days.

Ro. Exposing the package to a thermal test environment of 800°C for 30 minutes

- Applying the heat transfer by convection of the surrounding fluid of 800°C. The coefficient of heat transfer α used for the analysis was $10W/(m^2°C)$, a value retrieved from the IAEA transport regulations TS-G1.1 728.30. Ansys surface effect elements were used to apply the heat transfer.

- Applying the radiation of heat from the external surfaces of the outer receptacle to the surrounding space at an atmospheric temperature of 800°C. A radiation factor of 0.9 for the flame surface and of 0.8 for the external surface of the outer receptacle in accordance with the IAEA transport regulations TS-G1.1 728.28

and 728.29. As Ansys provides for only one value for the radiation factor to be applied, the following equation was adopted:

$$\text{Radiation factor } F_\varepsilon = \frac{\varepsilon_1 \varepsilon_2}{1 - (1 - \varepsilon_1)(1 - \varepsilon_2)}$$

Ansys surface effect elements were used to apply the radiation.

Ha. Applying natural cooling after fire

- Applying the heat transfer by convection of the surrounding fluid at 38°C. The coefficient of heat transfer α was regarded as a function of the Nusselt number. The Nusselt number was retrieved from the IAEA transport regulations TS-G1.1 728.31 (for details of the calculation of α, refer to section "B.2. Thermal Properties of Contents"). Ansys surface effect elements were used to apply the heat transfer.

(b) Heat transfer according to Appendix 4-1 to Public Notice

The following set of two conditions was used as conditions for item Yi (see above). Only the condition for the daytime is integrated into the preceding conditions Ro and Ha.

Yi: Applying a heat input with the specified heat flux and a heat release by radiation to simulate a thermal condition in the daytime as follows:

- According to the tables in Appendix 4-1 to the Public Notice, the following energies are applied:

800 W/m² to the external horizontal and upward-facing surfaces of the packaging

200 W/m² to the external vertical surfaces of the packaging

400 W/m² to the other surfaces.

These energies should be directly applied with heat flux to the relevant external surfaces of the packaging. The energy condition for "the other surfaces" is applied to the inclined surfaces of the damaged portions.

- Applying radiation of heat from the external surfaces of the outer receptacle to the surrounding space (atmospheric temperature: 38°C). A radiation factor of 0.8 was adopted in accordance with the IAEA transport regulations TS-G1.1 728.29. Ansys surface effect elements were used to apply the radiation.

Ro. Applying heat release by radiation to simulate a thermal condition in the nighttime

- Applying radiation of heat from the external surfaces of the outer receptacle to the surrounding space (atmospheric temperature: 38°C), similarly to the item Yi. A radiation factor of 0.8 was adopted in accordance with the IAEA transport regulations TS-G1.1 728.29. Ansys surface effect elements were used to apply the radiation.

(c) Coefficient of heat transfer

The coefficient of heat transfer α for the interface between the external surfaces of the outer receptacle and the surrounding fluid during fire, 10W/(m²°C), was retrieved from the IAEA transport regulations TS-G1.1 728.30. The α-values adopted for other states are those shown in section "B.4.1.1. Analytical model, (2) Analysis conditions, (c) Heat transfer to packaging surfaces by convection of surrounding fluid" on the assumption that thermal balance occurs on the external surfaces of the outer receptacle by convection of the surrounding fluid, which is kept at 38°C.

Table II-B-8 shows the heat transfer conditions.

Table II-B-8: Heat Transfer Conditions (Accident Conditions of Transport)

Conditions		Heat transfer through surrounding air (heat transfer condition applied)	Inflow of solar radiation (heat flux applied)	Radiation by flames (heat transfer by radiation applied)	Radiation through surrounding air (heat transfer by radiation applied)	Radiation through the air in packaging voids (outer recept. internal surface⇔inner recept. external surface, inner recept. internal surface ⇔ contents external surface)
Before Fire	Temperature rise by solar radiation (daytime)	ON Surrounding air at 38°C Temperature-dependent coefficient of heat transfer	ON Horizontal/upward-facing surfaces: 800 Vertical surfaces: 200 Horizontal/downward-facing surfaces: 0	OFF	ON (ε of packaging external surface=0.1)	ON (ε=0. 1)
	Natural cooling (nighttime)		OFF			
Fire	Ongoing fire	ON (coefficient of heat transfer =10 surrounding air at 800°C)	ON Horizontal/upward-facing surfaces: 800 Vertical surfaces: 200 Horizontal/downward-facing surfaces: 0	ON (ε of flame=0.9 ε of packaging external surface=0.8)	OFF	
After Fire	Natural cooling after fire	ON Surrounding air at 38°C Temperature-dependent coefficient of heat transfer		OFF	ON (ε of packaging external surface =0.1)	

(3) Flow of analysis

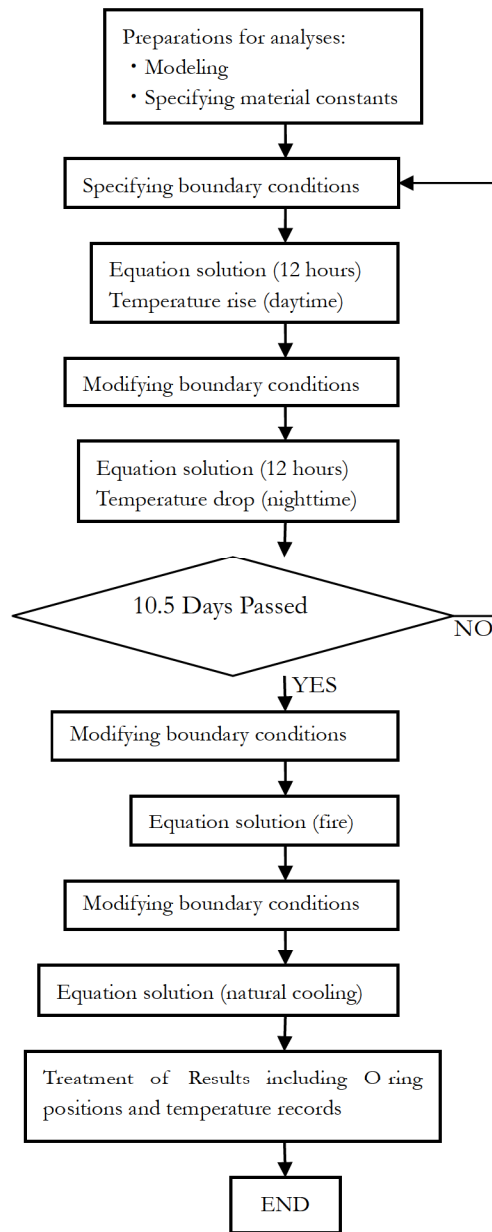Fig. II-B-20 shows the flow of the thermal analysis.

```
                    ┌─────────────────────────────┐
                    │ Preparations for analyses:  │
                    │   • Modeling                │
                    │   • Specifying material     │
                    │     constants               │
                    └─────────────────────────────┘
                                  │
                                  ▼
                    ┌─────────────────────────────┐ ◄───────┐
                    │ Specifying boundary         │         │
                    │ conditions                  │         │
                    └─────────────────────────────┘         │
                                  │                          │
                                  ▼                          │
                    ┌─────────────────────────────┐         │
                    │ Equation solution (12 hours)│         │
                    │ Temperature rise (daytime)  │         │
                    └─────────────────────────────┘         │
                                  │                          │
                                  ▼                          │
                    ┌─────────────────────────────┐         │
                    │ Modifying boundary          │         │
                    │ conditions                  │         │
                    └─────────────────────────────┘         │
                                  │                          │
                                  ▼                          │
                    ┌─────────────────────────────┐         │
                    │ Equation solution (12 hours)│         │
                    │ Temperature drop (nighttime)│         │
                    └─────────────────────────────┘         │
                                  │                          │
                                  ▼                          │
                            ╱─────────────╲                 │
                          ╱  10.5 Days      ╲──── NO ────────┘
                          ╲  Passed         ╱
                            ╲─────────────╱
                                  │ YES
                                  ▼
                    ┌─────────────────────────────┐
                    │ Modifying boundary          │
                    │ conditions                  │
                    └─────────────────────────────┘
                                  │
                                  ▼
                    ┌─────────────────────────────┐
                    │ Equation solution (fire)    │
                    └─────────────────────────────┘
                                  │
                                  ▼
                    ┌─────────────────────────────┐
                    │ Modifying boundary          │
                    │ conditions                  │
                    └─────────────────────────────┘
                                  │
                                  ▼
                    ┌─────────────────────────────┐
                    │ Equation solution           │
                    │ (natural cooling)           │
                    └─────────────────────────────┘
                                  │
                                  ▼
                    ┌─────────────────────────────┐
                    │ Treatment of Results        │
                    │ including O ring positions  │
                    │ and temperature records     │
                    └─────────────────────────────┘
                                  │
                                  ▼
                            ┌───────────┐
                            │    END    │
                            └───────────┘
```

Fig. II-B-20: Flow of Analysis of Package under Accident Conditions of Transport

B.5.1.2. Test model

The analytical model described above was used to carry out thermal evaluations. Some data which we are unable to obtain with the analytical model should be collected in other ways. Thus, in parallel, a thermal test was carried out on Prototype No. 2 to acquire a temperature history for checking the relevance of the analytical model and to ascertain the behavior of the real packaging in fire test conditions. Appendix 1 to Chapter II-B shows details of the results of the thermal test of the prototype.

(1) Prototype

The prototype packaging used for the thermal test was the one which had already been subjected to various drop tests. Two prototype packagings were used during the drop tests: one (Prototype No. 1) was mainly to examine the orientation(s) of the specimen during the main part of the drop tests that would cause maximum damage, and the other (Prototype No. 2) was for the main part of the drop tests. The latter was tested in the orientation which would produce maximum damage: with one of its upper corners facing downward to strike the test target first. This upper corner was finally chosen for maximum damage because such orientations would allow the drop energy to be concentrated on it and produce significant deformation, and because this portion of the package was located close to the flange which was regarded as most vulnerable to thermal stresses during the thermal test and likely to suffer damage (cracking or cleaving) under drop energy to form a path for heat during the thermal test.

During the drop tests, deformations occurred in the package up to the flange. No openings were produced in the flange. None of the rod bolts for tightening the lid on the body of the outer receptacle were pulled out or fractured. The lid of the outer receptacle stayed in its required position. Cracks were produced in the welds of the lifting attachment, resulting in partial exposure of the insulator. Nevertheless, no portions of the insulator were lost . In the interior of the outer receptacle, the aluminum honeycomb elements were partially deformed. The inner receptacle and the pellet storage box assemblies suffered no significant deformation. Appendix 1 to Chapter II-A shows details of the results of the prototype drop tests.

The prototype packaging (No. 2) was subjected consecutively to the drop tests and the thermal test. Essentially, this prototype packaging has characteristics and constructions identical to those of a production model except for some small differences. The only differences from a production model will be described in the following paragraphs. Two pellet storage box assemblies "A" were used as the contents of the package during the drop tests to increase the overall weight of the package. The same dummy contents were used in the thermal test without modification.

Differences of Prototype from a production model:
- Dummy pellets (lead rods) used as substitute for the real contents. Differences in thermal characteristics between uranium and lead were taken into account in the analytical calculations;

   Thermocouples were installed on the packaging, and thermo labels and thermo paint were applied to the packaging for temperature measurements. Fig. II-B-21 shows the locations at which the thermocouples were installed;

- Small portions of the honeycomb elements in the outer receptacle were cut and removed to allow installation

of thermocouples in those voids, and holes corresponding to these thermocouples were created;

- A normal stainless steel was used instead of the boronic stainless steel used for real neutron absorbers.
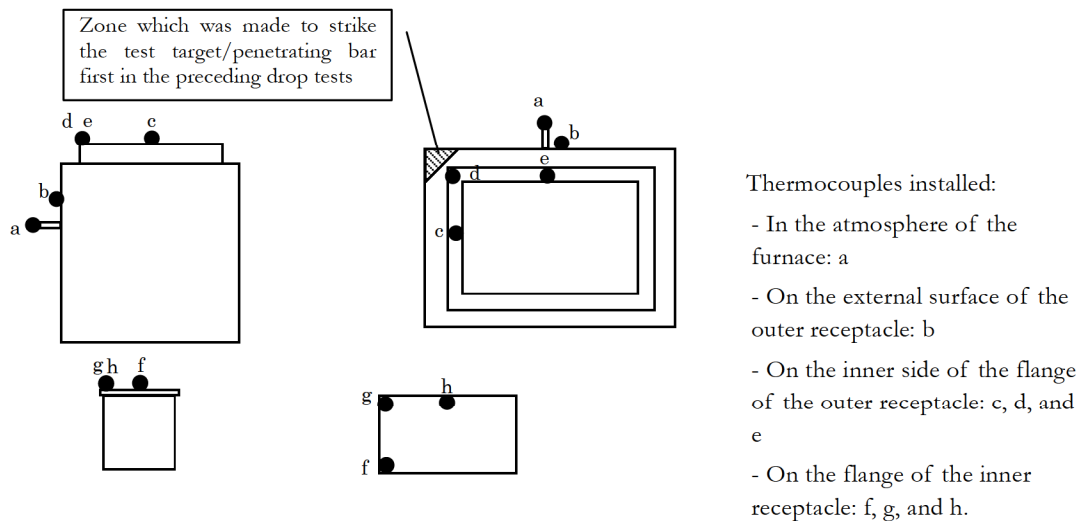
Fig. II-B-21: Locations of Thermocouples

(2) Method used for thermal test

As part of the thermal test under accident conditions of transport, a specimen of fissile package should be exposed to an environment of solar heat radiation of 38°C until it presents a constant surface temperature change pattern before being subjected to the thermal test. However, it is not possible to implement all these conditions in tests using a prototype. Thus, in our thermal test, the prototype was exposed to an environment of 800°C for 30 minutes and cooled in the ambient temperature. An analytical model created on the basis of collected data was subjected to analyses to integrate the results of the preceding tests. The required conditions were reproduced through analytical calculations to determine temperatures in the package.

The analyses for integrating the results of the preceding tests were preceded by a preliminary temperature rise test and a delivery procedure verification rehearsal. A method was then defined for the thermal test and the following procedure was applied:

① Raise the temperature in the furnace to 1000°C and maintain this temperature for at least 60 minutes.

② Have a forklift truck lifting the prototype (specimen) ready for delivery of the prototype in front of the furnace; open the port of the furnace and pull out the carriage.

③ Place the prototype in the predetermined location on the carriage and immediately place the prototype on the carriage into the furnace. Close the port of the furnace.

④ Set the temperature to 820°C±20. When a temperature of at least 800°C has been reached in the furnace and on the thermocouples installed for measuring in-furnace temperatures, wait 30 minutes while maintaining the current equipment status.

⑤ Recover the prototype in a sequence opposite to the procedure for introducing it, and leave it indoors to undergo natural cooling at room temperature until the next day.

(3) Test results

The rubber materials were burnt and lost, and the external surfaces of the prototype changed their colors. The prototype kept its geometrical shape of package and presented no significant deformation. The interior of the outer receptacle and the external surfaces of the inner receptacle changed their colors but presented no deformation or any trace of ignition. The interior of the inner receptacle and the contents kept their original colors and presented no alteration throughout the thermal test. Appendix 1 to Chapter II-B shows the details of the results of the thermal test.

Temperatures of up to 144°C were recorded in the silicone rubber O-ring provided on the inner receptacle flange. This O-ring retained its original elasticity. The type of O-ring used for the prototype has a normal service temperature of up to 180°C, and is a product which had demonstrated that it does not deteriorate significantly during a heat and aging resistance test at 225°C for 72 hours specified by the JIS standard. None of the 125°C thermo-labels applied to the internal surfaces of the inner receptacle responded during the test. This suggests that the temperature did not reach 125°C.in any part of the contents. A visual check of the interior of the inner receptacle revealed that it had not been affected by the heat during the thermal test. Table II-B-9 shows the highest temperatures in different selected zones of the package during the thermal test. Fig. II-B-21 shows a graph representing a history of temperature changes in various components of the prototype.

Table II-B-9: Measurements of Highest Temperatures with Thermocouples

Measured Locations		Thermocouple	Highest Temperature (°C)	Time for attaining the highest temperature (counting from end of test)
In-furnace temperature		(a)	818.6	—
External surface of outer receptacle		(b)	794.8	0:00:20
Outer receptacle	Flange on wider side	(e)	407.1	0:06:10
	Flange corner	(d)	343.8	0:08:44
	Flange on narrower side	(c)	394.6	0:07:46
-Inner receptacle	Flange on wider side	(h)	127.1	1:51:54
	Flange corner	(g)	143.7	1:24:50
	Flange on narrower side	(f)	141.9	1:48:16
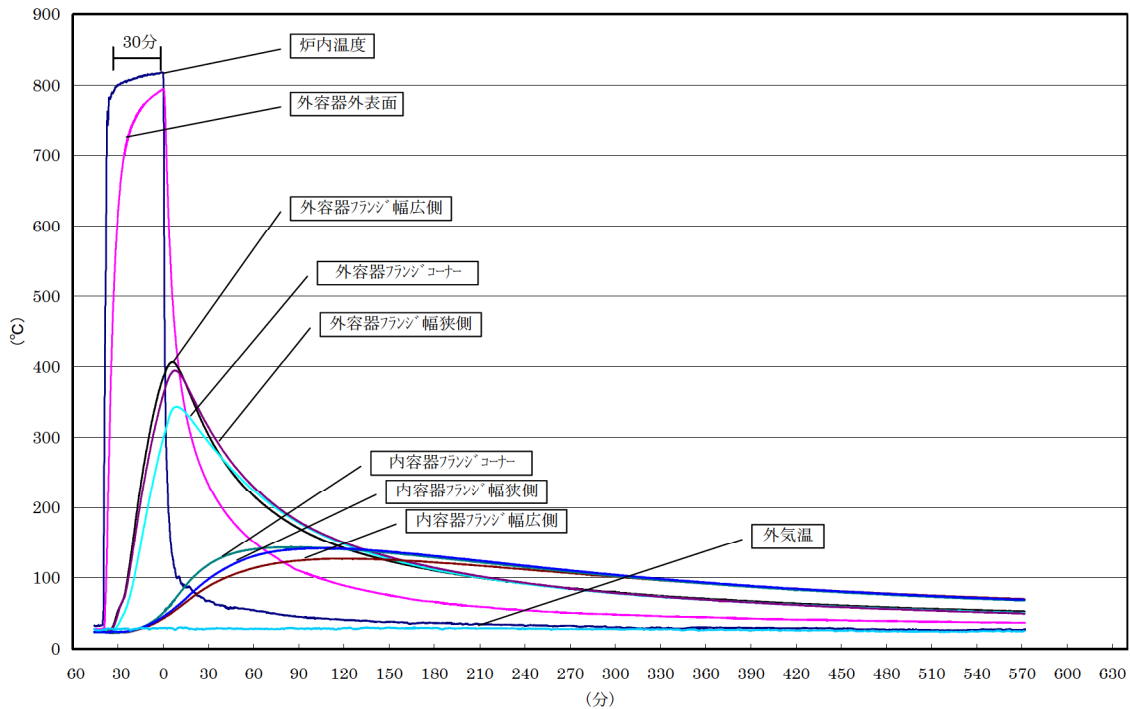
Fig. II-B-21: History Of Temperature Changes in Various Components of The Prototype

In-furnace temperature

External surface of outer receptacle

Flange on wider side of outer receptacle

Flange corner of outer receptacle

Flange on narrower side of outer receptacle

Flange corner of inner receptacle

Flange on narrower side of inner receptacle

Flange on wider side of inner receptacle

External air temperature

(°C) (minutes)

B.5.2.   Evaluation Conditions for the Package

The deformations on the package corner of the package, constituting the principal damage produced during the strength tests, were taken into account. The package is a box-shaped object (rectangular parallelepiped) and has joints of two surfaces on which drop energy is likely to be concentrated. Therefore, these joints are very liable to suffer deformation. Of these joints, eight corners or zones common to three surfaces are most vulnerable to deformation. If the specimen package is dropped in a test in such a way that one of its corner strikes the test target first, maximum deformation will occur. Furthermore, of these eight corners of either receptacle, the four upper corners are located close to the flange which is thought to be most vulnerable to heat during the thermal test. We therefore decided to adopt the package orientation with one of the four upper corners made to strike the test target first in the drop tests, supposing that the specimen would be most

affected by stresses during subsequent tests including the thermal test.

In fact, during the Drop I tests using Prototypes No. 1 and No. 2, deformation reached as far as the flange (refer to Appendix 1 to Chapter II-A). During the main parts (1.2-meter free drop under normal condition, Drop I (9 meters) and Drop II (1-meter target) under Accident Conditions of Transport) of the strength tests using Prototype No. 2, the specimen was dropped in an orientation in which the same corner zone might strike the test target first. These drop tests were followed by the thermal test.

The analytical model took into account the deformations generated in Prototype No. 2 during the strength tests. Most of the portions deformed were included in the conservatively simplified zone in the lid of the outer receptacle as described in section "B.5.1.1 Analytical model."

B.5.3.   Temperatures in Package

Fig. II-B-22 shows the history of temperature changes in the package under the accident conditions of transport described in section "B.5.1.1 Analytical model". Fig. II-B-23 shows the history of temperature changes in an environment of solar radiation of 38°C to which the specimen was exposed before the thermal test. Fig. II-B-24 shows the history of temperature changes during the thermal test and during the cooling period following the thermal test. Fig. II-B-25 shows the evaluation points. In the environment of solar radiation of 38°C, the top surface of the outer receptacle attained equilibrium at 129°C during the third day, and the lateral sides of the outer receptacle reached equilibrium at 62°C on the fifth day. Similarly, the O-ring on the inner receptacle reached equilibrium at 66°C on the fifth day.

The temperature of the O-ring in the inner receptacle started to rise during the thermal test and attained its highest level (170°C) approximately two hours after the start of the thermal test. . Table II-B-10 shows the highest temperatures at different locations of the package under Accident Conditions of Transport. Figs. II-B-26 to II-B-29 show the temperature distributions in the entire analytical model and in the zones of and around the O-ring and spacer at the moment immediately after the end of the thermal test at 800°C for 30 minutes and at the moment when the highest temperature was attained in the O-ring on the inner receptacle.

Throughout the thermal test using the prototype, the dummy pellets in pellet storage box assemblies (contents of the package) and the dummy neutron absorbers presented no change in condition. The thermolabels presented no thermal reaction for 125°C and over. This suggests that the highest temperature in the contents was obviously lower than that (144°C) in the inner receptacle flange. Thus, we will conservatively assume in the subsequent analytical processes that the temperature in the inner receptacle will become identical (170°C) to that in the O-ring on the flange.

Table II-B-10: Highest Temperatures in Different Locations of Package under Accident Conditions of Transport

Analysis Item	Highest Temperature (°C)	
	Before thermal test	After thermal test
Top of outer receptacle	129.0	798.2
Corner of outer receptacle	80.4	800.7
Wider lateral side of outer receptacle	61.8	736.1
Narrower lateral side of outer receptacle	62.2	737.4
O-ring on corner of inner receptacle	65.8	169.3
O-ring on wider lateral side of inner receptacle	66.2	155.3
O-ring on narrower lateral side of inner receptacle	66.5	169.7
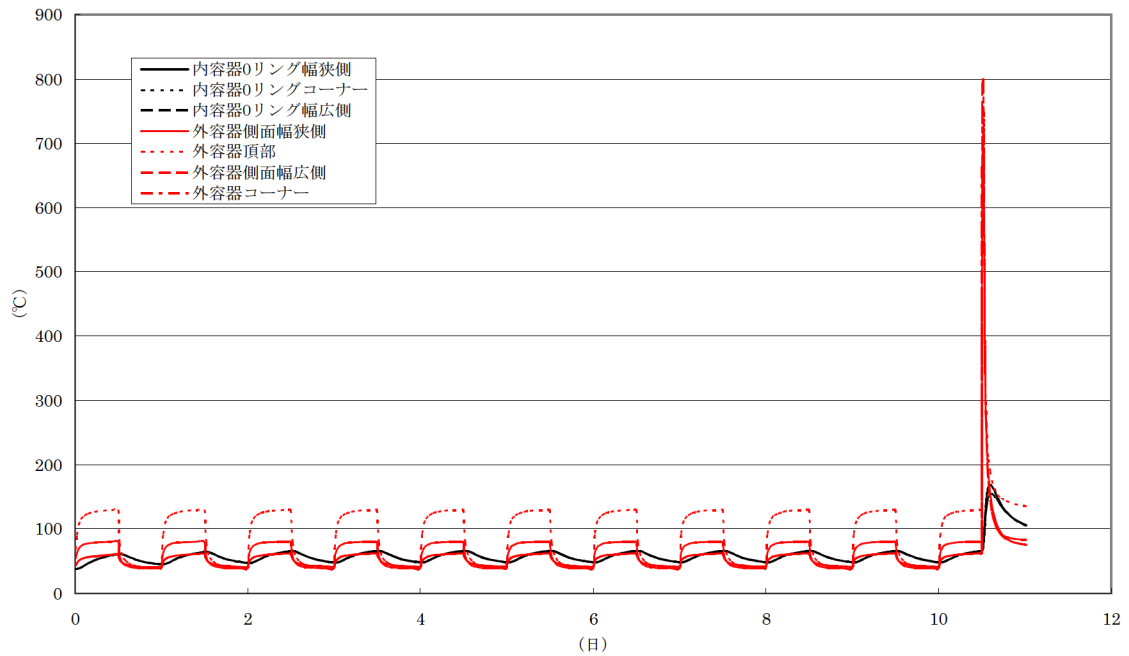
Fig. II-B-22: History of Temperature Changes under Accident Conditions of Transport (entire package)
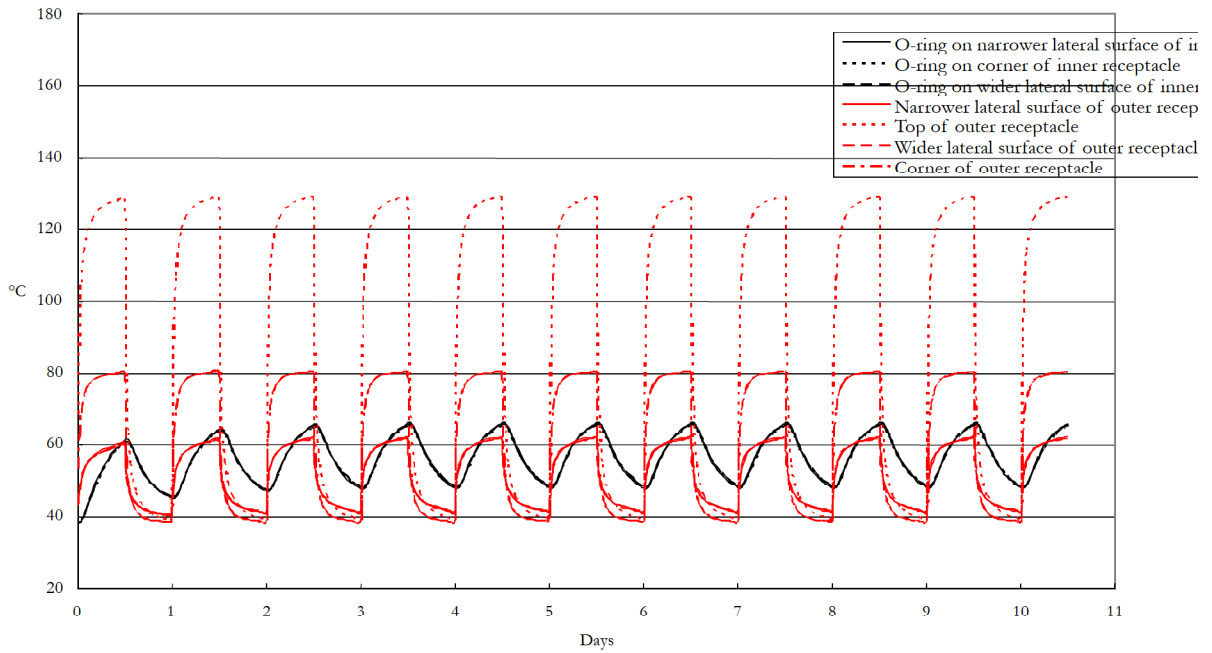
Fig. II-B-23: History of Temperature Changes under Accident Conditions of Transport (before thermal test)
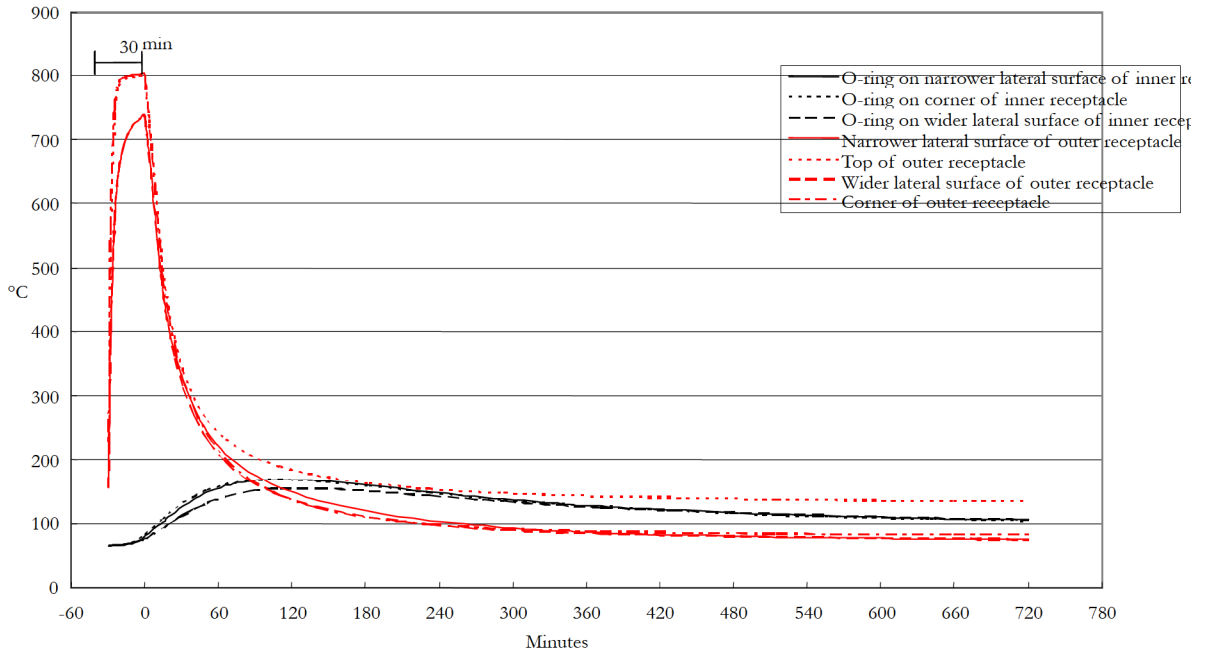
Fig. II-B-24: History of Temperature Changes under Accident Conditions of Transport (during/after thermal test)
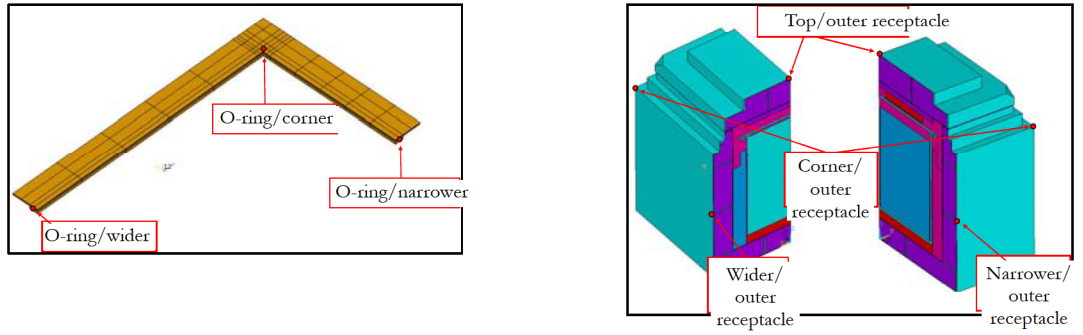
Fig. II-B-25: Temperature Evaluation Points
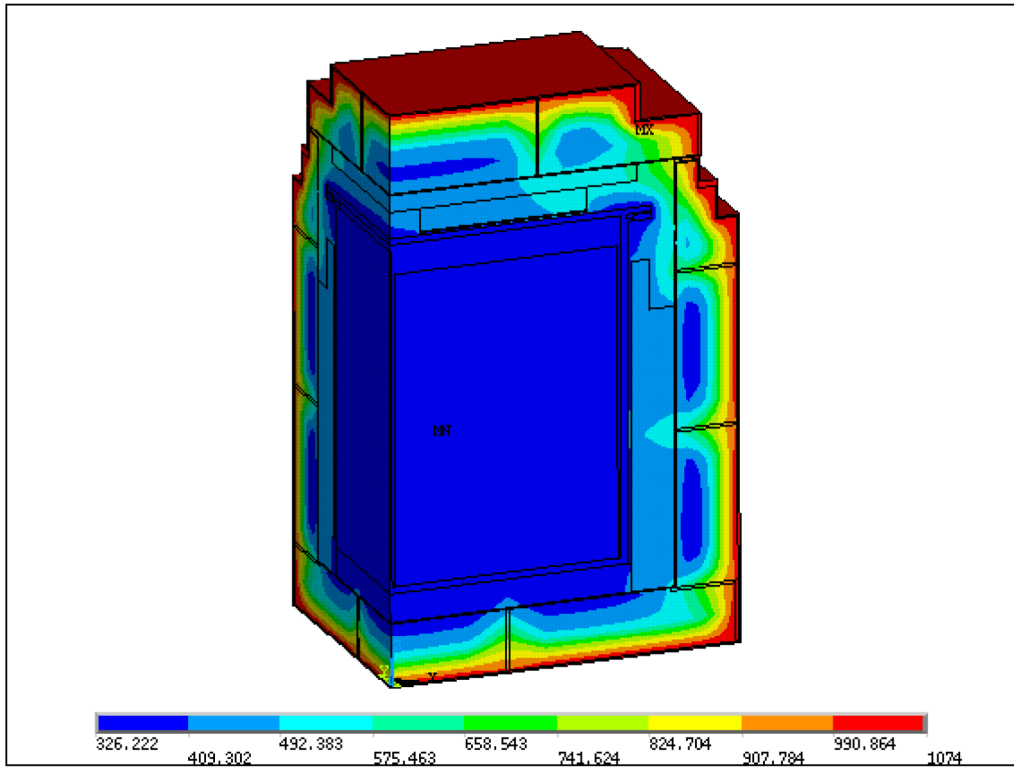
Fig. II-B-26: Temperature Distribution in Package (immediately after thermal test; unit in K)

338.219   338.644   339.069   339.493   339.918
   338.432   338.856   339.281   339.706   340.13
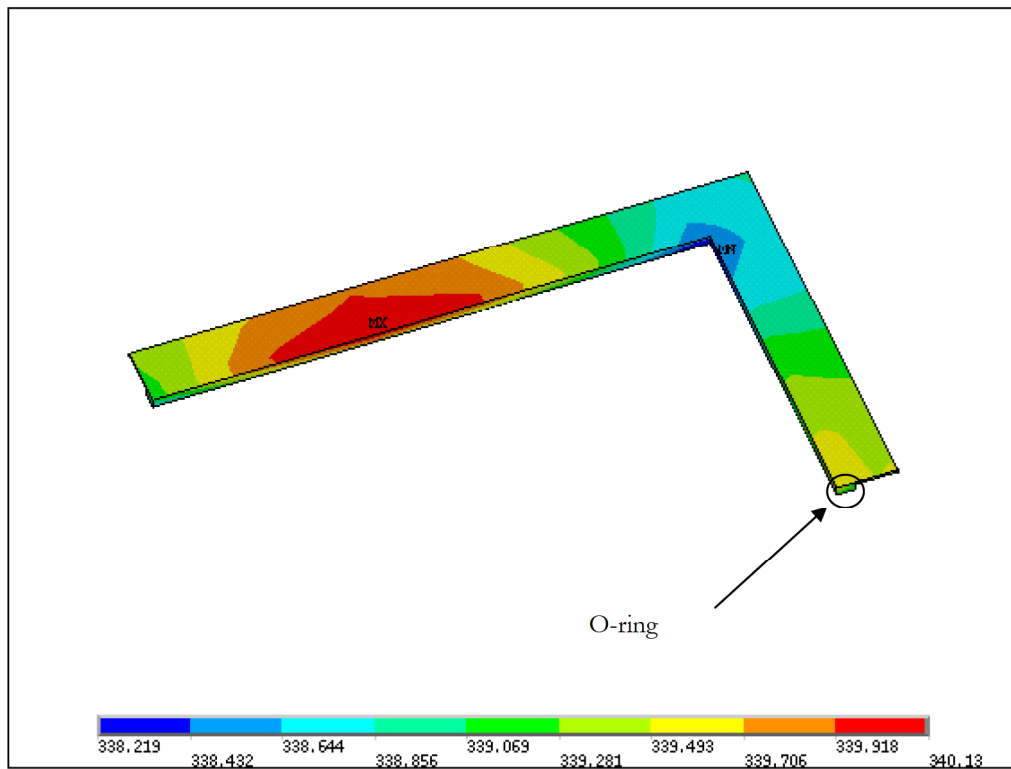
Fig. II-B-27: Temperature Distribution around O-ring Rubber (immediately after thermal test; units: K)

338.158   392.637   447.116   501.595   556.074
   365.397   419.876   474.355   528.834   583.314
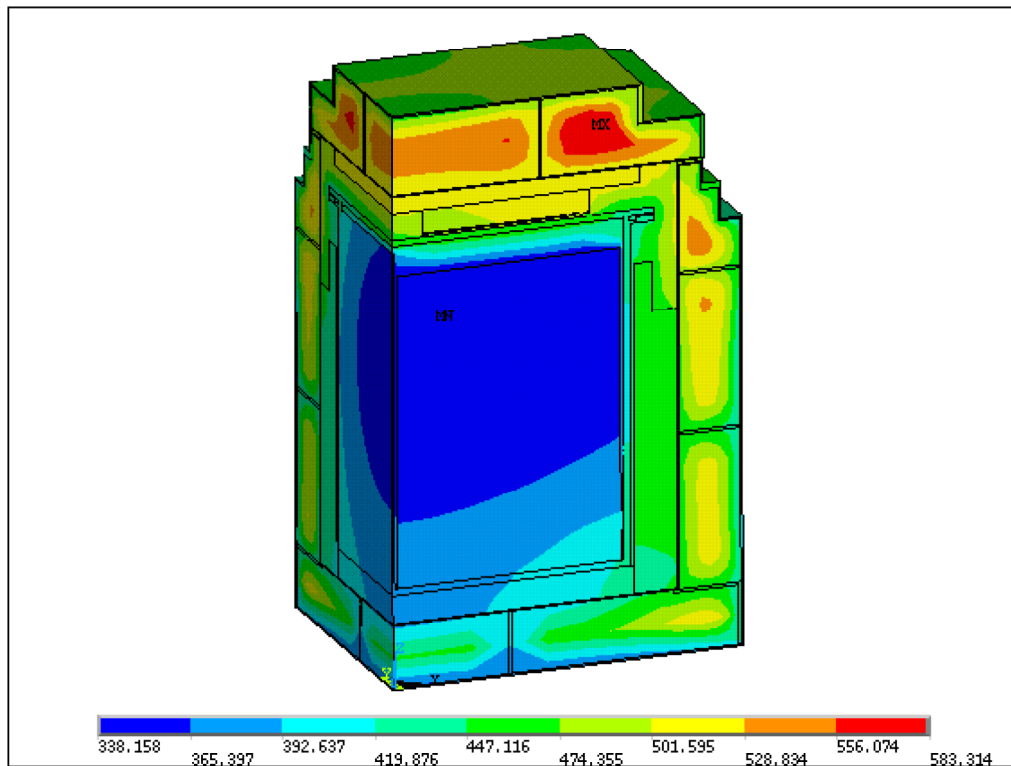
Fig. II-B-28: Temperature Distribution in Entire Package (at the moment when the highest temperature was attained in the O-ring; units: K)
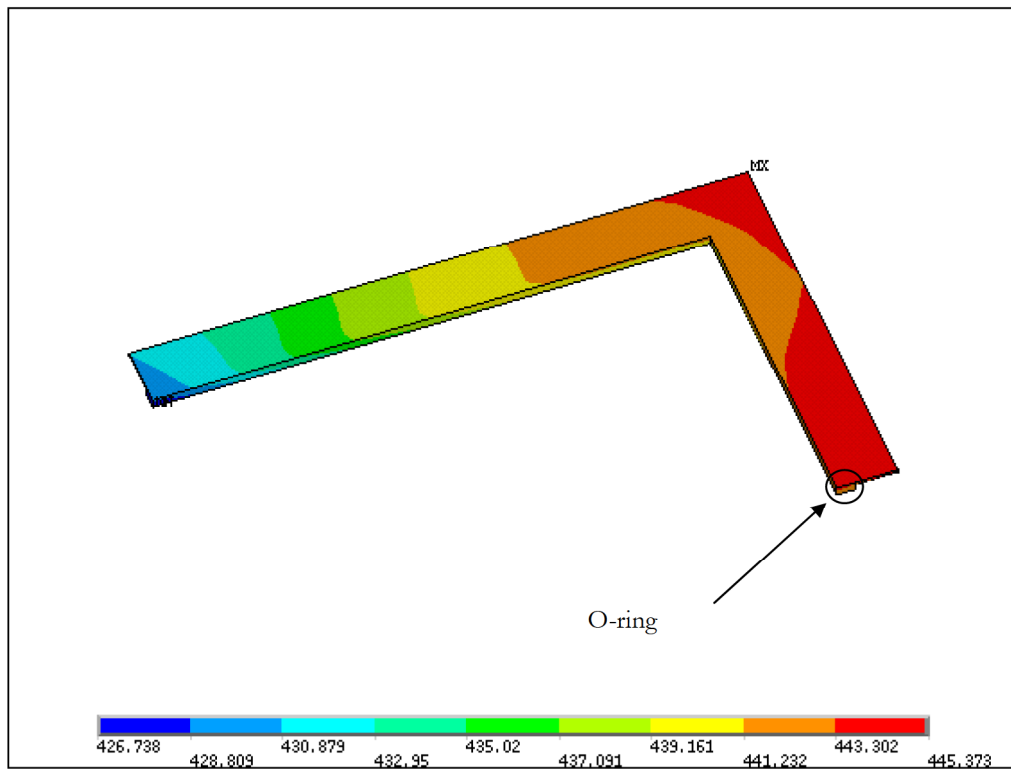
Fig. II-B-29: Temperature Distribution around O-ring Rubber (at the moment when the highest temperature was attained in the O-ring; units: K)

B.5.4. Highest Inner Pressure

As described in section "B.5.3 Temperatures in Package," the analysis for determining the highest inner pressure in the package under Accident Conditions of Transport assumed conservatively that a temperature of 170°C has been reached in the entire inner receptacle which would maintain its original leaktightness. In such cases, the inner receptacle presents an effect of thermal expansion, with a slight increase in internal volume. Such thermal expansion was neglected to stay conservative.

We assume here an initial inner pressure of 101 kPa (absolute) in the inner receptacle at an initial temperature of 0°C. When the temperature in the inner receptacle reaches 170°C, the inner pressure will increase as follows:

$$P = \frac{273+170}{273+0} \times 101 = 164 \quad \text{[kPa]}.$$

Hence, a gauge pressure of 63 kPa (=164–101 [kPa]) which corresponds to the pressure difference between the interior and the exterior of the inner receptacle acts on the internal surface of the inner receptacle.

B.5.5. Highest Thermal Stress

Fig. II-B-26 shows that a large temperature difference is produced among different portions of the package immediately after the thermal test. Nevertheless, as proved in the thermal test using a prototype, no deformation or other damage will occur under thermal stresses.

The inner receptacle is not fixed onto any parts of the outer receptacle. Even in thermally expanded condition, it will not suffer thermal stresses resulting from restraint. Geometrical changes due to thermal expansion will remain small in the inner receptacle. Therefore, the receptacle will not present deformation that might cause displacement or leak of the contents. Moreover, since different metals are not welded together in the packaging, no stresses will occur due to difference of thermal expansion between the package elements.

B.5.6.   Summary of Results and Evaluation

The highest temperatures in different parts of the package under accident conditions of transport are shown in section "B.5.3 Highest Temperatures."

In such conditions of transport, the temperatures of the external surfaces of the outer receptacle can reach 700 or 800°C. Nevertheless, there will be no deterioration in the main structural elements made of stainless steel of the packaging. There will be no occurrences of dissolution (fusion point of the stainless steel: 1398°C) or inflammation, or of deformations that should be taken into account in the subsequent criticality evaluation. . There will be no displacement or leakage of the contents out of the packaging. The temperature of the O-ring may reach 170°C, which is lower than its maximum service temperature (180°C). Furthermore, it has been proved that the material (silicone rubber) of the O-ring does not significantly deteriorate in the heat and aging resistance test at 225°C for 72 hours specified by the applicable JIS standard.

Even if conservatively the temperature of the boronic stainless steel plates as neutron absorbers reaches 170°C in the inner receptacle, no deformation or deterioration that should be taken into account in the criticality evaluation will occur. Moreover, displacement or leakage of the radioactive contents out of the packaging that should be taken into account in the criticality evaluation will not occur in the pellet storage box assemblies (contents).

Assuming that the inner pressure in the inner receptacle is kept in the leaktightness of the receptacle at a temperature equal to the measured highest temperature uniformly distributed in the receptacle, an inner pressure of up to 63 kPa acts on the internal surfaces of the receptacle. Stresses resulting from a rise of the inner pressure will not affect the capability of the packaging, as has been evaluated in section "A.9.2.3 Thermal test."

Table II-B-11 shows the summarized results of the thermal analyses of the package under accident conditions of transport.

Table II-B-11: General Evaluation of Package under Accident Conditions of Transport

Item	Criterion	Results	Evaluation
Highest temperatures:			
Entire package	–	801 °C	No deformation
O-ring *	180 °C	170 °C	Meets the requirements.
Neutron absorber	–	170 °C	No deterioration in performance
Highest inner pressure	–	63 kPa (g)	–
Highest thermal stress	–	No deformation during the thermal test of the prototype	No effect

Note *: No significant deterioration occurred in the heat and aging resistance test at 225°C for 72 hours specified in the standard JIS K 6257.

References:

- IAEA Safety Standards - Regulations for the Safe Transport of Radioactive Material, 2005 Edition, Safety Requirements No. TS-R-1.
- IAEA Safety Standards Series - Advisory Material for the IAEA Regulations for the Safe Transport of Radioactive Material, Safety Guide No. TS-G-1.1.
- Japan Stainless Steel Association, Manual for Stainless Steel
- The Japan Society of Mechanical Engineers, New Edition of Manual for Mechanical Engineering
- The Japan Society of Mechanical Engineers, Data for Heat Transfer Engineering, 4th revised edition
- D.L. Hargman, G.A. Reymann and R.E. Mason, "MATPRO-Version 11 (revision 2) - A Handbook of Materials Properties for Use in the Analysis of Light Water Reactor Fuel Rod Behavior", NUREG/CR-0497, TREE-1280, Rev. 2 (1981).
- N. Ogasawara, M. Shiratori, Yu Qiang and T. Kurahara, Evaluation of coefficient of orthotropic heat transfer of honeycomb material, report No. 99-0011, Bulletin (Title B) of The Japan Society of Mechanical Engineers, vol. 65, issue 639, 1999-11.

Results of Prototype Thermal Test

1. Introduction

The document describes the results of a prototype thermal test carried out on the Type GP-01 transport packaging developed by Nuclear Fuel Industries, Ltd. for containing and transporting pellets of uranium oxides or pellets of uranium oxides mixed with gadolinium, enriched to 5 weight percent or less. The specimen used for this thermal test was the prototype packaging which had been tested for mechanical strengths (drop tests). In those drop tests, the prototype packaging was made to drop and strike the test target and the penetrating bar with one of these corners first to suffer maximum mechanical damage.

2. Description of Transport Packaging

(1) Designation: Type GP-01

(2) Category of package: Type "A" fissile package

(3) Maximum enrichment: 5.0 weight %

(4) Contents: Two pellet storage box assemblies of category either "A" or "B"

(5) Limitations on content loading:
   - When two pellet storage box assemblies "A" are installed: 264 kg or less of UO_2
   - When two pellet storage box assemblies "B" are installed: 200 kg or less of UO_2.

(6) Dimensions:
   - Width: 830 mm
   - Length: 1144 mm
   - Height: 1060 mm.
Note: These values of dimension take into account the legs and the portions of the lifting attachments which protrude from the flush surfaces of the packaging.

(7) Weight
- Gross weight of a packaging: 730 kg or less
- Gross weight of a package (packaging + contents):   1300 kg or less

(8) Principal materials
- Structural material: Stainless steel
   Heat insulators: Ceramic fiber
- Neutron absorbers: Boronic stainless steel
- Shock absorbers (honeycomb element): Aluminum
- Rod bolts: Chrome molybdenum steel

- Nuts: Stainless steel

- Spacers and skids: Silicone rubber, neoprene rubber, urethane rubber.

(9) General Characteristics

Fig. II-B.App1-1 shows a general view of the package. The transport packaging consists of an outer receptacle and an inner receptacle which can be retrieved from the outer receptacle. The outer receptacle has a multi-caisson-shaped double structure composed of frames, inner plates, and outer plates. The voids between the inner plates and the outer plates are filled with a heat insulating material (ceramic fiber). The lid of the outer receptacle has the same structure as that of the body of the outer receptacle. The lid of the outer receptacle is firmly joined to the body of the outer receptacle by means of rod bolts. Fire-resistant rubber blocks are installed on the back of the lid of the outer receptacle. When the ambient temperature exceeds the normal level, these rubber blocks will expand to occlude voids in the outer receptacle.

The body of the inner receptacle as well as the lid of the inner receptacle has a caisson-shaped single structure composed of thick stainless steel plates. An O-ring is provided for sealing on the flange surfaces. Like the outer receptacle, the lid of the inner receptacle is joined to the body of the inner receptacle by means of rod bolts. One of the boronic stainless steel plates is installed as partition between two pellet storage box assemblies (contents).

The packaging is designed to store two assemblies of pellet storage boxes which contain pellets (minimum elements of nuclear fuel). To construct an assembly, pellet storage boxes are stacked alternately with partitions which are penetrated by six pillars. The stacks of pellet storage boxes are fixed with nuts at the threaded top of the pillars. All the partitions except for the uppermost and lowermost one are boronic stainless steel plates which serve as neutron absorbers.

Two configurations can be selectively adopted for the pellet storage box assembly depending on the type of the pellet storage box: assembly "A" consisting of twelve (12) pellet storage boxes which can store up to 11 kg of UO_2 per box and assembly "B" consisting of five (5) pellet storage boxes which can store up to 20 kg of UO_2 per box. An assembly "A" has a maximum capacity of 132 kg of UO_2 and an assembly "B" has a maximum capacity of 100 kg of UO_2.

Lifting attachment

Lid of Outer Receptacle

Fusible plug

(166)

Flange

Lid of Inner Receptacle

Pellet storage box assembly

Body of Outer Receptacle

Outer receptacle rod bolt

Inner receptacle rod bolt

Flange spacer

Aluminum honeycomb element

Body of Inner Receptacle

Assembly cover

Inner plate

(894)

Outer plate

Insulator

Fork guard

(1134)

Leg

(820)
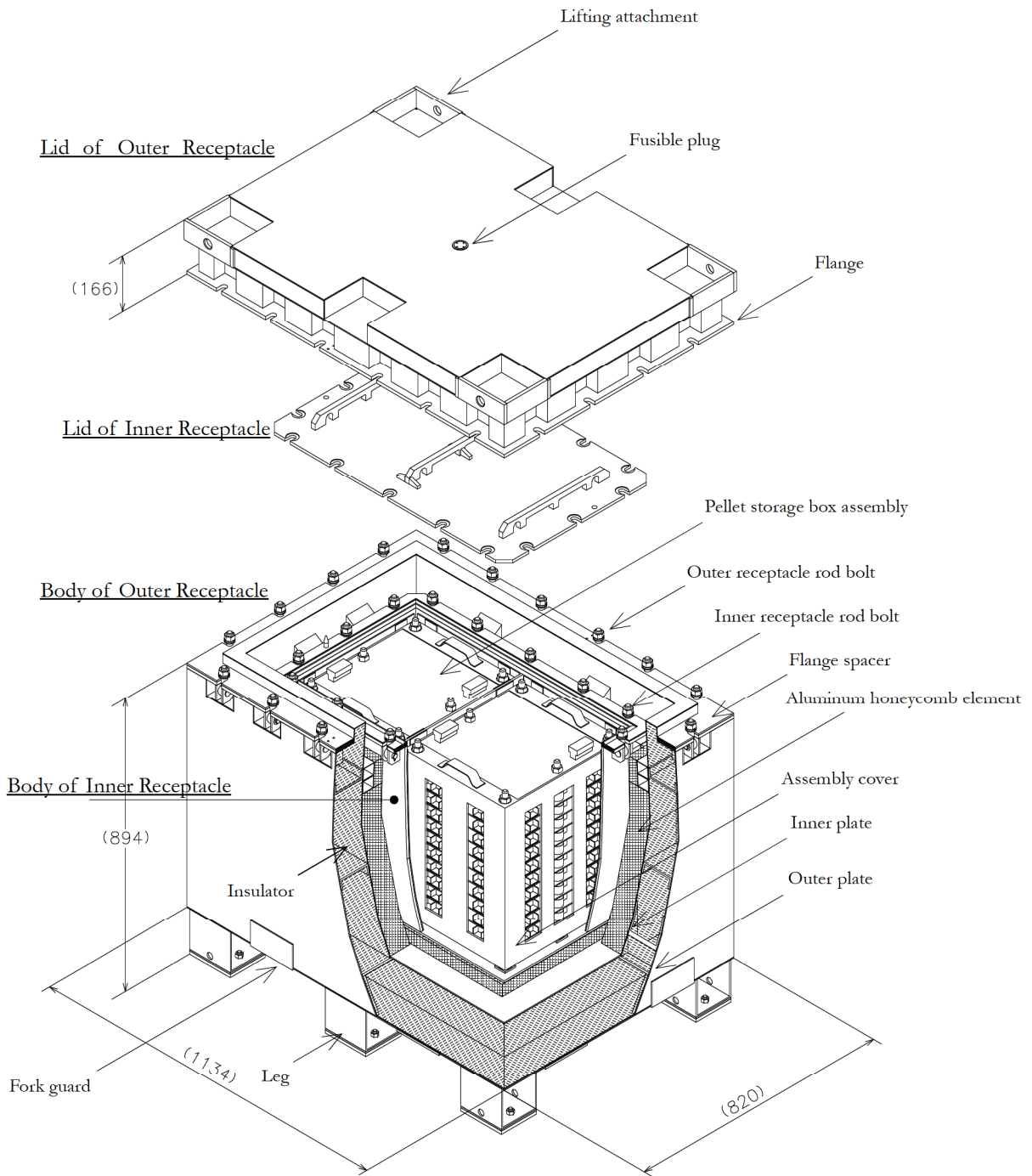
Fig. II-B.App1-1: General View of Type GP-01 Transport Package

3. Tests

3.1. Prototype Packaging

Prototypes No. 1 and No. 2 were used for the preceding drop tests. Prototype No. 1 was mainly used for examining and verifying orientations of the package to be adopted for the main part of the drop tests. Prototype No. 2 was used for the main part of the thermal test. During the drop tests, this prototype was dropped in the orientation determined in the preliminary tests with Prototype No. 1. This orientation was supposed to cause maximum damage to the upper corner of the package. The specimen was released from a height in such an orientation that this zone might strike the test target plate or the penetrating bar first. This upper corner was chosen for maximum damage because such orientations would concentrate the drop energy on it to produce significant deformation and because this portion of the package was located close to the flange which was regarded most vulnerable to thermal stress during the thermal test and would present opening under drop energy to form a path for heat during the thermal test.

Appendix 1 to Chapter II-A shows the detail of the results of the prototype drop tests. During these tests, deformations occurred in the package up to the flange. No opening was produced in the flange and none of the rod bolts for tightening the lid on the body of receptacle were pulled out or fractured. The lid of the outer receptacle stayed in its required position. Small cracks were produced in the welds of the lifting attachment, and the insulator got partially exposed but was not lost at all (Photos B.App1-1 to B.App1-3).

In the interior of the outer receptacle, the aluminum honeycomb elements were partially deformed. The inner receptacle and the pellet storage box assemblies suffered no significant deformation (Photos B.App1-4 to B.App1-6).

The prototype packaging (No. 2) was subjected consecutively to the drop tests and the thermal test. This prototype packaging has essentially been designed with characteristics and constructions identical to those of a production model except for some small differences. The differences from a production packaging will be described in the following paragraphs. Two pellet storage box assemblies "A" were used as contents of the package during the drop tests because of the greater loading capacity of the type of assembly. The same dummy contents were used in the thermal test.

(1) Dummy contents

The prototype to be subjected to the thermal test contains lead rods (dummy pellets) instead of real pellets of uranium oxides since a packaging containing real pellets of uranium oxides cannot be subjected to physical tests. The total weight of the dummy pellets was adjusted to become greater than the maximum possible total weight of real pellets that can be loaded in the pellet storage boxes. Lead has thermal properties which differ from those of uranium oxides. Therefore, the thermal analyses which will be carried out on the bases of results of the thermal test will use corrected data.

(2) Attaching thermocouples (Photo B.App1-7 to B.App1-14)

Upon completion of all the drop tests, Prototype No. 2 was sent to a facility of the company Sakaguchi Seisakusho. The accelerometers used for drop tests were removed. Thermocouples, thermo-labels and thermo-paint were applied instead to the package for temperature measurements. It was imperative, but not possible in the normal way, to remove the lid of the outer receptacle to attach these measuring means. A rod

bolt located near the deformed zone of the outer receptacle could not be removed in the normal way and had to be cut with a grinder. Opening or closing of the inner receptacle was possible only by loosening the rod bolts.

Fig. II-B.App1-2 shows the locations where thermocouples were attached. Thermo-labels were applied to the flange of the inner receptacle where lower temperatures were likely to prevail. Thermo paints were applied to the internal side of the flange of the outer receptacle where higher temperatures were likely to be produced during the thermal test.

The model of thermocouple used was suitable for measurement of temperatures during the thermal test since it is capable of measuring 1000°C and over. The large diameter of this model is suitable for avoiding short-circuiting due to the heated sheath which is exposed to flames in the furnace. The sheath was covered with a ceramic fiber heat insulator before the thermal test.

The thermo-label is capable of indicating a range of five temperature change points. Three kinds of thermo-labels which correspond to three temperature ranges were prepared. Five types of thermo-paint were prepared. They were applied to surfaces which would be exposed to higher temperatures.

The technical data of the thermocouples, thermo-labels and thermo-paints are shown below.

Thermocouples

- Manufacturer: Sukegawa Denki Company, Ltd.

- Type/category: Type T35, category K

- Sheath dimensions: φ4.8mm × 15000 mm (length)

Thermo-labels and Thermo-paints

- Manufacturer: Nichiyu Giken Kogyo Co., Ltd.

- Types of thermo-label: 5E-125 (125-160°C), 5E-170 (170-210°C),

                            5E-210 (210-250°C)

- Types of thermo-paint::   No. 25 (250°C), No. 31 (310°C), No. 36 (360°C), No. 41 (410°C), and No. 45 (450°C)

Thermocouples installed:
- In the atmosphere of the furnace: a
- On the external surface of the outer receptacle: b
- On the inner side of the flange of the outer receptacle: c, d, and e
- On the flange of the inner receptacle: f, g, and h.
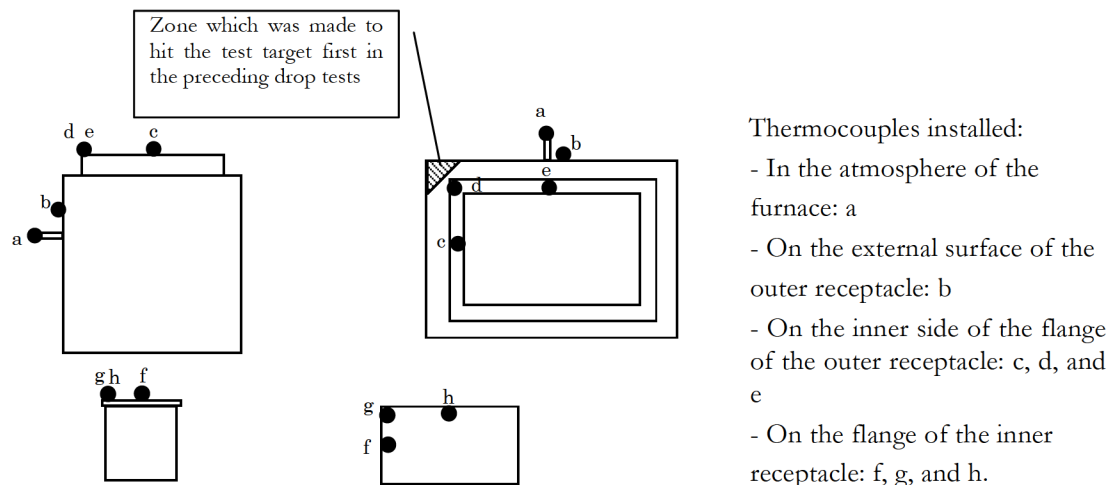
Fig. II-B.App1-2: Locations of Thermocouples

(3) Additional measures for installing thermocouples

The portion of honeycomb element which had been set aside for avoiding contact with the accelerometers during the drop tests was reworked: one end was cut off for providing room for installing thermocouples and was reinstalled in the void. The bracket for accelerometer which had been attached for the preceding drop tests was removed.

The hole arrangement which had been used for the cabling of the accelerometer was reused for routing the thermocouples. This routing hole is 30 mm in inner diameter. The portion of the insulator concerned had been removed and a steel pipe had been welded on the hole (Photo B.App1-15). When the installation of thermocouples was complete, the hole was plugged with fragments of ceramic fiber insulator set aside when the hole was made, to prevent flames from entering.

To fix the sheathed sections of the thermocouples, small thin stainless steel strips were spot-welded on the receptacles. For the sheathed section of the thermocouples for O-ring on the inner receptacle, small pieces of stainless steel rectangular pipe were spot-welded on the pellet storage box assemblies, and these fragments were covered with small pieces of stainless steel plate. All these fixing materials are small and can be neglected for thermal consequences.

(4) Dummy neutron absorbers

Instead of real neutron absorbers made of boronic stainless steel plate for inner receptacle and pellet storage box assembly, stainless steel plates of the same dimensions were used. Use of these dummy neutron absorbers will not affect the outcome of the thermal test.

(5) Other measures taken

The weight adjusting materials used for the preceding drop tests were removed when the thermocouples were installed.

(6) Differences of prototype packaging from production model of packaging

The characteristics of a definitive production model of packaging will be fixed only when several improvements in features and handling procedures have been identified after completion of manufacture of these prototype packagings and all the tests described in this document have been taken into account. Table II-B.App1-1 shows the modifications in the prototype packaging which have thus been adopted. These modifications will not lead to reduction of the margin of safety for the thermal characteristics of the production model of the type GP-01 packaging.

Table II-B.App1-1: Modifications of Prototype Packaging Adopted for Production Model

Element	Modifications	Improvements	Consequences of Modifications
Outer receptacle flange spacer	Spacer width was reduced to allow the spacer to avoid the uneven weld surface on the flange. The dimensions around the rod bolts were increased.	Adhesiveness during construction was improved. Interference was eliminated for better workability.	The element concerned does not contribute to safety.
Lifting attachment	Sharp portions on the bottom end of the corners were chamfered additionally.	Operational safety was improved.	This modification does not affect the strength.
Outer receptacle positioning pin	Additional machining for better flatness.	Workability during tightening was improved.	The element concerned does not contribute to safety.
Process of attaching outer receptacle positioning pin	Nuts were welded on the back surface of the flange: portions of the flange were threaded additionally.	Machinability during construction was improved.	The element concerned does not contribute to safety.
Aluminum honeycomb element	Honeycomb elements were no longer fixed with an adhesive, but with a dedicated cover and screws.	Maintainability was improved. Repairability was improved.	The characteristics of the honeycomb element were not modified. This modification will not affect results of drop tests.
	Fixing process was changed to eliminate the gaps between blocks	Possibility of entry of foreign matter into the gaps was eliminated.	
	Fixing method for the aluminum plate cover on the honeycomb plates was modified to avoid use of adhesive agent.	Maintainability was improved. Repairability was improved.	
	The width of honeycomb for the narrower lateral surface was changed.	Non-functioning zones were removed.	The zones concerned do not work. The modification does not affect test results.
Urethane rubber guide	MC nylon was applied to the tip of the urethane rubber guide.	Slidability during introduction/retrieval of the inner receptacle was improved.	The element concerned does not contribute to safety.
Lid of the outer receptacle	Internal frame gaps were modified and reinforcing plates were added. Spacing for ventilation holes was modified.	Strength under severe service conditions was enhanced.	The strength of the outer receptacle frame is enhanced.
Flange	Flange clearance was reviewed.	Machinability during construction was improved. Workability was improved.	Strength is not affected.
Leg	Bottom corner was chamfered.	Positioning for two-stage stacking was facilitated.	The element concerned is not
Dimensions of skid	Skid was shortened.	Positioning for two-stage stacking was facilitated.	The element concerned is not

Process of attaching a skid	Nut was no longer welded on the leg, but a threaded boss was imbedded.	Maintainability was improved. Repairability was improved.	The element concerned is not
Edge of lid of the inner receptacle and lid rod	Additional chamfering was carried out.	Workability was improved. Operational safety was enhanced.	This modification does not affect the strength.
External surface of the inner receptacle	Mirror finishing is no longer carried out.	Maintainability was improved.	This modification does not affect the strength.
Spacing between rod bolts for inner receptacle	Modification as a result of the modification of frame gaps of the lid of the outer receptacle	Interference during collision is prevented.	This modification does not affect the strength.
Rod bolt seat on inner receptacle	Rod bolt seat was designed as a longer hole.	Workability was improved.	This modification does not affect the strength.
Threaded portion of pillar for pellet storage box assembly	Threaded portion was made longer.	Dimensions after tightening were optimized.	This modification does not affect the strength of the assembly.
Process of fixing pillar for pellet storage box assembly	Welding was replaced by a detachable structure.	Maintainability was improved. Repairability was improved.	This modification does not affect the strength of the assembly.
Process of lifting pellet storage box assembly	"Insert an eye bolt into the threaded hole" was replaced by "Attach an eye nut to the pillar."	Design was simplified.	This modification does not affect the strength of the assembly.
Eye nut holder	Eye nut holders were added on the top surface of the pellet storage box assembly	Workability was improved.	This addition of elements does not affect the gross weight of the package.
Rubber block for positioning pellet storage boxes	Lugs were added at both ends.	Workability was improved.	This modification does not affect the storage box's pellet retaining capability.
Pellet storage box assembly cover	The width of the handle was reduced.	Workability was improved.	The element concerned does not contribute to safety.

Note: Since each or the sum of these modifications does not affect the thermal characteristics of the package, the validity of the test results will be maintained.

3.2. Test Facility

A heat treatment furnace installed at Kawanetsu Company was used as our thermal test. Kawanetsu has several heat treatment furnaces of different sizes. That we selected was the No. 3 furnace (smaller furnace) because it takes short time for return operation for overshoot and downshoot and has a sufficient capacity for storing the prototype packaging. The small furnace presents steep temperature drop while being opened after preheating process. But this characteristic is an advantage at the same time because it can be controlled easily for raising the temperature (Photo B.App1-16).

Technical Data on Test Facility: No. 3 furnace, annealing furnace with double carriage
- Internal dimensions: W 2.08 m × H 1.95 m × L 7.1 m (effective dimensions: W 2.0 m × H 1.2 m × L 6.0 m)
- Fuel: Utility gas
- Treatment temperature: Service temperatures: 625°C to 950°C; 1300°C maximum
- Temperature tolerance: ± 10°C
- Capacity: 20 tons/charge (maximum).

3.3. Method for Thermal Test

(1) Method

As part of the thermal test under accident conditions of transport specified by Appendix 12 to the Public Notice, a specimen of fissile package should be exposed to:
- An environment of solar radiation kept at 38°C until it presents a constant surface temperature change pattern,
- An environment of 800°C for 30 minutes, and then
- An environment of solar radiation of 38°C for cooling.

It is not realistic and possible to implement the whole set of conditions in our thermal test using a prototype. Thus, we decided to expose the specimen to an environment of 800°C for 30 minutes and then cool it in the ambient temperature. An analytical model created on the basis of collected data was subjected to analysis for integrating the results of the preceding tests. And then analytical calculations are carried out with all the three conditions to determine temperatures in the package.

The thermal test was preceded by a preliminary temperature rise test and a delivery procedure verification rehearsal. For the preliminary temperature rise test, the following procedure was applied (Photo B.App1-17):

① Raise the temperature in the furnace up to 1000°C, and then keep the operating conditions of the furnace for at least 60 minutes.

② Manipulate a forklift truck to lift the specimen and make it ready for delivery of the specimen in front of the furnace; open the port of the furnace and pull out the carriage.

③ Place the prototype at the predetermined location on the carriage and immediately introduce the prototype on the carriage into the furnace. Close the port of the furnace.

④ Set the temperature to 820°C±20. Once a temperature of at least 800°C is attained in the furnace and on the thermocouples installed for measuring in-furnace temperatures, wait 30 minutes while keeping the current operating conditions of the furnace.

⑤ Retrieve the specimen in a sequence opposite to the procedure for introducing it, and subject the specimen to natural cooling at the room temperature until the next day.

(2) Collecting temperature data

Temperatures in the prototype were measured with nine (9) thermocouples: eight installed on the Prototype "A" and one at a location outside the package in the furnace. The measurement was started shortly before the specimen was introduced into the furnace and ended in the morning of the next day. A sampling interval of two seconds was adopted for each measuring point (Photo B.App1-18).

3.4.   Description and Interpretation of Thermal Test (Photos B.App1-19 to B.App1-26)

The urethane rubber on the sole of the legs started to burn intensely in flames immediately after being placed on the carriage of the furnace. The thermocouples for measuring in-furnace temperatures indicated 800°C nine minutes after the furnace port was closed, and the test facility was maintained in the current operating conditions for further 30 minutes. In view of the fact that the thermocouple for furnace control indicated an attainment of 800°C earlier than those installed on the prototype, the temperature of the entire atmosphere of the furnace must have uniformly attained 800°C.

Retrieved from the furnace, the prototype was still burning red on the carriage for a short time until it cooled down. The general surfaces of the package were oxidized in black but half covered with a white substance on its upper portion around the flange. This white substance was estimated to be ash of the burnt rubber parts. The prototype was checked visually. No change in shape was observed in the prototype. Dissolution or deformation resulting from burning was not found in the appearance of the specimen. The molten solder in the fusible plugs showed that they had worked correctly. Small flames were seen through the thermocouple routing hole but went out soon. These flames were presumably of the tape used for filling the hole with fragments of insulator.

Table II-B.App1-2 shows the highest temperatures attained at various locations during the thermal test. Fig. II-B.App1-3 shows the fluctuations of the recorded temperatures.

Table II-B.App1-2: Highest Temperatures Recorded on Thermocouples

Measured Locations		Thermocouple	Highest Temperature (°C)	Time for attaining the highest temperature (counting from end of test)
Interior of furnace		(a)	818.6	—
External surface of the outer receptacle		(b)	794.8	0:00:20
Outer receptacle	Flange on wider side	(e)	407.1	Outer receptacle
	Flange corner	(d)	343.8	
	Flange on narrower side	(c)	394.6	
Inner receptacle	Flange on wider side	(h)	127.1	Inner receptacle
	Flange corner	(g)	143.7	
	Flange on narrower side	(f)	141.9	

Fig. II-B.App1-3: Evolutions of Temperatures (1/2)

Fig. II-B.App1-3: Evolutions of Temperatures (2/2)

Flange on wider side of the outer receptacle

Corner flange of the outer receptacle

Flange on narrower side of the outer receptacle

Corner flange of the inner receptacle

Flange on narrower side of the inner receptacle

Flange on wider side of the inner receptacle

℃

Minutes
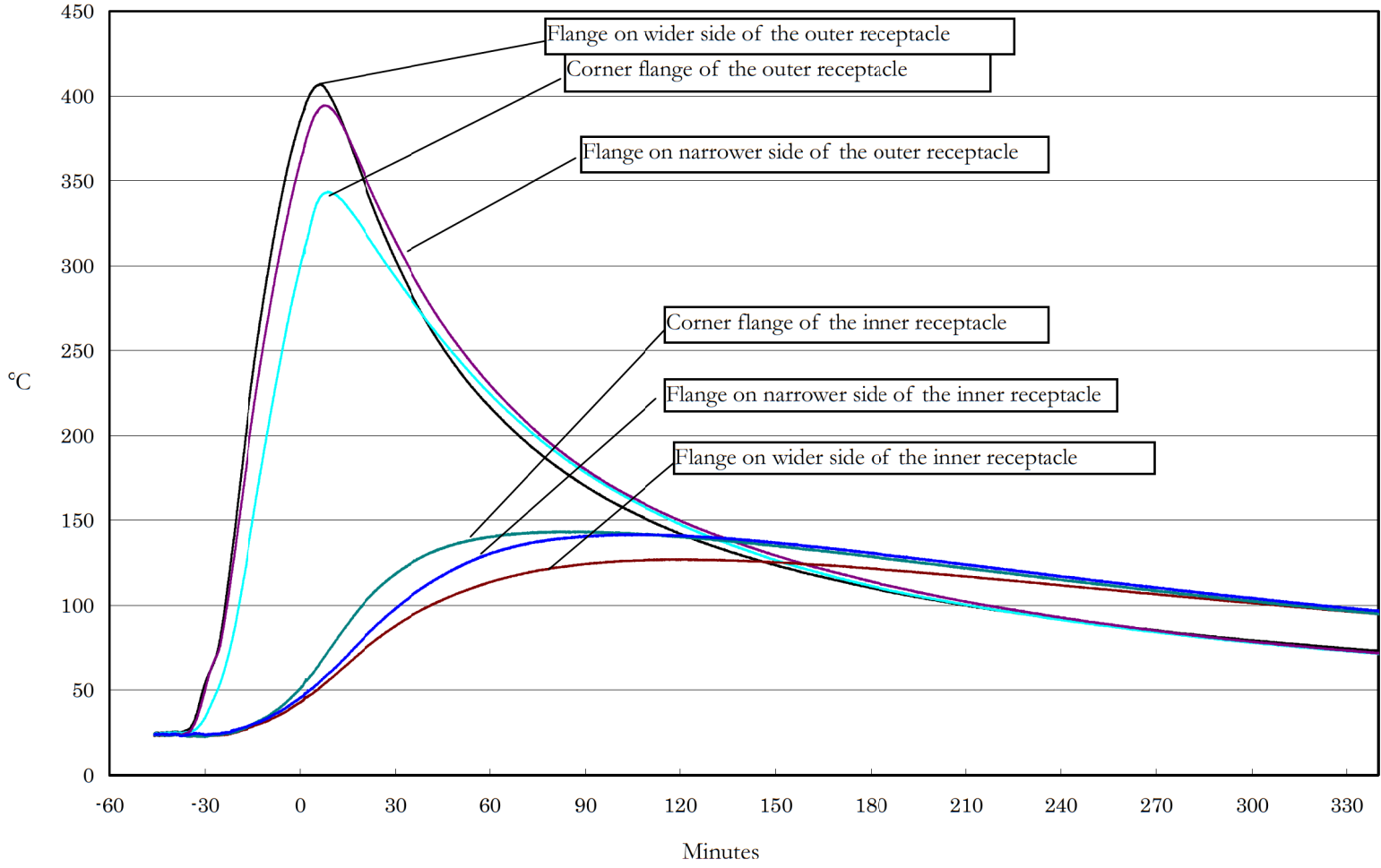
4. Inspections after Thermal Test

After the thermal test was complete, the specimen was opened at NFI's facility (Kumatori Works) to inspect its interior. The outer receptacle was once opened to install the thermocouples before this test. The lid was easily removed and no alteration in shape was observed in the general appearance of the package.

(1) The silicone rubber was found to have been carbonized or transformed into ash on the outer receptacle flange after burning (Photo B.App1-27).

(2) The external surfaces of the inner receptacle turned brown and the internal surface of the outer receptacle turned gray. Nevertheless, there was no sign that suggested entry of flame into the specimen (Photo B.App1-28).

(3) The 250°C to 450°C thermo-paints applied to the back of the inner receptacle turned brown. Exact description of the color changes is not possible (Photo B.App1-29).

(4) Expanded and altered fire-resistant rubber was found adhering to the top of the outer receptacle body, which suggests that the rubber material worked effectively to plug up the voids in the receptacle (Photos B.App1-30 to B.App1-34).

(5) The 250°C thermo-paints changed their color and the 310°C thermo-paints did not change their color. At several locations, some thermo-paints only changed their upper portion of their color. in different temperature zones. These partial changes of color were attributed to expanded fire-resistant rubber applied to the outer receptacle flange: it probably came over the internal surface of the outer receptacle and the thermo-paints. This fire-resistant rubber was estimated to have been excessively heated; those thermo-paints came into contact with the expanded fire-resistant rubber and changed their color; and accordingly they showed temperature indications different from those of those not affected by the expanded rubber. This explains how the thermo-couples c, d, and e showed results (343.8°C to 407.1°C) different from those indicated by these thermo-paints affected by the expanded rubber, and how the thermocouple at the receptacle corner which was not covered with fire-resistant rubber indicated values lower than those indicated by the other ones (Photo B.App1-35).

(6) Most of the thermo-labels (for 125°C to 250°C indication) applied to the rubber plate on the inner receptacle flange adhered once to the back of the inner receptacle lid and then were separated from it. These thermo-labels touched the rubber plate as well. They probably show the temperature of the inner receptacle lid. All the thermo-labels indicate that the temperature around them reached 200°C or 210°C. The thermo-labels applied to the entire zone along the inner receptacle flange indicated similar states of temperature. This suggests that the temperature distribution was uniform in the inner receptacle and was not affected by the presence of the hole for thermocouple routing (Photos B.App1-36 to B.App1-39).

(7) The spacers (silicone rubber plates) on the inner receptacle flange kept their elasticity though they turned

brown on their perimeter similarly to the external surfaces of the inner receptacle (Photo B.App1-40).

(8) The O-ring on the inner receptacle flange also kept it elasticity and did not alter their properties and color (Photos B.App1-41 to B.App1-44).

(9) The contents and the interior of the inner receptacle did not alter their color and there was no physical evidence proving high temperatures in the interior and contents of the inner receptacle (Photo B.App1-40).

(10) The thermo-labels applied to the dummy neutron absorbers (stainless steel plates) showed no reaction and demonstrated that the temperature of the dummy neutron absorber did not attain 125°C (Photos B.App1-45 to B.App1-48).

4.3.   Summary of Test Results

The thermal test caused change in color of the external surfaces of the outer receptacle. The deformations and damage which had been generated during the preceding drop tests were not aggravated during the thermal test. The thermal load of the test caused no holes in the specimen and no damage to the tightening rod bolts. The outer receptacle lid did not change its initial required position. The silicone rubber spacers on the flange were carbonized and turned into ash.

The internal surfaces of the outer receptacle and the external surfaces of the inner receptacle changed their colors but suffered no additional deformations and present no trace of ignition.

The dummy contents and interior of the inner receptacle only changed their colors but suffered no significant change or deformation during the thermal test. The highest temperature recorded of the silicone rubber O-ring on the inner receptacle flange was lower than 144°C. This O-ring kept its required elasticity. The type of O-ring adopted for this thermal test is a proven product which has a maximum service temperature of 180°C and has passed the heat and aging resistance test at 225°C for 72 hours specified by the applicable JIS standard. The temperature of the dummy contents did not exceed 125°C, proving that it was not affected by the thermal load during the thermal test.
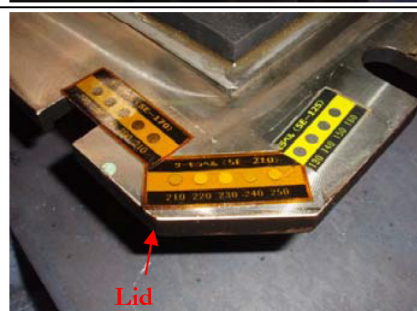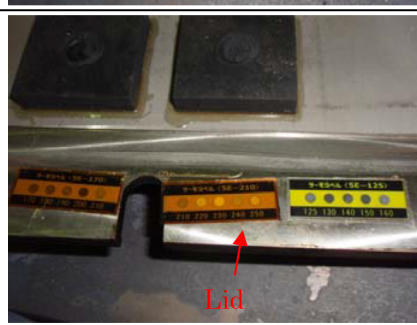
5.   Conclusion

The specimen (prototype packaging) which had been tested repeatedly for strength against drop impact was subjected to the 30-minute thermal test at 800°C. The thermal stresses imposed by the test caused loss by burning of the rubber material applied to the external surfaces of the package, but not significant changes in the package. These results show that the prototype packaging tested has the required heat resistance. This thermal test was carried out under conditions which partially differ from those required for ambient temperature and solar radiation heat by the Public Notice. For this reason, the values of the measured temperatures will be corrected by the subsequent thermal analysis. Results of analytical corrections will be taken into account in the definitive evaluation of the prototype.

Photo B.App1-1: General view of the Package which underwent drop tests		Photo B.App1-2: General view of the Package which underwent drop tests (from another angle)	
Photo B.App1-3: Cleft in the weld on the corner (O)		Photo B.App1-4: Interior of the outer receptacle	
Photo B.App1-5: External view of the inner receptacle	Zone behind the outer receptacle corner which was made to strike the test target or penetrating bar first in the preceding drop tests	Photo B.App1-6: General view of pellet storage box assembly	
Photo B.App1-7: Thermocouple (external surface of the outer receptacle and surrounding atmosphere)		Photo B.App1-8: Thermocouple, thermo-label, and thermo-paint (corner of the inner/outer receptacle)	
Photo B.App1-9: Thermocouple, thermo-label, and thermo-paint (narrower-side flange of the inner/outer receptacle)		Photo B.App1-10: Thermocouple, thermo-label, and thermo-paint (wider-side flange of the inner/outer receptacle)	
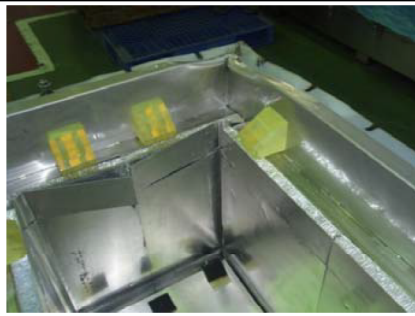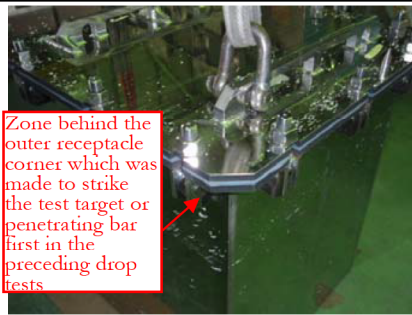
Photo B.App1-11: Positions of thermocouples on the inner receptacle		Photo B.App1-12: Thermocouple routing	
Photo B.App1-13: All thermocouples installed on the inner receptacle		Photo B.App1-14: All thermocouples installed	
Photo B.App1-15: Thermocouple routing hole		Photo B.App1-16: Interior of the furnace (before temperature raising)	
Photo B.App1-17: Test rehearsal for checking the setting position for the specimen		Photo B.App1-18: Measuring instrumentation	
Photo B.App1-19: Carriage retrieved from the furnace in which the required temperature has been attained		Photo B.App1-20: Setting the specimen on the carriage	
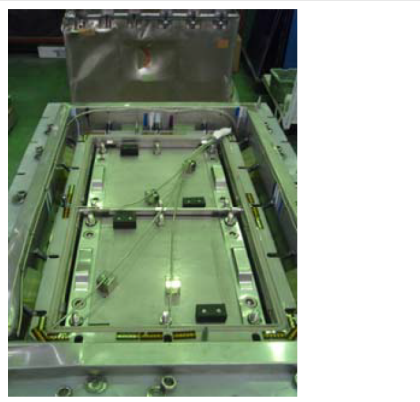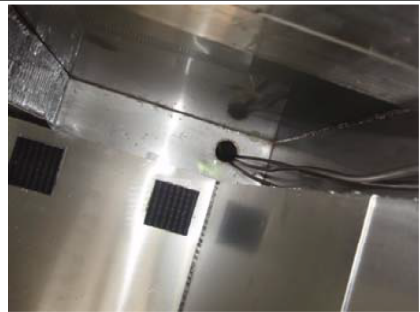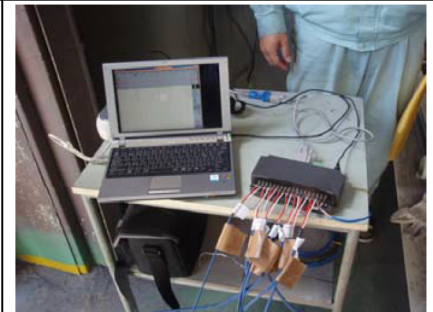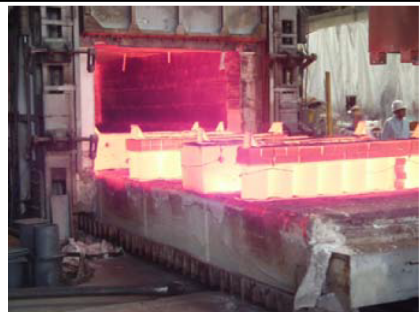
Photo B.App1-21: Specimen which has just been set on the carriage		Photo B.App1-22: Introducing the specimen into the furnace	
Photo B.App1-23: Port of the furnace opened at the end of the thermal test		Photo B.App1-24: Specimen on the carriage just retrieved from the furnace	
Photo B.App1-25: General view of the specimen shortly after the test		Photo B.App1-26: Thermocouple and fusible plug on the external surface of the specimen	
Photo B.App1-27: Outer receptacle flange		Photo B.App1-28: Interior of the outer receptacle	
Photo B.App1-29: Thermo-paints on the back of the inner receptacle lid		Photo B.App1-30: Fire-resistant rubber and thermo-paints on internal surface of the outer receptacle	

Photo B.App1-31: Fire-resistant rubber on the internal surface of the outer receptacle	
Photo B.App1-32: Fire-resistant rubber on the internal surface of the outer receptacle (from another angle)	
Photo B.App1-33: Fire-resistant rubber and thermo-paints on the internal surface of the outer receptacle	
Photo B.App1-34: Fire-resistant rubber	
Photo B.App1-35: Thermo-paints on the internal surface of the outer receptacle after removal of fire-resistant rubber (same location as in Photo B.App1-33)	
Photo B.App1-36: Thermo-label on the inner receptacle flange	
Photo B.App1-37: Thermo-labels applied side-by-side on the inner receptacle flange	
Photo B.App1-38: Other thermo-labels on the inner receptacle flange (corner)	
Photo B.App1-39: Other thermo-labels on the inner receptacle flange	
Photo B.App1-40: Inner receptacle without the lid	

Photo B.App1-41: O-ring on the corner flange of the inner receptacle		Photo B.App1-42: O-ring on a wider-side flange of the inner receptacle	
Photo B.App1-43: O-ring on a narrower- side flange of the inner receptacle		Photo B.App1-44: Inner receptacle corner, O-ring removed	
Photo B.App1-45: Thermo-labels on the top surface of the content (near the corner which was made to strike the test target or penetrating bar first during the preceding drop tests)		Photo B.App1-46: Thermo-labels on the top surface of the content (near the hole for thermocouple routing)	
Photo B.App1-47: Thermo-labels on the dummy neutron absorber (stainless steel plate)		Photo B.App1-48: Thermo-labels on the top surface of the content (near the hole for thermocouple routing)	

Results of Thermal Model Analysis
for Integrating Thermal Test Results

1. Introduction

The Type GP-01 transport packaging developed by Nuclear Fuel Industries, Ltd. for transporting pellets of uranium oxides or pellets of uranium oxides mixed with gadolinium, enriched to 5 weight percent or less, is classified as type "A" fissile transport package. Fissile packages must be subjected to the thermal test specified in Appendix 12 to the Public Notice. Accordingly, a thermal test was carried out using a prototype for this type of packaging. However, the requirements stipulated in the Public Notice include those which cannot be met in actual thermal tests, such as those for application of solar radiation. Thus, our definitive evaluation of the model of packaging will take into account results of analytical calculations. For this purpose, an analytical thermal model which conservatively includes the results of the actual thermal test should be created to carry out thermal analyses of the packaging under normal and accident conditions of transport.

Thus, the analysis for integrating thermal test results using a prototype were carried out to be able to justify the analytical model and to be able to enhance the accuracy of the thermal analysis. This document will describe the results of the analysis for integrating thermal test results.

2. Prototype and Results of Prototype Tests

2.1. Prototype Packaging

The prototype packaging was subjected consecutively to the drop tests and the thermal test. This prototype packaging has essentially been designed with characteristics and constructions identical to those of a production model of GP-01 packaging except for small differences. The only differences from an actual packaging will be presented in the following paragraphs. Two pellet storage box assemblies "A" were used as the contents of the package during the drop tests because of its greater loading capacity than the assembly "B." The same dummy contents were used in the thermal test.

(1) Dummy contents

The prototype to be subjected to the thermal test contains lead rods (dummy pellets) which simulates the weight of real pellets of uranium oxides. Lead has its own thermal properties which differ from those of uranium oxides. The thermal analysis to be carried out subsequently correct results of the thermal test.

(2) Attaching thermocouples

The accelerometers used for the drop tests were removed. Thermocouples had to be applied instead to the specimen for temperature measurements. For this purpose, it was imperative to open the outer receptacle to apply these measuring means. Several rod bolts located near the deformed zone of the outer receptacle could not be loosened for removal in the normal way and had to be cut. They were not replaced by new rod bolts or any substitute materials.

Fig. II-B.App2-1 shows the locations where thermocouples were attached. Thermo-labels and thermo-paints were applied to the flange of the inner receptacle. Thermo paints were applied to the internal sides of the outer receptacle near the inner receptacle flange.

The thermal analysis conducted after the thermal test simulated the temperatures recorded by these thermocouples.

Thermocouples installed:
- In the atmosphere of the furnace: a
- On the external surface of the outer receptacle: b
- On the inner side of the flange of the outer receptacle: c, d, and e
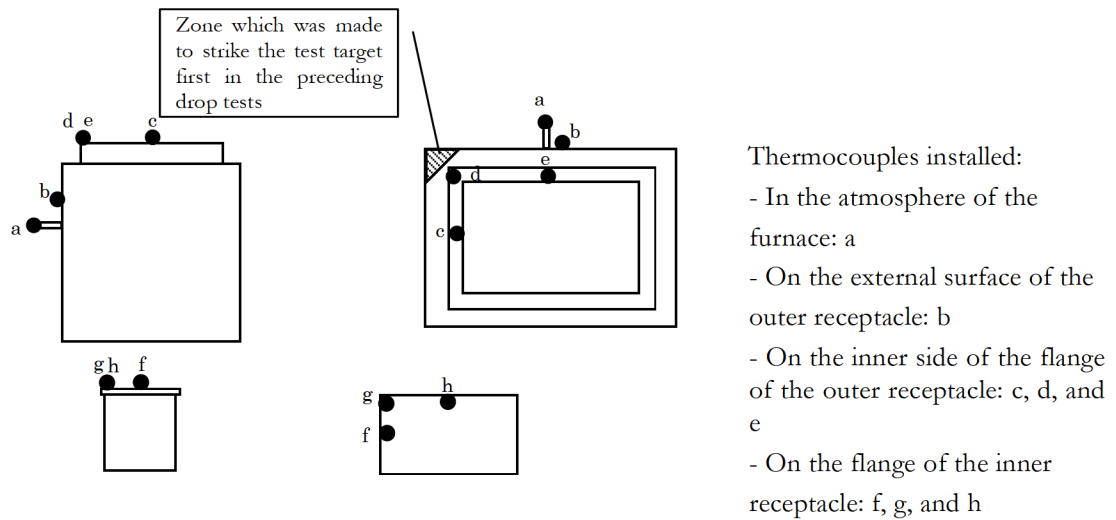- On the flange of the inner receptacle: f, g, and h

Fig. II-B.App2-1: Locations of Thermocouples Attached

(3) Additional measures for installing thermocouples

The hole arrangement which had been used for the cabling of the accelerometers was reused for routing the thermocouples. This routing hole is 30 mm in inner diameter. The portion of the insulator which bothered the routing was removed and a steel pipe welded on the internal surface of the hole. The hole was plugged with the remaining fragments of ceramic fiber insulator removed to prevent flames from entering, fragments produced when the hole was made.

The portions of honeycomb elements near the hole were reworked (ends cut off) for installing/routing the thermocouples.

(4) Dummy neutron absorbers

For real neutron absorbers made of boronic stainless steel plate for inner receptacle and pellet storage box assembly were substituted stainless steel plates of the same dimensions. Use of these dummy neutron absorbers does not affect the thermal test.

(5) Supplementary notes

The characteristics of a definitive production model of packaging will be fixed only when several improvements in features and handling procedures have been identified after completion of manufacture of these prototype packagings and all the tests described in this document have been taken into account. Table II-B.App1-1 shows the modifications in the prototype packaging which have thus been adopted. These modifications will not lead to reduction of the margin of safety for the thermal characteristics of the production model of the type GP-01 packaging.

2.2.   Results of Prototype Tests

(1) Drop tests

Prototypes No. 1 and No. 2 were used for the preceding drop tests. Prototype No. 1 was mainly used for examining and verifying orientations of the specimen to be adopted for the main part of the drop tests.

Prototype No. 2 was used for the thermal test. During the drop tests, this prototype was dropped in the orientation determined in the preliminary tests with Prototype No. 1. This orientation was supposed to cause maximum damage to the upper corner of the package. The specimen was released from a height in such an orientation that this zone might strike the test target plate or the penetrating bar first. This upper corner was chosen for maximum damage because such orientations would concentrate the drop energy on it to produce significant deformation and because this portion of the package was located close to the flange which was regarded most vulnerable to thermal stress during the thermal test and would present opening under drop energy to form a path for heat during the thermal test.

Appendix 1 to Chapter II-A shows the detail of the results of the prototype drop tests. During the drop tests, deformations occurred in the package up to the flange. No opening was produced in the flange and none of the rod bolts for tightening the lid on the body of receptacle were pulled out or fractured. The lid of the outer receptacle stayed in its required position. Small cracks were produced in the welds of the lifting attachment, and the insulator got partially exposed but was not lost at all. The cumulative deformations are modeled in Fig. II-B.App2-2.

In the interior of the outer receptacle, the aluminum honeycomb elements were partially deformed. The inner receptacle and the pellet storage box assemblies suffered no significant deformation.

Deformation on the outer receptacle corner which was made to strike the test target first during drop tests:

R1: 220 mm
R2: 300 mm
R3: 180 mm
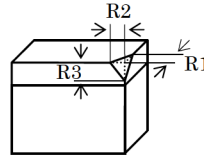
Fig. II-B.App2-2: Deformation during Drop Tests

(2) Thermal test

The thermocouples for measuring in-furnace temperatures indicated 800°C nine minutes after the furnace port was closed, and the test facility was maintained in the current operating conditions for further 30 minutes. Retrieved from the furnace, the prototype was still burning red on the carriage for a short time until it cooled down. The general surfaces of the package were oxidized in black. The prototype was checked visually. No change in shape was observed in the prototype. Dissolution or deformation resulting from burning was not found in the appearance of the specimen.

The thermal test caused change in color of the external surfaces of the outer receptacle. The deformations and damage which had been generated during the preceding drop tests were not aggravated during the thermal test. The thermal load of the test caused no holes in the specimen and no damage to the tightening rod bolts. The outer receptacle lid did not leave its initial position. The silicone rubber spacers on the flange were carbonized and turned into ash.

The internal surfaces of the outer receptacle and the external surfaces of the inner receptacle changed their colors but suffered no additional deformations and present no trace of ignition.

The dummy contents and interior of the inner receptacle only changed their colors but suffered no significant change or deformation during the thermal test. The highest temperature recorded of the silicone rubber O-ring on the inner receptacle flange was lower than 144°C. This O-ring kept its required elasticity. The type of O-ring adopted for this thermal test is a proven product which has a maximum service temperature of 180°C and has passed the heat and aging resistance test at 225°C for 72 hours specified by the applicable JIS standard. The temperature of the dummy contents did not exceed 125°C, proving that it was not affected by the thermal test.

Table II-B.App2-1 shows the highest temperatures attained at various locations during the thermal test. Fig. II-B.App2-3 shows the fluctuations of the recorded temperatures.

Table II-B.App2-1: Highest Temperatures Recorded on Thermocouples

Measured Locations		Thermocouple	Highest Temperature (°C)	Time for attaining the highest temperature (counting from end of test)
Interior of furnace		(a)	818.6	—
External surface of the outer receptacle		(b)	794.8	0:00:20
Outer receptacle	Flange on wider side	(e)	407.1	Outer receptacle
	Flange corner	(d)	343.8	
	Flange on narrower side	(c)	394.6	
Inner receptacle	Flange on wider side	(h)	127.1	Inner receptacle
	Flange corner	(g)	143.7	
	Flange on narrower side	(f)	141.9	

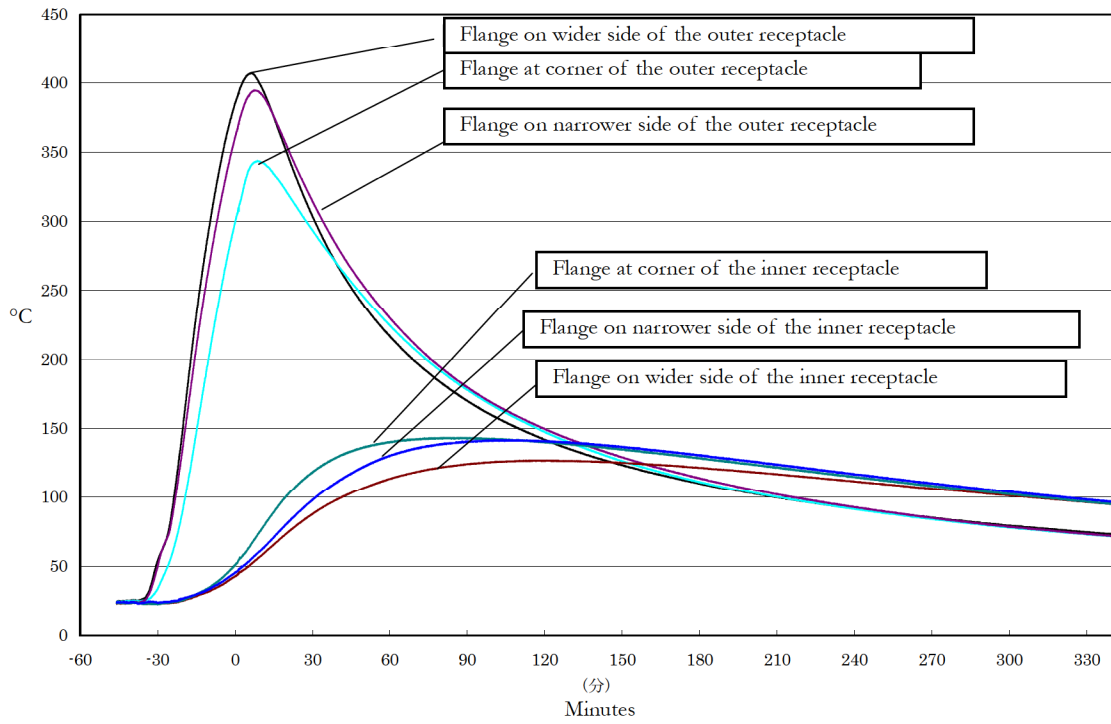Fig. II-B.App2-3: Evolutions of Temperatures (1/2)

Fig. II-B.App2-3: Evolutions of Temperatures (2/2)

II - B.App2 - 6

3. Methodology for Analysis

3.1. Geometrical Modeling

The type GP-01 package is a small and caisson-shaped object. Preliminary examinations led to the conclusion that assigning this package a 2-dimensional model (such as axisymmetrical model or slice model often used for thermal analysis of cylindrical objects) will greatly underestimate the heat input through the lateral surfaces of the package. Thus, a 3-dimensional model was adopted.

The prototype subjected to various drop tests including free drop, Drop I and Drop II was deformed in particular manners (refer to section "2.2. Results of Prototype Tests," (1) Drop tests). It is hardly possible to model the prototype in its real deformed shape and dimensions. Thus, we decided to cut a triangular pyramid which corresponds to the crushed portion (Fig. II-B.App2-2) from a no-damage analytical model to prepare an model to be used for our analysis. The insulator behind the cut zone should not be left exposed. Therefore, a 10-mm thick stainless steel plate is assigned to the damaged portion.

Since the prototype contains dummy pellets of uranium oxides (lead rods), the analysis for integrating thermal test results takes into account the thermal properties of lead.

3.2. Setting Analysis Conditions

This section shows the thermal boundary conditions. Table II-B.App2-2 shows summarized boundary conditions.

(1) Heat transfer between package components

All the components and parts of the packaging are assumed to be in tight contact with each other as long as they are in contact geometrically. The analysis assumes no loss of heat transfer because the model was created with the nodes shared by the relevant elements.

(2) Heat transfer simulating the thermal test conditions

The following conditions are applied consecutively.

(a) Assuming the package to be in an isothermal state which roughly corresponds to the ambient temperature before a fire breaks out

(b) Placing the package under the conditions of the thermal test

The analysis adopted the in-furnace temperatures recorded in the thermal test (Fig. II-B.App2-3) to simulate the temperature of flames (or temperature of external atmosphere) during a fire. The coefficient of heat transfer α used for the analysis was 10W/(m²°C), value retrieved from the IAEA transport regulations TS-G1.1 728.30. Ansys surface effect elements were used to define the heat transfer.

A radiation of heat from the external surfaces of the outer receptacle to the surrounding space is defined. A radiation factor of 0.9 for the flame surface and that of 0.8 for the external surface of the outer receptacle in accordance with the IAEA transport regulations TS-G1.1 728.28 and 728.29. As Ansys provides for only one value of radiation factor available for the definition, the following equation was adopted:

$$\text{Radiation factor } F_\varepsilon = \frac{\varepsilon_1 \varepsilon_2}{1-(1-\varepsilon_1)(1-\varepsilon_2)}$$

Ansys surface effect elements were used to define the radiation.

(c) Defining natural cooling after fire

Heat transfer by convection of the surrounding fluid at an ambient temperature is defined. The coefficient of heat transfer α was regarded as function of Nusselt number. The Nusselt number was retrieved from the IAEA transport regulations TS-G1.1 728.31 (for detail of the calculation of α, refer to the section describing the properties of the materials below). Ansys surface effect elements were used to define the heat transfer. Since the prototype packaging was cooled indoors in the thermal test, we assume in the analysis that no solar heat input will occurs.

(3) Heat transfer by radiation through air in the packaging

A real package contains air between the outer surfaces of the inner receptacle and the internal surfaces of the outer receptacle and between the internal surfaces of the inner receptacle and the outer surfaces of the pellet storage box assemblies. Assuming that no convection is occurring in the internal air, this air was handled as a heat transferring material (or solid for which physical properties corresponding to the air are defined) in our analysis. For the internal surfaces of the packaging which are in contact with air, heat transfer by radiation was defined. Aluminum honeycomb elements occupy most of the internal surfaces of the outer receptacle. The *Heat Transfer Engineering Data* (4th revised edition, The Japan Society of Mechanical Engineers, 1986) includes data on the radiation factor for aluminum in Figure 1(a), page 184. It indicates a range of 0.01 to 0.05. We adopted 0.1 to stay conservative. To carry out the analysis with a symmetric model, radiosity was used.

(4) Symmetry boundary condition

Symmetric surfaces are handled as a heat insulating condition. Surfaces for which no condition is specified are handled as heat insulating conditions in the heat transfer analyses.

(5) Initial temperature condition

The analysis should be started with the object to be analyzed which has a uniform temperature of 38°C under normal and accident conditions. In our analysis for integrating thermal test results using a prototype, the analysis was started for a state of uniform temperature of 25°C in order to ensure accord with the initial temperature for the thermal test.

Table II-B.App2-2: Thermal Boundary Conditions

Conditions	Heat transfer through surrounding air (heat transfer condition defined)	Inflow of solar radiation (heat flux defined)	Radiation by flames (heat transfer by radiation defined)	Radiation through surrounding air (heat transfer by radiation defined)	Radiation through the air in packaging voids (outer recept. internal surface ⇔inner recept. outer surface inner recept. internal surface ⇔? outer surface)
Ongoing fire	ON Surrounding air: measured temperature Coefficient of heat transfer =10	OFF Conditions of the prototype	ON (ε of flame=0.9 ε of packaging outer surface=0.8)	OFF	ON (ε=0. 1)
Natural cooling after fire	ON Surrounding air: room temperature Temperature-dependent coefficient of heat transfer		OFF	ON (ε of packaging outer surface =0.1)	

3.3. Flow of Analysis

Fig. II-B.App2-4 shows the flow of the analysis.
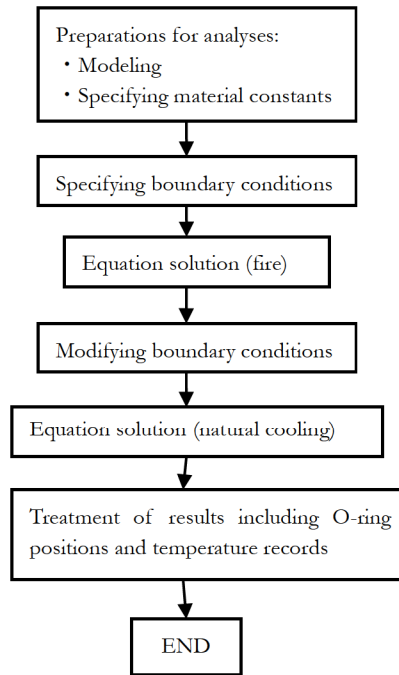
Fig. II-B.App2-4: Flow of Analysis for Integrating Thermal Test Results

4. Analytical Model

Since the package to be analyzed has a symmetric shape, our analysis concerns a modeled quarter symmetric zone (hatched zone in Fig. II-B.App2-5) of the package. Our modeling excluded small parts of the packaging because they were regarded negligible in terms of thermal consequences.
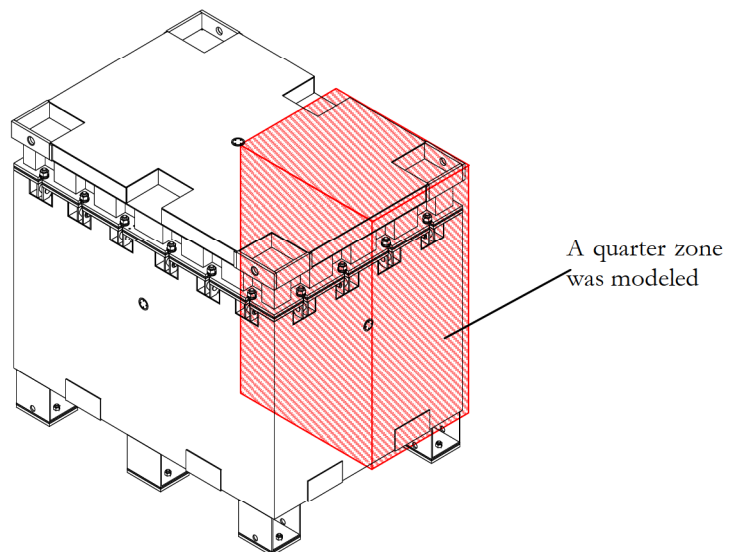

Fig. II-B.App2-5: Modeled Zone for 3-Dimensional Analysis

By design, the outer receptacle lid contains no heat insulating material outside the external surfaces of the frames and on the six recesses (including the four at the corners on which lifting attachments are provided) which can be engaged with the legs of another outer receptacle when stacked. The preliminary examinations revealed that these recesses of the outer receptacle do not affect the temperature distribution in the inner receptacle.

Thus, we excluded from our analysis those portions of the lid of the outer receptacle which are located outside the frames. The model is all the more conservative because it has contiguous stacking recesses for the legs of another outer receptacle on the lid of the outer receptacle and contiguous bolt seats on the body of the outer receptacle.

In the mechanical prototype tests, the honeycomb elements were slightly deformed but not completely crushed. To avoid reducing our conservatism, the honeycomb elements were assumed to be free from deformation and form heat conduction paths to the inner receptacle.

As described in section "3.1 Geometrical Modeling," a zone (triangular pyramid) of the model adopted was cut off in a simple manner to simulate the actual shape of the package subjected to several drop tests. Moreover, the analytical model was simplified in external dimensions to increase the conservatism and reduce the model scale. As a result, most of the verified deformations (in number and volume) are included in the simplified zone. Fig. II-B.App2-6 shows the resulting analytical model. Figs. II-B.App2-7 to II-B.App2-10 show cutaway images of this damage model. The adopted quarter symmetric model corresponds to a full model with four damaged zones. This partial compressing would contribute to increasing the volumetric insulating property, but the geometrical model simply has a cutaway portion and conserves its original thermal characteristics to maintain the conservatism.

The zone corresponding to contents (loaded pellet storage box assemblies) was assumed to be homogenized.
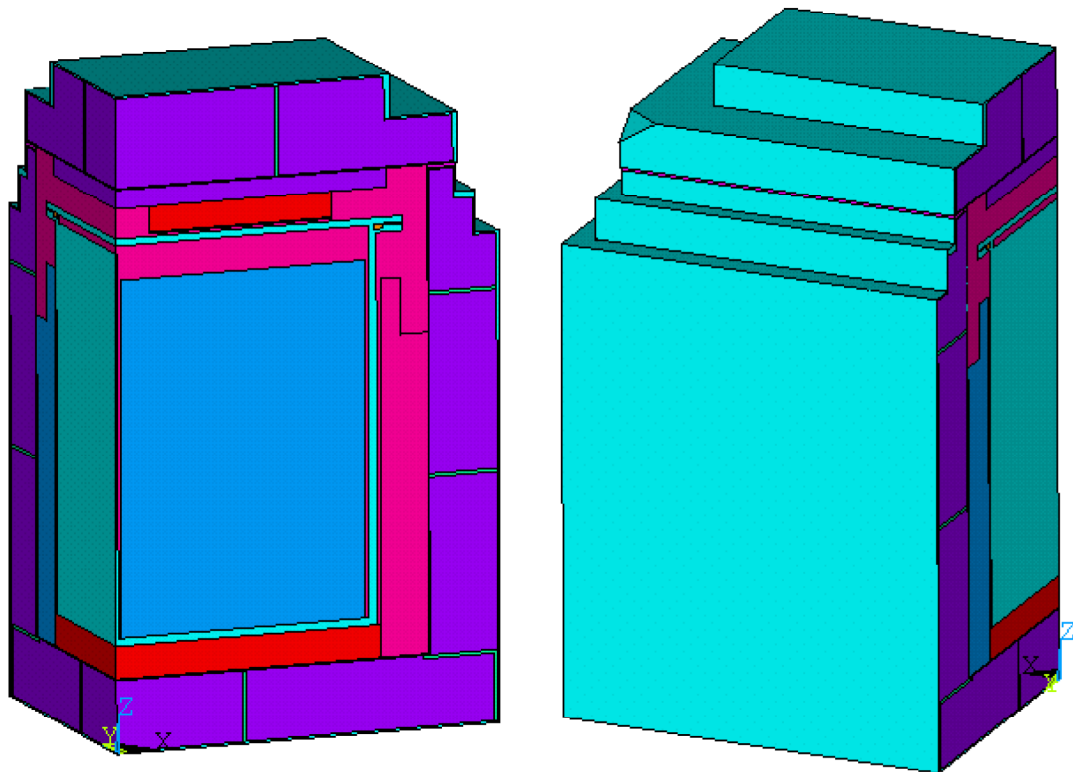
(a) View from –Y direction   (b) View from +Y direction

Fig. II-B.App2-6: General View of Analytical Model (entire damage mode)
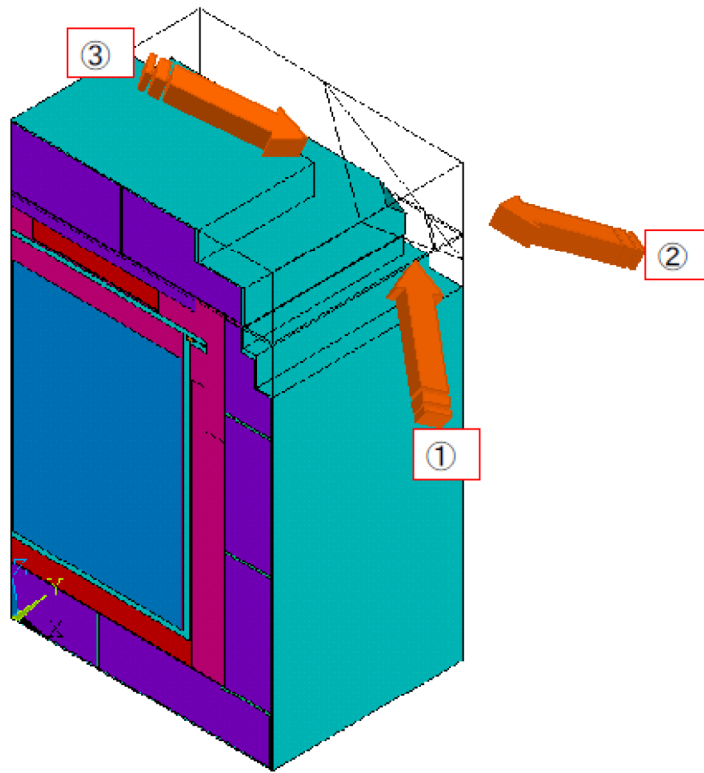
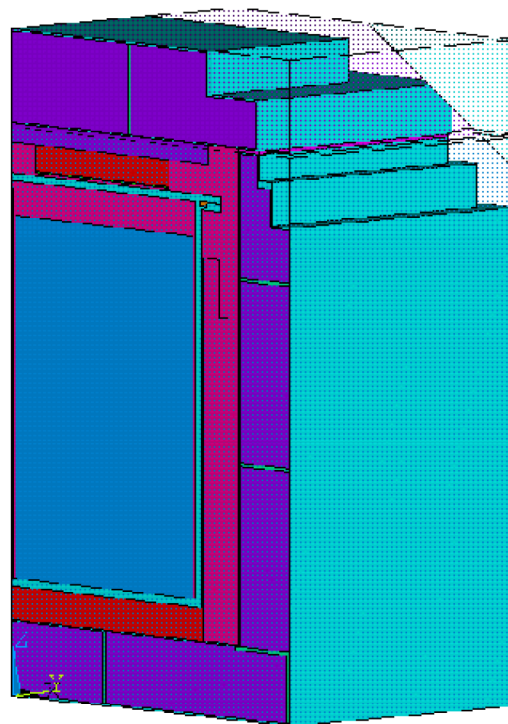Fig. II-B.App2-7: Cutaway Image of Damage Model (1/4)

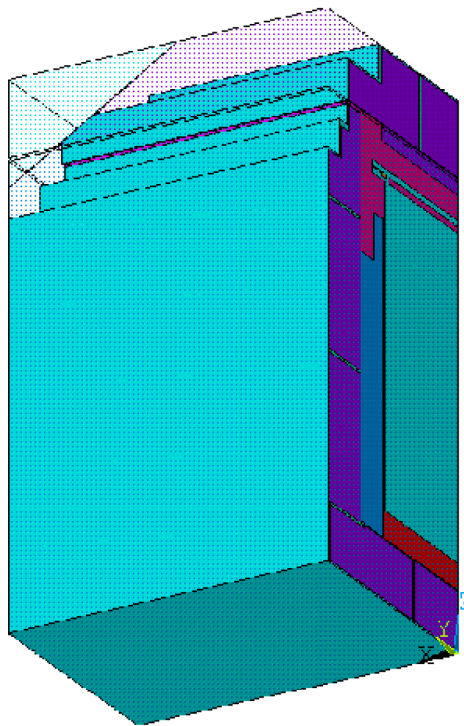Fig. II-B.App2-8: Cutaway Image of Damage Model (2/4) (view from ①)

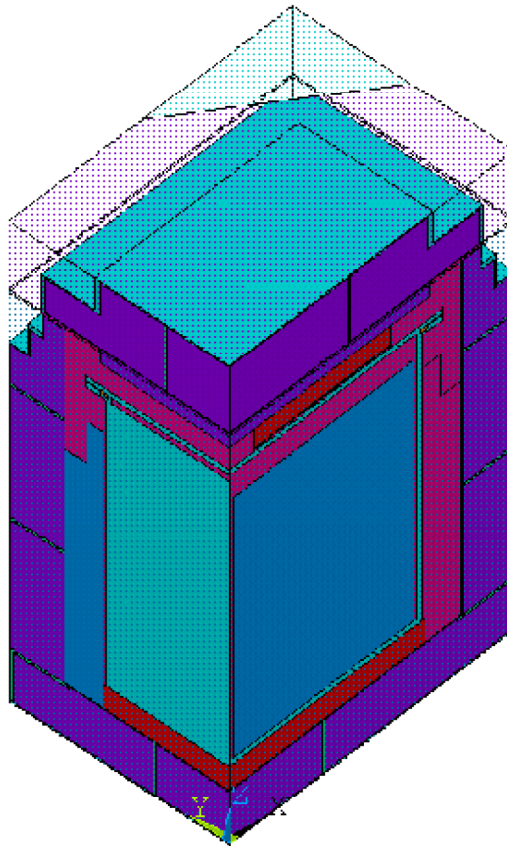Fig. II-B.App2-9: Cutaway Image of Damage Model (3/4) (view from ②)

Fig. II-B.App2-10: Cutaway Image of Damage Model (4/4) (view from ③)

The analytical model is embraced by three elements created for analyzing heat transfer through air, heat transfer by radiation during natural cooling and heat transfer by radiation of flames, respectively. Heat transfer by radiation is taken into account for the border between the internal air and the surrounding constructions. The finite element model was created in the same way as that for the no-damage analytical model. The model has 102,279 nodes and 125,973 finite elements. Figs. II-B.App2-11 to II-B.App2-13 show the finite element models used.
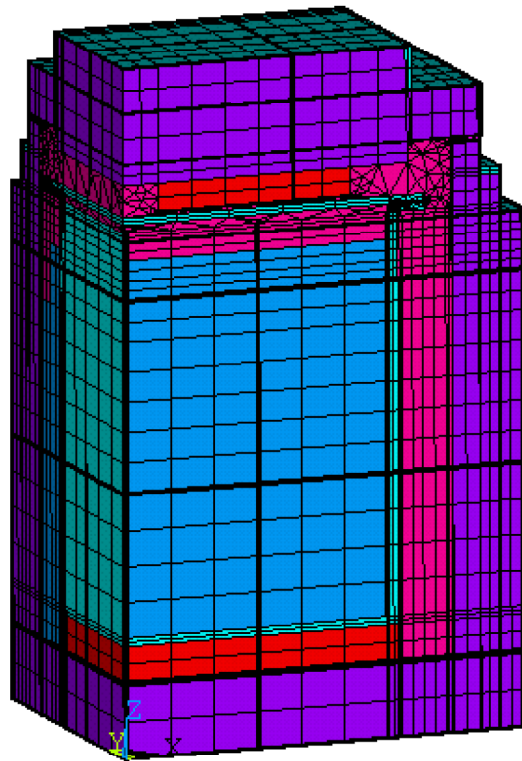

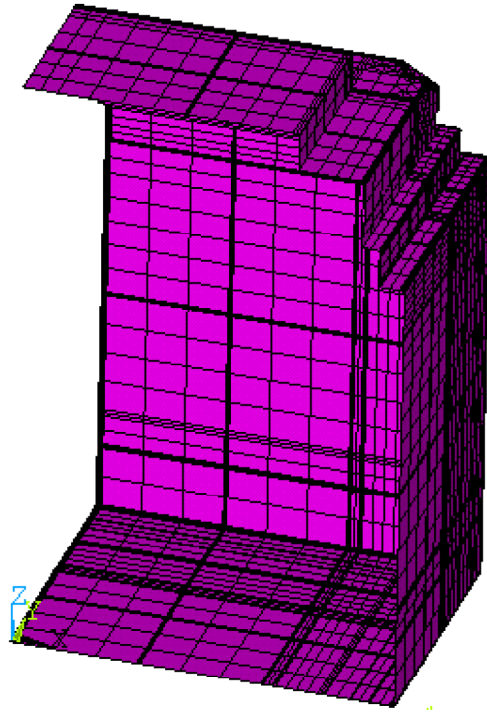Fig. II-B.App2-11: Finite Element Model (entire)

Fig. II-B.App2-12: Finite Element Model (segment for calculating surface effect)
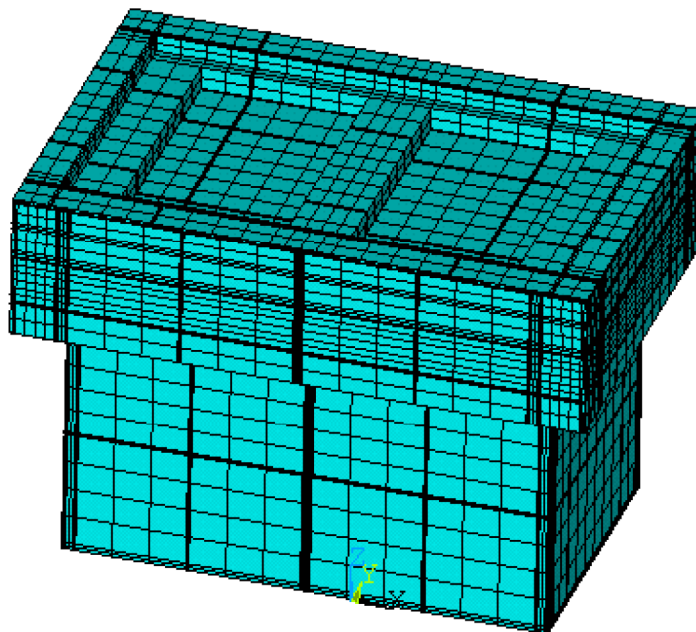

Fig. II-B.App2-13: Finite Element Model (segment for calculating surface effect and internal radiation)

5. Physical Properties of Materials

(1) Thermal properties of contents

The prototype packaging contains weight-simulating lead rods instead of pellets of uranium oxides. Therefore, the analysis for integrating thermal test results took into account thermophysical properties of lead.

The pellet storage box assemblies (contents) have no leaktightness and thus are not affected by rise of the inner pressure resulting from temperature rise. Moreover, the uranium oxides (pellets), nuclear fuel, and the component materials of the pellet storage box assembly are negligible in terms of fusion, gasification or gas leakage resulting from temperature rise. Thus, it is almost needless to determine temperature distribution in the contents. Thus, the analytical model contains a homogenized zone which represents the contents of the packaging. We used equivalent thermophysical property values which had been determined from volumetric ratios of the component materials/substances.

The densities and coefficients of heat transfer for these materials/substances were determined by summing the thermophysical property values multiplied by their volumetric ratios. The specific heat values were determined with the equation $\Sigma \rho_i \cdot c_i / \rho$ (ρ_i and $c_i p$ are density and specific heat of a material/substance and ρ is average density). Table II-B.App2-3 shows the thermophysical properties of the contents used for the analysis.

(2) Thermophysical properties of aluminum honeycomb element

The honeycombs element has an appearance shown in Fig. II-B.App2-14. The honeycomb element literally resembles the periodical pattern of bees' cells in structure. Therefore, the honeycomb element, a heat conducting body, can be handled as a homogenized material which has thermophysical properties equivalent to those of these different materials/substances. However, it should be noted that it has specific heat conducting characteristics depending on the directionality.
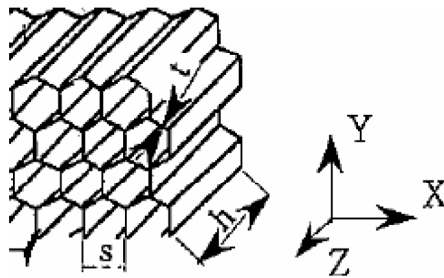

Fig. II-B.App2-14: Structure of Aluminum Honeycomb Element

A reference (N. Ogasawara, M. Shiratori, Yu Qiang and T. Kurahara, *Evaluation of coefficient of orthotropic heat transfer of honeycomb material*, report No. 99-0011, Bulletin (Title B) of The Japan Society of Mechanical Engineers, vol. 65, issue 639, 1999-11) presents an equation for determining the coefficients of heat transfer for different directions of this structure:

$$\lambda_x = \lambda_{air} + \lambda_{al} R$$
$$\lambda_y = \lambda_{air} + \frac{3}{2}\lambda_{al} R$$
$$\lambda_z = \lambda_{air} + \frac{8}{3}\lambda_{al} R$$
$$R = \frac{t}{s}$$

For our analysis, the coefficients of heat transfer λx, λy, and λz were defined with account taken of the orientations of the installed honeycomb material and the directionality depending on their location. The equivalent density and the equivalent specific heat were determined as follows:

$$\rho = \rho_{air} + 8/3\,\rho_{al} R$$
$$C = \left(C_{air}\rho_{air} + 8/3\,C_{al}\rho_{al} R\right)/\rho$$

Table II-B.App2-4 shows the thermophysical properties of the aluminum honeycomb element used for the analysis.

(3) Thermophysical properties of insulator
The values of the thermophysical properties of the insulator used for our preliminary analysis conservatively exceed those published by the manufacturer. Initial results of the preliminary analysis were found incompatible with the results of the preceding thermal test. Further examination using the manufacturer's data which we slightly complemented on thermophysical properties led to results compatible with those of the thermal test. The definitive results of the preliminary analysis are conservative. Accordingly, the analytical model achieved is conservative as well and has high compatibility with the results of the thermal test. Table II-B.App2-5 shows the thermophysical properties of the insulator.

(4) Thermophysical properties of other component materials
Table II-B.App2-6 shows the thermophysical properties of component materials other than the insulator.

(5) Determining coefficient of heat transfer
The coefficient of heat transfer α between the external surface of the outer receptacle and the surrounding fluid under fire conditions used for the analysis was 10W/(m²°C), value retrieved from the IAEA transport regulations TS-G1.1 728.30.

The coefficient of heat transfer α for other conditions was regarded as function Nusselt number:

$$\alpha = Nu \cdot \lambda / l \quad (\lambda : \text{heat conductivity}, l : \text{representative length (outer receptacle height exc. legs} : 0.915 \text{ m}$$

The Nusselt number was calculated with the formula shown in the IAEA transport regulations TS-G1.1 728.31:

$$Nu = 0.13(PrGr)^{1/3}$$

where
Prandtl number $Pr = \nu / \varkappa$ (ν: kinetic viscosity; $\varkappa$: coefficient of thermal diffusivity ($=\lambda / \varrho c$); ϱ: density; c: specific heat)
Grashof number $Gr = g \cdot \beta \ (T_w - T_\infty) \ l^3 / \ \nu^2$ (g: gravitational acceleration; β: coefficient of volumetric expansion; T_w: wall temperature; T_∞: air temperature)

Table II-B.App2-7 shows the calculated coefficients of heat transfer.

Table II-B.App2-3: Thermophysical Properties of Contents

Temperature (K)	Density (g/cm³)	Specific heat (J/kg·K)	Heat conductivity (W/m·K)	Temperature (K)	Density (g/cm³)	Specific heat (J/kg·K)	Heat conductivity (W/m·K)
293	3.799	402	9.33	693	3.668	459	9.85
313	3.794	402	9.33	713	3.660	463	9.90
333	3.789	404	9.33	733	3.652	467	9.95
353	3.783	405	9.34	753	3.644	471	10.00
373	3.778	407	9.35	773	3.635	474	10.06
393	3.772	409	9.36	793	3.626	478	10.11
413	3.766	411	9.38	813	3.618	481	10.17
433	3.760	414	9.40	833	3.609	484	10.23
453	3.754	416	9.42	853	3.600	487	10.29
473	3.748	419	9.44	873	3.590	490	10.36
493	3.741	422	9.47	893	3.581	493	10.42
513	3.735	426	9.50	913	3.571	495	10.49
533	3.728	429	9.53	933	3.561	498	10.56
553	3.721	433	9.56	953	3.552	499	10.63
573	3.714	436	9.60	973	3.542	501	10.70
593	3.707	440	9.63	993	3.531	502	10.77
613	3.699	444	9.67	1013	3.521	503	10.85
633	3.692	448	9.71	1033	3.511	504	10.92
653	3.684	452	9.76	1053	3.500	504	11.00
673	3.676	455	9.80	1073	3.489	504	11.08

Table II-B.App2-4: Thermophysical Properties of Aluminum Honeycomb Element

Temperature (K)	Density (g/cm³)	Specific heat (J/kg·K)	Heat conductivity (W/m·K)		
			X	Y	Z
300	0.0776	907	2.554	3.818	6.767
320	0.0775	921	2.552	3.814	6.759
340	0.0774	934	2.550	3.810	6.751
360	0.0772	946	2.548	3.806	6.743
380	0.0771	957	2.546	3.802	6.735
400	0.0770	966	2.543	3.798	6.727
420	0.0768	975	2.541	3.794	6.719
440	0.0767	983	2.539	3.790	6.711
460	0.0766	991	2.537	3.786	6.702
480	0.0765	998	2.534	3.782	6.694
500	0.0764	1005	2.532	3.778	6.686
550	0.0760	1022	2.526	3.768	6.665
600	0.0757	1040	2.520	3.758	6.645
650	0.0754	1060	2.491	3.712	6.562
700	0.0750	1083	2.462	3.667	6.480
800	0.0743	1140	2.404	3.577	6.315
900	0.0734	1213	2.345	3.487	6.150
1000	0.0725	1300	2.286	3.395	5.984
1100	0.0715	1391	2.226	3.304	5.817

Table II-B.App2-5: Thermophysical Properties of Insulating Material

Temperature (K)	Density (g/cm³)	Specific heat (J/kg·K)	Heat conductivity (W/m·K)
291	0.16	1050	0.031
373	0.16	1050	0.036
473	0.16	1050	0.044
573	0.16	1050	0.053
673	0.16	1050	0.064
773	0.16	1050	0.081
873	0.16	1050	0.098
973	0.16	1050	0.120
1073	0.16	1050	0.145
1173	0.16	1050	0.173

Note: These data are cited from the technical data published by the manufacturer with some modifications.

Table II-B.App2-6: Thermophysical Properties of Component Materials Adopted for Thermal Analyses

Component	Material	Temperature (K)	Density (g/cm³)	Specific heat (J/kg·K)	Heat conductivity (W/m·K)
Inner/Outer Receptacle	Stainless steel [1]	300	7.92	449	16.0
		400	7.89	511	16.5
		600	7.81	556	19.0
		800	7.73	620	22.5
		1000	7.64	644	25.7
Rubbers	Fire-resistant rubber [2]	300	0.86	2200	0.36
	Silicone rubber	293	0.97	1600	0.20
		400	0.97	1500	0.19
	Neoprene rubber	293	1.23	2200	0.25
		400	1.23	2200	0.23

Notes: (1) *Heat Transfer Engineering Data*, 4th revised edition, JSME, 1986

(2) The properties of ethylene propylene rubber (main component) are substituted.

Table II-B.App2-7: Coefficients of Heat Transfer

Temperature (K)	Coefficient of heat transfer (W/m²·K)	Temperature (K)	Coefficient of heat transfer (W/m²·K)
311	0	550	7.942
320	3.858	600	7.988
340	5.460	650	7.975
360	6.250	700	7.965
380	6.742	800	7.878
400	7.082	900	7.783
420	7.326	1000	7.619
440	7.509	1100	7.448
460	7.643	1200	7.273
480	7.748	1500	6.758
500	7.826	—	—

6.　Results of Analysis for Integrating Thermal Test Results

Figs. II-B.App2-15 shows the results of the analysis for integrating thermal test results. Figs. II-B.App2-16 to II-B.App2-19 show contour diagrams for the model at the moment of thermal test completion and at the moment when the highest temperature was attained in the inner receptacle flange.

The analysis was carried out to evaluate the points of the model which correspond to the different locations of the inner and outer receptacle flanges on which temperatures had been measured during the thermal test. Good accord is observed between the temperature fluctuations of these flange points and those indicated in "Fig. II-B.App2-3: Evolutions of Temperatures (1/2)" and "Fig. II-B.App2-3: Evolutions of Temperatures (2/2)." More precise comparison of the analysis results with the test results revealed that the former is 8 to 10 percent more conservative for the flange points of the inner receptacle and 4 to 14 percent more conservative for the flange points of the outer receptacle than the latter. Table II-B.App2-8 shows the highest temperatures on these flange points calculated in comparison with the real measurements. The temperature variation between the analysis and the test is greater for the flange points of the outer receptacle than for those of the inner receptacle. Since the analysis for integrating thermal test results was focused on the reactions in the inner receptacle, we concluded that an analytical model compatible with the thermal test results was created, keeping a higher conservatism over the thermal test results. Thus, we are ready for carrying out thermal analyses of the prototype package under normal and accident conditions of transport.
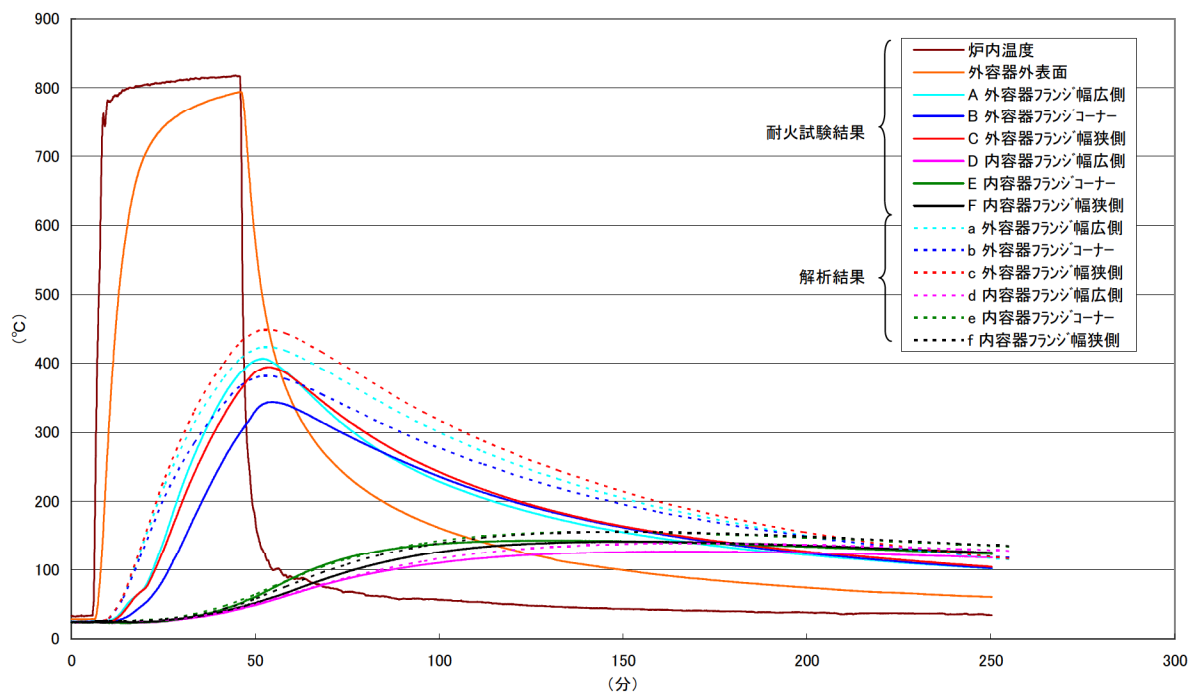

Fig. II-B.App2-15: Results of Analysis for Integrating Thermal Test Results

Results of thermal test:

In-furnace temperature

External surface of the outer receptacle

A: Flange on wider side of the outer receptacle

B: Flange at corner of the outer receptacle

C: Flange on narrower side of the outer receptacle

D: Flange on wider side of the inner receptacle

E: Flange at corner of the inner receptacle

F: Flange on narrower side of the inner receptacle

a: Flange on wider side of the outer receptacle

b: Flange at corner of the outer receptacle

c: Flange on narrower side of the outer receptacle

d: Flange on wider side of the inner receptacle

e: Flange at corner of the inner receptacle

f: Flange on narrower side of the inner receptacle

Table II-B.App2-8: Highest Temperatures Compared between Test Results and Analysis Results

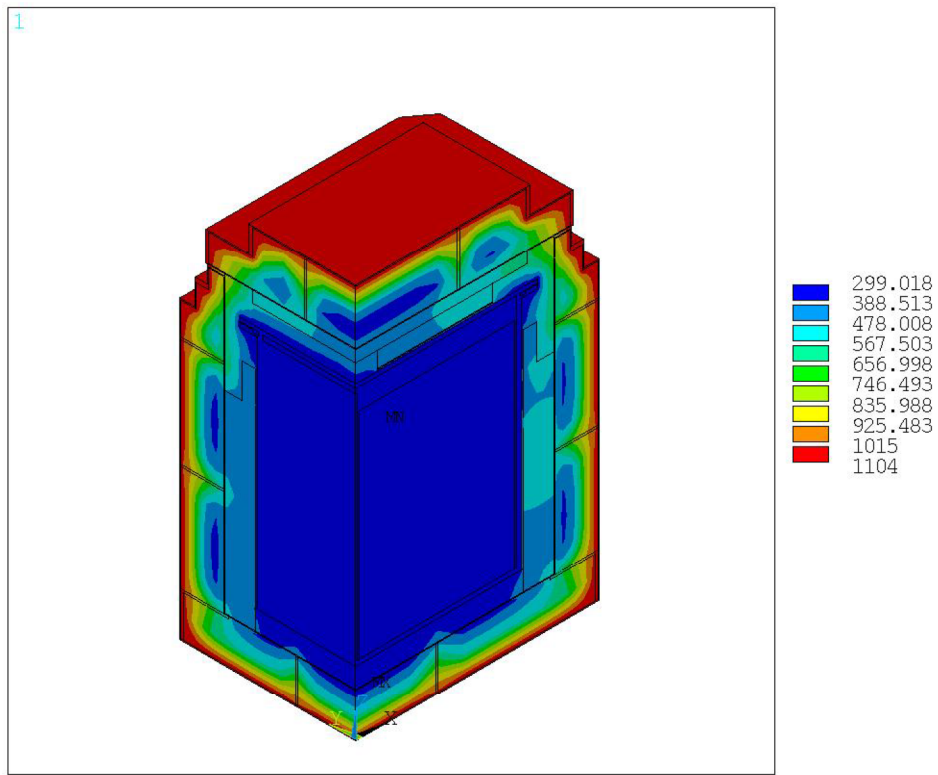|	Inner Receptacle Flange			Outer Receptacle Flange		
	Narrower	Corner	Wider	Narrower	Corner	Wider
Test Results	141.9	143.7	127.1	394.6	343.8	407.1
Analysis Results	155.5	155.3	138.8	449.0	381.4	423.9
Increase	9.6%	8.1%	9.2%	13.8%	10.9%	4.1%

Fig. II-B.App2-16: Temperature Distribution in the Entire Packaging at End of Thermal Test (unit: K)
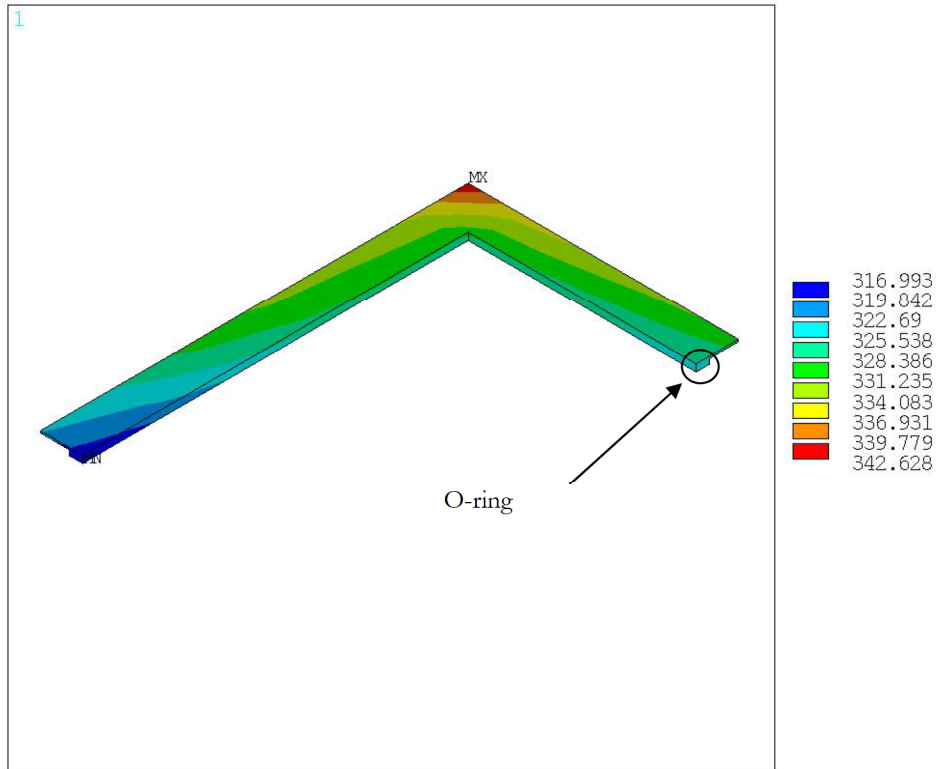

Fig. II-B.App2-17: Temperature Distribution in Rubber near O-ring at End of Thermal Test (unit: K)
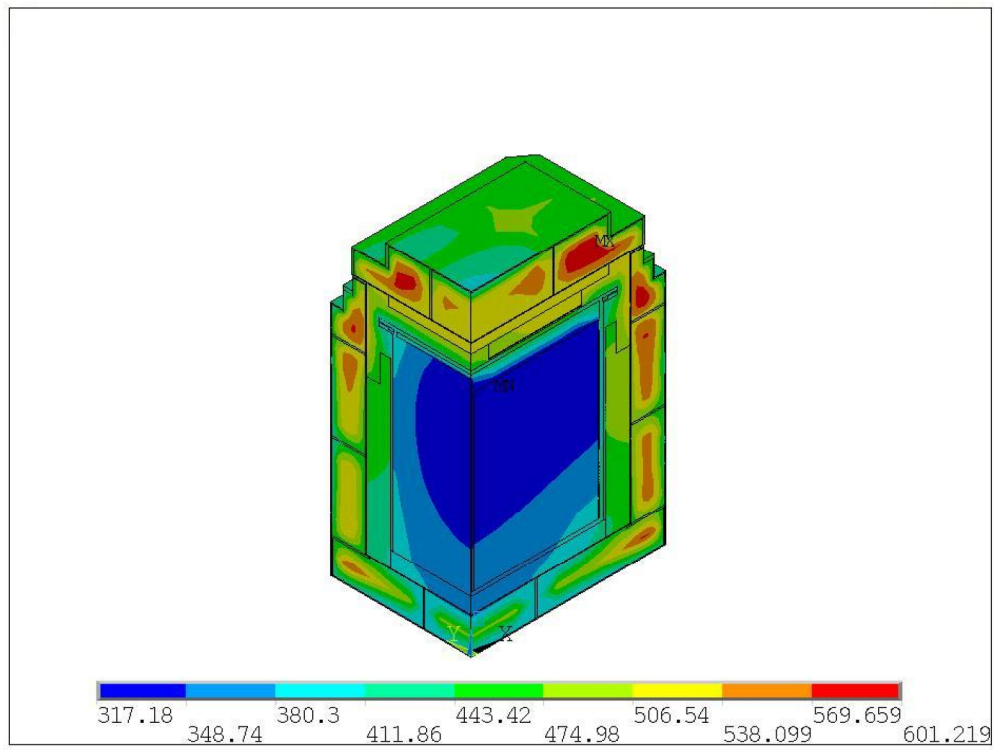
Fig. II-B.App2-18: Temperature Distribution in Entire Package (when the highest temperature was attained in O-ring; unit: K)
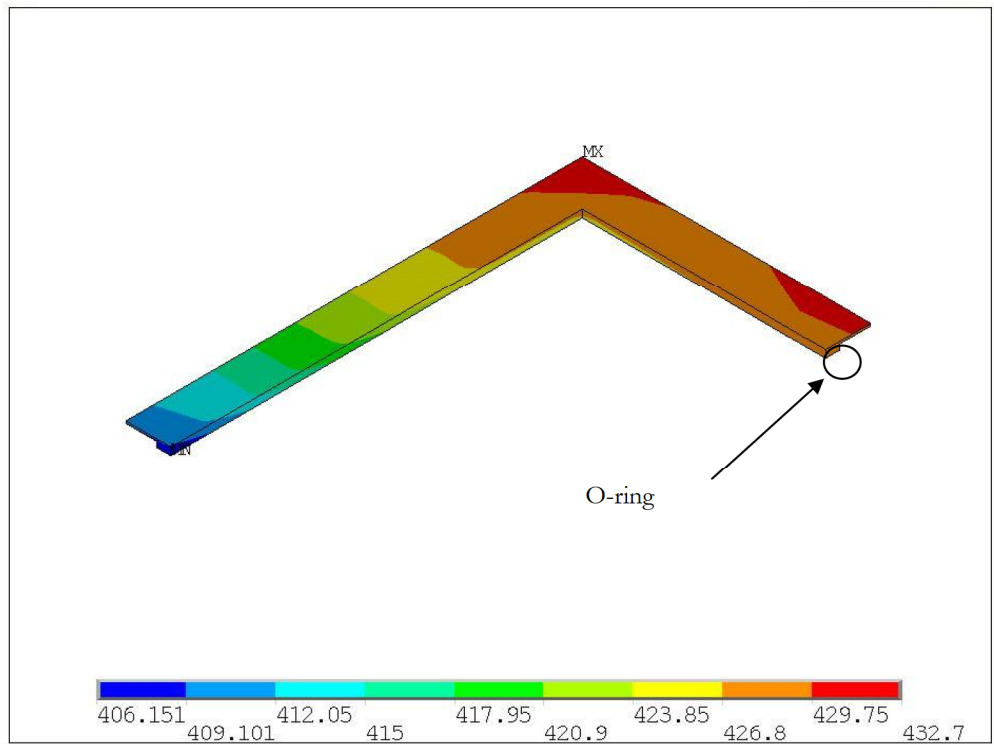

Fig. II-B.App2-19: Temperature Distribution in Rubber near O-ring (when the highest temperature was attained in O-ring; unit: K)

II-C.   Leaktightness Analysis

C.1.   General

The type GP-01 transport packaging consists of an outer receptacle and an inner receptacle which can be retrieved from the outer receptacle without being dismantled. The inner receptacle is designed to contain two pellet storage box assemblies (contents). The outer receptacle has the principal function of protecting the inner receptacle which forms the containment boundary of the package.

The inner receptacle includes an upper lid which allows pellet storage box assemblies to be loaded and retrieved vertically while it is opened. The lid is joined to the body of the inner receptacle by means of rod bolts. An O-ring is provided for sealing on the flange surface.

The packaging is designed to store two assemblies of pellet storage boxes which contain pellets (minimum elements of nuclear fuel) of uranium oxides. To construct an assembly, pellet storage boxes are stacked alternately with partitions which are penetrated by six pillars. The stack of pellet storage boxes is fixed with nuts at the threaded top of the pillars. Pellets are ceramic non-dissipative solids prepared by press-molding and sintering (at higher than 1000°C) process. This packaging is not designed to contain nuclear fuel materials in liquid or gaseous phase.

In the containment boundary formed by the inner receptacle, the pellet storage box assemblies have no gaps which might cause pellets to leak out from the pellet storage boxes, and have a rigid structure.

(1) Normal conditions of transport

Packages configured with the type GP-01 packaging are classified as type "A" packages. This chapter will describe how radioactive materials or substances do not leak from the package under normal conditions of transport according to the Regulations, Article 10.

(2) Accident conditions of transport

Packages configured with the type GP-01 packaging do not need to have the leaktightness required by the Regulations under accident conditions of transport. This chapter will describe how radioactive materials or substances are contained in the inner receptacle forming the containment boundary under accident conditions of transport.

C.2.   Containment System
C.2.1.   General

The inner receptacle of the package consists of a lid and a main body. The lid consists of a monolithic stainless steel plate 10 mm in thickness and the main body is composed of stainless steel plates 6 to 8 mm in thickness, welded in the form of a box. Stainless steel plates 12 mm in thickness are machined and welded as flanges onto the upper part of the body of the inner receptacle. All the joints contributing to the containment boundary are finished with continuous welding.

A silicone rubber O-ring 10 mm in diameter is provided at the interface of the body and the lid of the inner receptacle which are joined by means of rod bolts to ensure leaktightness of the inner receptacle.

The entire finished inner receptacle is inspected for leaktightness in water at least one meter in depth or under an equivalent hydraulic pressure for at least one hour.

C.2.2.   Penetrations in Containment System

The lid covers the entire top surface of the inner receptacle which forms the containment system for pellet storage box assemblies, contents of the package. The containment boundary is completed with sixteen (16) rod bolts for firmly tightening the lid on the body of the inner receptacle. The type GP-01 packaging is not designed for containing liquids or gases and has no valves.

C.2.3.   Gasket and welds of containment system

The material (silicone rubber) of the O-ring provided on the inner receptacle flange maintains its thermal strength in a temperature range from –50°C to +180°C. Deterioration does not occur in the material in the temperature range of –40°C to +70°C. The inner receptacle of the packaging is constructed by continuous welding of stainless steel plates which are not liable to deformations that might affect its leaktightness or confinement.

Loading of contents is performed at room temperature and under room atmospheric pressure. Thus, no pressure differences will be generated between the interior and the exterior of the inner receptacle, and loading operations will not affect the performance of the O-ring and the welds of the inner receptacle.

C.2.4.   Lid of inner receptacle

The lid of the inner receptacle consists of one single stainless steel plate 10 mm in thickness. Sixteen (16) rod bolts are used to join the lid to the main body of the inner receptacle to create a containment boundary.

Under normal conditions of transport, the leaktightness of the inner receptacle is maintained by the lid firmly joined to the body by means of rod bolts.

Packages configured with the Type GP-01 packaging are classified as type "A" fissile transport packages and do not need to meet the regulatory requirements for leaktightness under accident conditions of transport. The firm connection of the lid with the body of the inner receptacle thus maintained by the rod bolts contributes to containing pellet storage box assemblies in the inner receptacle.

C.3.   Normal Conditions of Transport

As described in section "A.5.7. Summary of results and evaluation," the evaluation of the package under normal conditions of transport has revealed that the leaktightness of the inner receptacle keeps radioactive materials/substances in its substantial containment system and prevents them from leaking out.

(1) Thermal test

Packages configured with the Type GP-01 packaging are categorized as type "A" fissile packages and do not need to undergo regulatory thermal tests. As presented in section "B.4.6. Summary of Results and Evaluation," a thermal analysis showed that the temperature in the O-ring attains 68°C. This level is, however, far below the service temperature (180°C) for the material of the O-ring. Therefore, the material of the O-ring will not deteriorate at such temperatures. The highest attainable temperature in the inner receptacle is 75°C. The analysis

proved that all the materials of the inner receptacle will maintain their performance integrity even if the inner pressure in the inner receptacle is increased by a temperature rise in the surrounding atmosphere. Thus, the thermal test will not affect the leaktightness of the package.

(2) Water Spraying

As described in section "A.5.2. Water Spray Test," the main structural materials of the packaging are stainless steel and will not deteriorate in water. Moreover, the packaging has a structure which prevents water from entering the interior of the package. Water spraying will not affect the leaktightness of the package.

(3) Free Drop Tests

As described in section "A.5.3.1. Prototype tests," a free drop will cause local deformation in the outer receptacle. Nevertheless, the containment boundary of the package was maintained (see section "A.5.3.2. Integrity of containment boundary"). Thus, free drop will not affect the leaktightness of the containment boundary of the package.

(4) Stacking Test

As described in section "A.5.4. Stacking Test," the load applied to the package during the stacking test was far below the allowable highest stress which might be generated on the package. Thus, the package/packaging will not be deformed. Since the inner receptacle does not support any part of the load generated during the stacking test, the leaktightness of the inner receptacle will not be affected.

(5) Penetration Tests

As explained in section "A.5.5. Penetrations," the test rod for the penetration test will not penetrate the outer plates of the outer receptacle.

C.3.1.   Leakage of Radioactive Materials

The results of the prototype tests and the structural analyses have revealed that the inner receptacle maintains its leaktightness under normal conditions of transport and that no leakage of radioactive materials from the inner receptacle will occur.

C.3.2.   Rise of pressure in containment system

The temperature of the inner receptacle may reach 75°C in an environment of solar radiation. At this temperature, no gases will be emitted from any of the materials including rubber and stainless steel of the inner receptacle, or from the pellets of uranium oxides. The only possible rise of pressure in the containment system is that which may result from a temperature rise of the atmosphere (air) in the inner pressure. As shown in section "A.5.1.3. Calculation of stresses," any rise of the inner pressure resulting from temperature rise will not affect the performance integrity of the inner receptacle.

C.3.3.   Contamination of Coolant

The package/packaging contains no coolant (cooling material or agent). Thus, no contamination of coolant

(cooling material or agent) will occur.

C.3.4.   Loss of Coolant

The package/packaging contains no coolant (cooling material or agent). Thus, no loss of coolant or cooling (cooling material or agent) will occur.

C.4.   Accident Conditions of Transport

Packages configured with the type GP-01 packaging, type "A" fissile packages, do not need to meet the regulatory requirements for leaktightness under accident conditions of transport. Our tests and analyses have shown that the contents will be maintained in the package, and that none of the contents will leak from the package under accident conditions of transport. The following paragraphs summarize the results of the test and analysis of the package under accident conditions of transport.

(1) Drop I tests

As shown in section "A.9.2.1.5. Summary of results of Drop I tests," no cracks, fractures or penetration holes that might affect the interior of the package were generated in the outer receptacle, and the lid did not move from its required position. No cleft or hole was produced in the joints on the flange, so that any exposure of the inner receptacle was prevented.

The lid and body of the inner receptacle were deformed, and some of the rod bolts for tightening the receptacle were deformed. Nevertheless, none of the rod bolts was fractured or separated from the original locations, and the lid did not move from its required position.

The contents, pellet storage box assemblies, remained in the inner receptacle and did not leave their initial required positions. Thus, the pellets of uranium oxides will not leak from the storage boxes.

Prototype tests were conducted under very demanding test conditions for the prototypes: for example, every single prototype was subjected to five drop trials. Throughout the test, the dummy contents were retained in the inner receptacle. All these results show with sufficient conservatism that the inner receptacle will maintain its function of retaining the contents in its leaktight body.

(2) Drop II tests

As described in section "A.9.2.2.1. Summary of results of Drop II tests," several dents were produced on the external surface of the outer receptacle. No penetration or crack/cleft or hole was generated on its external surfaces. The drop tests did not affect, or produce any deformation to, the internal zones of the outer receptacle, and never affected the inner receptacle or contents.

(3) Thermal test

As shown in section "B.5.6. Summary of Results and Evaluation," the load applied during the thermal test caused no remarkable deterioration in the package components. Dissolution, inflammation, or deformation resulting from alteration will not occur in the components of the package. The contents will not leave their original locations and will not leak from the package. The temperature of the O-ring on the inner receptacle flange may reach 170°C, far below the maximum service temperature (180°C) of its material (silicone rubber).

Even if the inner temperature of the inner receptacle reaches 170°C under unfavorable conditions, nuclear fuel materials will not move in the inner receptacle or leak from the containment boundary.

(4) Water immersion

Our criticality analysis takes account of entry of water into the inner receptacle. However, the immersion test under 0.9-meter water head as stipulated by the Public Notice was not conducted. Even in case of immersion in water or entry of water into the inner receptacle, the nuclear fuel material will not change its property of insolubility in water. Furthermore, because of this property, no fuel material will be released from the packaging even if such external water flows out from the inner receptacle.

C.4.1.   Fission product gases

Pellets of unirradiated uranium oxides to be contained in the inner receptacle will not generate any fission product gas.

C.4.2.   Leakage of radioactive materials

Even under accident conditions of transport, the contents will remain sealed (confined) in the inner receptacle.

C.5.   Summary of Results and Evaluation

The package has been evaluated for leaktightness under normal conditions of transport. The results of the evaluation prove that the inner receptacle maintains its integrity of containment boundary.

It has been verified that the contents will be sealed or confined in the inner receptacle under accident conditions of transport.